

COMPREHENSIVE INVITED REVIEW

**REDOX HOMEOSTASIS IN PHOTOSYNTHETIC ORGANISMS: NOVEL
AND ESTABLISHED THIOL-BASED MOLECULAR MECHANISMS**

Mirko Zaffagnini¹, Simona Fermani², Christophe H. Marchand³, Alex Costa⁴, Francesca Sparla¹, Nicolas Rouhier⁵, Peter Geigenberger⁶, Stéphane D. Lemaire³, and Paolo Trost¹

¹ Department of Pharmacy and Biotechnology, University of Bologna, Bologna, Italy

² Department of Chemistry Giacomo Ciamician, University of Bologna, Bologna, Italy

³ Laboratoire de Biologie Moléculaire et Cellulaire des Eucaryotes, UMR8226, Centre National de la Recherche Scientifique, Sorbonne Université, Institut de Biologie Physico-Chimique, Paris, France

⁴ Department of Biosciences, University of Milan, Milan, Italy

⁵ Université de Lorraine, Inra, IAM, F-54000 Nancy, France

⁶ Ludwig-Maximilians-Universität München, LMU Biozentrum, Department Biologie I, Martinsried, Germany

WORD COUNT: 23615

REFERENCES NUMBER: 595

NUMBER OF GRAYSCALE ILLUSTRATIONS: 0

NUMBER OF COLOR ILLUSTRATION: 17 (online 17 and hardcopy 0)

“Reviewing Editors: Plamena Angelova, Monica Balsera, Maria Borisova-Mubarakshina, Christine Foyer, Christian Gruber, Jean-Pierre Jacquot, Robert Hancock and Thomas Kieselbach”

Addresses correspondence to:

Mirko Zaffagnini

Laboratory of Molecular Plant Physiology

Department of Pharmacy and Biotechnology

University of Bologna

Via Irnerio 42, 40126, Bologna (BO)

Italy

E-mail: mirko.zaffagnini3@unibo.it

Paolo Trost

Laboratory of Molecular Plant Physiology

Department of Pharmacy and Biotechnology

University of Bologna

Via Irnerio 42, 40126, Bologna (BO)

Italy

E-mail: paolo.trost@unibo.it

ABSTRACT

Redox homeostasis consists of an intricate network in which reactive molecular species (RMS), redox modifications and redox proteins act in concert to allow both physiological responses and adaptation to stress conditions. This review highlights established and novel thiol-based regulatory pathways underlying the functional facets and significance of redox biology in photosynthetic organisms. This cannot be all-encompassing, but is intended to provide a comprehensive overview on the structural/molecular mechanisms governing the most relevant thiol switching modifications with emphasis on the large genetic and functional diversity of redox controllers (*i.e.* redoxins). We also summarize the different proteomic-based approaches aimed at investigating the dynamics of redox modifications and the recent evidence that extends the possibility to monitor the cellular redox state *in vivo*. Lastly, the physiological relevance of redox transitions is discussed based on reverse genetic studies confirming the importance of redox homeostasis in plant growth, development, and stress responses.

I. INTRODUCTION

The research field of redox regulation and signaling in aerobic organisms, including humans and microbes, has received a great impetus from early studies conducted on plants. During the sixties and the seventies of the last century, a decade after the discovery of the photosynthetic CO₂ fixation cycle, now known as the Calvin-Benson (CB) cycle, it was observed that some CB cycle enzymes were activated in the light and inactivated in the dark, indicating that the CB cycle was temporally coupled to the light reactions of photosynthesis (397) (for a recent review see (339)). Light activation *in vivo* was first demonstrated for chloroplast glyceraldehyde-3-phosphate dehydrogenase (GAPDH) (13,595), and in the next years for phosphoribulokinase (PRK) (279), and the two phosphatases, namely fructose-1,6-bisphosphate phosphatase (FBPase) (23) and sedoheptulose-1,7-biphosphate phosphatase (SBPase) (12). A mechanistic explanation of these results was essentially provided by Bob Buchanan and collaborators (Peter Schürmann and Ricardo Wolosiuk *in primis*) in a series of papers that marked the birth of the plant redox field (57,58,455,457,538,540,541). Light activation of CB cycle enzymes was proposed to depend on a novel electron chain made by the interaction of three types of stromal proteins: ferredoxin (FDX, an iron-sulfur (Fe-S) protein, where electrons come in from photosystem I), FDX:thioredoxin reductase (FTR, a protein containing an Fe-S sulfur cluster functionally and physically connected with a disulfide) and thioredoxin (TRX), which also contains two cysteines (Cys) able to reversibly form a disulfide bond (Figure 1A). By means of this transduction chain, target enzymes are reduced and hence activated in the light (Figure 1B). In the absence of light, electrons were believed to return to oxygen leaving oxidized enzymes in the inactive form (456). Interestingly, at that time TRX was only known as a protein involved in ribonucleotide reduction in bacteria and the demonstration of its role in the regulation of chloroplast metabolism opened a wide array of possibilities for the development of redox biology concepts in all aerobic organisms (54). Once established the FDX-FTR-TRX system (hereafter named FDX-TRX system) in plants, new discoveries in the field were obtained in the following decades. By the end of the century the targets of the system approached the number of 25, including 4 enzymes and 2 regulatory proteins of the CB cycle (529,539,587), several other metabolic enzymes including NADP-malate dehydrogenase (NADP-MDH) (240,448) and glucose-6-phosphate

dehydrogenase (G6PDH), the latter remaining the prototypical example of enzymes that are inhibited, rather than activated, by disulfide reduction in plants (448). Moreover, the FDX-TRX system was found to be operative also in amyloplasts (non-photosynthetic plastids) where FDX is reduced by metabolically produced NADPH rather than by light (25). Knowledge on TRX diversity was limited to chloroplastic TRX *f* and *m*, with the addition of cytoplasmic TRX *h*, which can be reduced by NADPH:TRX reductase (NTR) using NADPH as electron donor (Figure 1B). The first structural studies on TRX regulated enzymes (FBPase and NADP-MDH) appeared in the late nineties providing nice explanations of how redox regulation could operate at the atomic level, at least in these proteins (55,286,339,456). NADP-MDH, in particular, constituted an interesting case. Its mechanism of regulation, based on C- and N-terminal extensions containing Cys pairs able to form internal disulfides under the control of TRXs, was found to be similar to other proteins like GAPDH (143) and CP12 (144). Another important achievement of the recent past was the ability to determine, *in vitro*, the redox potential of the different dithiol/disulfide interchange reactions (223), which allowed the development of hypotheses concerning the reciprocal influence between TRX and target proteins redox states *in vivo* (92,93,222,223,266,267,322).

Besides the chloroplast pathway for regulatory disulfides reduction, mechanisms of disulfides formation were also investigated. Current knowledge suggests that formation of regulatory disulfides in chloroplasts may involve particular types of TRXs (111,133,561) that shuttle electrons from reduced target proteins to 2-Cys peroxiredoxin (2-Cys PRX) and then to hydrogen peroxide (H₂O₂) (see section VII). These findings imply that H₂O₂, rather than oxygen, may be the terminal electron acceptor used for down-regulating the TRX-activated enzymes. This example nicely fits into the general concept, largely developed in the last decades, that the manifold interactions between reactive molecular species (RMS) and active protein thiols often play essential physiological roles. However, protein disulfides may also play structural rather than regulatory roles and the formation of structural disulfides is a compulsory step in the correct folding of several proteins. Systems controlling the oxidative protein folding generally rely on two types of proteins, isomerase and oxidase, forming an electron chain that connects the target protein (where the disulfide is formed) to the terminal acceptor (430). In plant cells, systems of this type are

present, at least, in the lumen of the endoplasmic reticulum (190), in the lumen of thylakoids (256) and in the intermembrane space of mitochondria (72). Different protein components and final electron acceptors are used in the different locations. For detailed analyses of oxidative protein folding in plants the reader might refer to other reviews that cover the subject (7,192,334,384).

At the end of the last century, redox regulation in plants was perceived as an established physiological mechanism somehow limited in scope, as it appeared to be essentially required for separating photosynthetic carbon fixation occurring in the light, from catabolic reactions occurring in the dark in the same organelle, thereby preventing dangerous futile cycles (54). Twenty years later the concept is still valid and strongly supported by experimental data, but the field of redox regulation in plants has witnessed an incredible expansion in many new directions. In this context, this comprehensive invited review tries to give the right credit to the recent explosion of thiol-based redox regulation and signaling studies in plants.

The review is organized in sections (section II-VII) focused on the topics that in our view represent most significantly the scientific developments achieved in the plant redox field in recent times. The section on redox biochemistry of protein thiols (section II) recognizes the recent transition from a redox biology dominated by TRXs and disulfides, to a more articulated subject that takes into consideration how reactive oxygen, nitrogen and sulfur species (ROS, RNS and RSS, respectively) may induce up to ten different post-translational modifications (PTMs) of protein Cys, in a complex interplay that involves also glutaredoxins (GRXs) and glutathione, besides classical TRXs. Section III witnesses the impressive development of redox proteomic techniques that occurs during the last two decades. Emphasis is given to the methodological principles and future technical developments in redox proteomics. To date, these approaches have already allowed the list of putative redox targets to include hundreds or thousands of members with different known redox PTMs on specifically identified Cys in different photosynthetic organisms. The biodiversity of plant TRXs and GRXs and their reducing systems is described in Section IV. Note that before the genomic revolution that in plants started with the sequencing of the genome of *Arabidopsis thaliana* in 2000, the different known TRXs could be counted on one hand and GRXs were almost unknown. With 20 classes of TRXs and 6 classes of GRXs, photosynthetic

organisms are now believed to contain a potential for redox regulation and signaling that seems to largely exceed that of non-photosynthetic organisms. The state of the art of the structure/function relationships studies in TRXs and GRXs, including their mechanisms of action and interactions with the targets is included in Section V. Section VI deals with the determination of redox couples *in vivo* by means of genetically encoded probes and fluorescence microscopy. This section witnesses the adaptation of green fluorescent probe (GFP)-based techniques in the redox field leading, for the first time, to dynamically determine redox states *in vivo*. Most of the section is dedicated to glutathione and the popular roGFP probes. Finally yet importantly, section VII shows that only recently the original model of redox regulation of chloroplast enzymes is receiving experimental confirmation by reverse genetic data. These experiments open the new avenue of redox plant physiology *in vivo*, including the role of redox regulatory systems in primary productivity, development and environmental adaptation.

II. REDOX BIOCHEMISTRY OF PROTEIN THIOLS

II.A. Production and detoxification of reactive molecular species (RMS) in plants and algae

Redox regulation mainly occurs through different types of PTMs of Cys residues that may occur either through dithiol-disulfide exchange reactions or through reactions in which particular proteins Cys are attacked by RMS. Biologically relevant RMS are based on oxygen (ROS), nitrogen (RNS) or sulfur (RSS), and plant cells may properly synthesize or accidentally release different RMS types by many different mechanisms, both under stress and non-stress conditions.

II.A.1. Reactive oxygen species (ROS)

Light reactions of photosynthesis constitute a fundamental source of ROS in plants. On the one hand, it is believed to be a consequence of the sessile nature of plants since ROS may be produced when the amount of energy obtained from light harvested by photosystems exceeds the combined capacity of downstream metabolic activities and heat dissipation mechanisms (112,123,442). On the other hand, ROS are signals that illuminated chloroplasts continuously produce, even in the absence of stress, as the energetic state of the photosynthetic electron transport (PET) chain is affected by varying environmental or metabolic conditions (184). ROS signals produced by altered states of the PET are involved

in controlling nuclear gene expression by chloroplast retrograde signaling, leading to long-term acclimation responses (184).

Photosynthesis can produce different types of ROS with different mechanisms (Figure 2). When light energy absorbed by chlorophylls is not rapidly dissipated, photo-excited chlorophylls in the triplet state accumulate in photosystems II and may generate singlet oxygen (1O_2) by interacting with molecular (triplet) oxygen (Figure 2) (148). This reaction is prevented in light-harvesting antennae where chlorophyll triplet states are quenched by xanthophyll-type carotenoids that dissipate the excitation energy as heat (442). Tocopherols and carotenoids provide a primary protection against the destructive action of 1O_2 , which primarily results in lipid peroxidation, but also oxidative modification of protein residues including Cys (137,270,391).

Photosystem I is also a potential source of ROS because it contains low potential Fe-S clusters that easily reduce molecular oxygen to the superoxide ion ($O_2^{\bullet-}$) (Figure 2), when downstream acceptors of the photosynthetic electron transport chain are limiting because they are already reduced. This condition notably arises when carbon fixation by the CB cycle is limited by partial activation of its light-dependent regulated enzymes or low CO_2 supply from the atmosphere due to stomata closure. Chloroplast superoxide dismutase (SOD) isoforms guarantee a rapid conversion of $O_2^{\bullet-}$ to H_2O_2 that ascorbate peroxidases (APXs), glutathione peroxidases-like (GPLXs), and PRXs may then reduce to water (Figure 2) (377). Ascorbate, glutathione, pyridine nucleotides, TRXs and their reductases, constitute an interlinked, powerful system of chloroplasts that tries to keep under control the unavoidable production of H_2O_2 during photosynthesis (155,377). Under particular conditions, H_2O_2 can react with ferrous ion leading to the formation of hydroxyl radical ($^{\bullet}OH$) (Figure 2), the most reactive and damaging ROS molecule.

Although iron-containing components of photosystem I are the major source of $O_2^{\bullet-}$ in chloroplasts in the so-called pseudocyclic electron transfer, photosynthetic oxygen reduction may also occur by other mechanisms. These include a long suspected role of the plastoquinone pool in generating ROS signals (524). However, it is still uncertain whether oxygen reduction might depend on the activity of the plastid terminal oxidase (365) or occur at the site of plastoquinone oxidation on cytochrome b_6f (31) or even result

from the direct reaction between the plastoquinone pool and oxygen or $O_2^{\bullet-}$ (516) (Figure 2).

Another important source of ROS is peroxysomal glycolate oxidase (GOX) that, in the photorespiratory pathway, generates H_2O_2 in stoichiometric amounts with the oxygenase activity of ribulose-1,5-bisphosphate carboxylase/oxygenase (RubisCO) (Figure 2). Given the relevant share of photorespiration on photosynthetic metabolism in C3 plants (up to half of carboxylation at 30 °C (594)), this is arguably one of the most important sources of ROS in green cells, at least in organisms with no CO_2 -concentrating mechanisms. Moreover, photorespiration of C3 plants is also another way by which photosynthesis unavoidably produces ROS independently from stress conditions (378). However, huge amounts of catalase (CAT), together with APXs, limit H_2O_2 from escaping peroxisomes (Figure 2) (337,377).

Similar to animal systems, mitochondria are also in plants a potential source of ROS (Figure 2) (230). Complexes I and III are able to transfer single electrons to oxygen thereby producing $O_2^{\bullet-}$, particularly under conditions of low ADP or low oxygen availability (358,418). Similar to chloroplasts, mitochondria contain SODs and H_2O_2 detoxifying systems relying on APXs, GPLXs, and PRXs (Figure 2).

Like H_2O_2 , also $O_2^{\bullet-}$ may be enzymatically produced in plant cells. NADPH-oxidases of the respiratory burst oxidase homolog (RBOH) family being probably the major source (Figure 2). A gene family of about ten members in higher plants encodes these NADPH-dependent flavo-cytochromes. Some of them at least reside at the plasma membrane and release $O_2^{\bullet-}$ in the apoplast in response to either abiotic or biotic stress and developmental processes (310). In *Arabidopsis*, RBOH is responsible for the oxidative burst triggered by incompatible pathogens. Together with nitric oxide ($^{\bullet}NO$), the resulting superoxide $O_2^{\bullet-}$ orchestrates the hypersensitive response against the pathogens (117). Interestingly, $^{\bullet}NO$ is also involved in a feedback loop that inhibits *Arabidopsis* RBOHD activity via S-nitrosylation of Cys-890 (570). Except for the presence of SOD and low concentrations of ascorbate, the apoplast is poor in antioxidant systems (19,157), suggesting that apoplastic H_2O_2 may accumulate more easily than in other cell compartments.

II.A.2. Reactive nitrogen species (RNS)

Sources of RNS in photosynthetic organisms are diverse and still not fully described. In land plants, reductive pathways converting nitrite (NO_2^-) to $\bullet\text{NO}$ seem to prevail over oxidative pathways that release $\bullet\text{NO}$ from arginine (Figure 2) (21). Nitrate reductase (NR) can slowly produce $\bullet\text{NO}$ by reducing NO_2^- , instead of its normal substrate nitrate (NO_3^-), using NADH as an electron donor. Since the affinity of NR for NO_3^- is higher than for NO_2^- , and since NO_3^- inhibits the reduction of NO_2^- , $\bullet\text{NO}$ production by NR is expected to be favored by stress conditions that lead to toxic nitrite accumulation (418). In any case, the role of NR in $\bullet\text{NO}$ production in *Arabidopsis* is supported by reverse genetic studies (21). Alternatively to NR, NO_2^- can be also reduced to $\bullet\text{NO}$ by components of the mitochondrial electron transport chain (complexes III and IV) (Figure 2) (196), particularly when oxygen is scarce. Recently, a complex involving NR and NO-forming nitrate reductase (NOFNiR) was shown to constitute a new $\bullet\text{NO}$ biosynthetic system in the green microalga *Chlamydomonas reinhardtii* (74). The role of NR in the complex is to transfer electrons from NAD(P)H to NOFNiR. Whether a similar complex also exists in land plants is currently unknown.

Oxidative pathways for $\bullet\text{NO}$ production from arginine seem to be operative in plants (Figure 2), but the proteins involved remain to be identified. An ortholog of animal NO synthases is found in the alga *Ostreococcus tauri* (151) but not in other algae and higher plants, where the oxidative release of $\bullet\text{NO}$ from arginine may involve distinct mechanisms (21).

Similar to biogenesis, regulation of intracellular $\bullet\text{NO}$ levels may also follow different pathways. Non-symbiotic hemoglobins convert $\bullet\text{NO}$ to NO_3^- (356), but as part of $\bullet\text{NO}$ in the cell is bound to GSH to form nitrosogluthathione (GSNO), the activity of GSNO reductase (GSNOR) which releases ammonia from GSNO (300,575) is potentially very relevant to modulate $\bullet\text{NO}$ availability and also the levels of GSNO, an important trans-nitrosylating agent (see section II.C.4.).

II.A.3. Reactive sulfur species (RSS)

In plants, hydrogen sulfide (H_2S) generation occurs through three pathways that differ in the underlying mechanisms and the subcellular compartments in which they take place. The primary source of H_2S is the chloroplast where it is produced in the reductive sulfate-assimilation pathway through the action of sulfite reductase (SiR, Figure 2) (488).

Alternative pathways occur in both mitochondria and cytoplasm. β -cyanoalanine synthase (CAS-C1), catalyzing the conversion of cyanide and Cys to β -cyanoalanine and H_2S , is found in mitochondria (Figure 2) (11). In the cytoplasm, the enzyme L-Cys desulfhydrase (DES1) catalyzes the desulfuration of Cys yielding sulfide, ammonia and pyruvate (Figure 2) (9,10,185). In any case, the production of H_2S in subcellular compartments where ROS or RNS may also be produced can result in non-enzymatic reactions, including the one-electron oxidation of H_2S to hydrogen disulfide (H_2S_2) (Figure 2), which may lead to persulfidation of protein Cys (see section II.C.5.).

II.B. Reactivity of cysteines is strictly controlled by the protein microenvironment

In plants, RMS (including ROS, RNS, and RSS) actively participate in redox homeostasis. In this context, proteins play an essential role as central mediators of RMS-dependent signaling events. Many of these proteins rely on modifications of Cys residues for modulating their redox activity whereas a few of them use other residues (*e.g.* methionines or tyrosines) for the same purpose, but knowledge on methionine- and tyrosine-dependent signaling pathways is still limited to a few studies (35,237,238,265,327).

Cys-based redox modifications have been extensively investigated and they are widely accepted to play a prominent role in regulatory and signaling networks that support plant development, metabolic functions, and responses to varying environmental conditions. The functionality of Cys residues in redox biology depends on the chemical reactivity and structural flexibility of their sulfur atom. Sulfur can form covalent bonds with different types of atoms present in living organisms (C, H, O, P, and N) and establish stable complexes with transition metals (Zn, Fe, and Cu). In addition, being weak acids, Cys thiols ($-SH$) are found in equilibrium with the deprotonated thiolate form ($-S^-$) over a physiological range of pH to flexibly optimize the function of specific protein Cys (Figure 3A). Compared to the protonated forms, Cys thiolates are more sensitive to the intracellular redox environment and susceptible to RMS-dependent oxidative modifications. Altogether, these features allow Cys residues to play fundamental structural and catalytic roles, and to function in RMS-mediated redox signaling as reversible molecular switches (321,508,537).

The acid dissociation constant (pK_a) of a Cys designates its tendency to dissociate. The pK_a of the sulfhydryl groups of free Cys is ~ 8.3 (395,434,502). A slightly higher pK_a value (8.8, (440)) is attributed to the Cys thiol of reduced glutathione (GSH). These pK_a values imply that these Cys thiols are largely found in the protonated form at neutral pH, while thiolate forms might progressively accumulate only at alkaline pH values. For example, the percentage of GSH thiolate (GS^-) at pH 7 is only 2%, but this value increase to 14% when the pH raises to 8. This variability is particularly important in subcellular compartments that experience a shift from neutral to slightly alkaline pH as observed in the chloroplast stroma during dark to light transitions (215,221,503).

Although the vast majority of protein Cys harbors a pK_a above 8, some of them are acidic due to the microenvironment in which they are located (395,508). Selected protein Cys involved in thiol switching reactions have pK_a values ranging between 3 and 6.5 (508), allowing these residues to be predominantly or fully deprotonated at physiological pH (Figure 3B). The structural features that contribute to modulate the acidity of Cys thiols mainly include the proximity of amino acids like lysine, histidine or arginine, that by attracting the proton of the thiol become positively charged and form an ion-pair with the negatively charged thiolate (Figure 3C) (96,508). These types of interactions are found in enzymes such as GAPDH (36,576), isocitrate lyase (ICL) (37) and PRXs (368). In other proteins, hydrogen-bonding networks may also be relevant (Figure 3C); in TRXs and GRXs, for instance, the hydrogen-bonding network is believed to be the major structural determinant of the acidity of the catalytic Cys (434). Finally, the location of the Cys residue at the N-terminus of an α -helix generating an electric macrodipole may also contribute to its acidity (Figure 3C) and, in general, desolvation can also have an impact on thiol pK_a by decreasing the dielectric constant of water and thus enhancing electrostatic interactions that occur in catalytic sites (146). In many other cases, the relative influence of each structural factor to the thiol pK_a is still undefined and difficult to derive from the protein tridimensional structure, such that it needs to be determined experimentally (508).

Although thiolates are stronger nucleophiles than thiols, it should be remembered that the nucleophilicity of a thiolate actually decreases with decreasing pK_a of the Cys. In other words, the most reactive Cys are often Cys that are acidic enough to be largely deprotonated at neutral pH, but not too acidic to loose completely their nucleophilicity

(146,508). Moreover, the protein microenvironment affects the reaction between Cys and RMS also in other ways, not directly dependent on Cys pK_a .

The H_2O_2 -dependent oxidation of Cys thiolate nicely exemplifies this latter point. By comparing the reactivity towards H_2O_2 of two thiolate-containing proteins, namely PRX and GAPDH (pK_a values of ~ 5 and ~ 6 , respectively), it was observed that PRX reacts with H_2O_2 10^4 - 10^5 times faster than GAPDH (508,536). Since the catalytic Cys of both PRX and GAPDH are fully or almost fully deprotonated at neutral pH, other factors than thiolate availability and exposure should be taken into account to explain the vastly different reactivity. Indeed, the stabilization of the transition state ($-S\cdots O\cdots O\cdots H$) by active-site residues was recently proposed to sustain the catalytic power of PRX (207,362). A counter example is given by GRX S12, that contains a highly acidic catalytic Cys (pK_a value < 4.0 ; (102,573)) but exhibits a reactivity towards H_2O_2 that is comparable to GAPDH ($pK_a \sim 6$; (508,573,576)). Based on these observations, we can conclude that although oxidation mainly affect acidic Cys, the Cys microenvironment can control the reaction kinetics with H_2O_2 and possibly other RMS, as detailed in the following subsections.

II.C. Cys residues may be modified in many different ways by RMS or enzymes

The cellular capacity for RMS-mediated regulatory pathways depends on different types of Cys modifications that allow oxidant signals to be transduced into biological responses. In the following subsections, the chemistry and mechanisms of oxidative modifications induced by each class of RMS molecules, namely ROS, RNS and RSS, are discussed. Alternative mechanisms of protein Cys oxidation catalyzed by enzymatic systems or mediated by intermediate Cys oxoforms (*i.e.* sulfenic acids and nitrosothiols) or oxidant molecules (*e.g.* oxidized glutathione, GSSG) are also described.

II.C.1. ROS-dependent redox modifications of protein thiols

Protein Cys thiol can be oxidized by both radical ($O_2^{\bullet-}$, $\bullet OH$) and non-radical ROS molecules (1O_2 , H_2O_2). Singlet oxygen is a non-radical molecule that can react with sulfur-containing amino acids (*i.e.* Cys and methionine) but also with histidine, tryptophan and tyrosine residues (391). The oxidation of Cys thiols by 1O_2 occurs *via* formation of a short-lived zwitterionic intermediate ($RS^+(H)-OO^-$) which decomposes yielding oxidized sulfur species such as sulfonic acids ($-SO_3H$) or alternatively, disulfides if another Cys residues is able to react with the initial intermediate (Figure 4) (360,391). Although 1O_2 is believed to play a

signaling role in chloroplasts (276), the molecular bases of its action are not fully understood.

The radical superoxide ($O_2^{\bullet-}$) is a relatively unreactive radical and its preferential targets appear to be other radical species such as $\bullet NO$ (395). In proteins, $O_2^{\bullet-}$ can react with Fe-S clusters and some transition metals (113,537), and shows low reactivity towards protein side chains, Cys being one of the less sensitive amino acids (113). However, if this reaction occurs, Cys may undergo cysteinyl (thiyl) radical ($-S^{\bullet}$) formation and possibly peroxidation (*i.e.* thiol peroxide formation) (Figure 4) (169,454). In contrast to $O_2^{\bullet-}$, $\bullet OH$ is highly reactive and is capable to oxidize nearly all protein residues with second order rate constants near the diffusion limit (*i.e.* 10^9 – $10^{10} M^{-1}s^{-1}$) (113). Protein Cys oxidation mediated by $\bullet OH$ is postulated to occur through hydrogen atom abstraction from S–H bonds yielding thiyl radicals ($-S^{\bullet}$, Figure 4) (15,113,477,519).

The aforementioned reactions are likely to occur under physiological conditions but their relevance in thiol-based redox signaling networks might be limited. These ROS molecules (1O_2 , $O_2^{\bullet-}$, $\bullet OH$) have high reactivity with biological macromolecules other than proteins. The abundance of these targets *in vivo* results in very short lifetimes and limited diffusion from the sites of generation. Therefore, oxidation by these ROS is restricted to proteins located at the proximity of production sites. In addition, they react with diverse protein side chains and display no specificity for reactive Cys.

Among ROS, H_2O_2 has the longest lifetime and is highly selective towards sulfur-containing residues, Cys thiolates being the most sensitive (226,395,453). The H_2O_2 -dependent two-electron oxidation of reactive Cys leads to the formation of a sulfenic acid ($-SOH$) (Figure 4). Sulfenic acids are emerging as redox signaling hubs implicated in different types of secondary modifications. Owing to their reactive nature, sulfenic acids are often considered as an unstable intermediate subjected to several alternative fates (Figure 4). In the presence of excess H_2O_2 , sulfenic acids can act as a nucleophile and be further oxidized to sulfinic ($-SO_2H$) and sulfonic acid ($-SO_3H$) (Figure 4), with reaction rates that are generally slower (0.1 – $10^2 M^{-1}s^{-1}$) than the primary oxidation event (10 – $10^7 M^{-1}s^{-1}$) (395,508). Sulfinic and sulfonic acids are usually considered irreversible forms except for sulfinated 2-Cys PRX (PRX- SO_2H), which can be reversibly reduced to the thiol form by sulfiredoxin (243). Sulfenic acids can alternatively serve as electrophiles reacting with the

backbone amide group of a neighboring residue forming a reversible cyclic sulfenamide or condensate with an interfacing additional sulfenic acid to generate a thiosulfinate (Figure 4). In most cases, however, sulfenic acids react with a proximal thiol from a protein Cys or a GSH (Figure 4) leading to the formation of intra/inter-molecular disulfide bonds (–S–S–) or a mixed-disulfide (–S–SG, S-glutathionylation). Besides protein Cys, H₂O₂ can also react with GSH yielding glutathione sulfenate intermediates (GSOH) but, owing to its pK_a, this reaction proceeds very slowly ($\sim 1 \text{ M}^{-1}\text{s}^{-1}$) (395).

II.C.2. Plant cysteine oxidases catalyze the enzymatic oxidation of protein cysteines to sulfinic acids

Besides protein disulfides, other oxidative modifications are found to be catalyzed by specific enzymes. Indeed, Cys oxidation to sulfinic acids can occur in the presence of plant Cys oxidases (PCOs). These enzymes are nonheme Fe²⁺-dependent dioxygenases catalyzing an essential step of the N-end rule pathway in plants that controls, for example, the stability of group VII ethylene response factors (ERF-VIIs). Whereas ERF-VIIs are rapidly degraded in normoxia, flooding-induced hypoxic conditions reduce the activity of PCOs allowing ERF-VIIs stabilization and consequently transcriptional adaptive responses (509,531,533). The molecular mechanisms underlying PCO activity have been recently established and Cys sulfinic acids are generated via an oxygen-dependent reaction (532,533). Besides oxygen, ROS and likely $\bullet\text{NO}$ are postulated to be involved in such reactions but the mechanisms are still not clarified (418).

II.C.3. RNS-dependent redox modifications of protein thiols

In biological systems, $\bullet\text{NO}$ and derived compounds (*i.e.* nitric dioxide ($\bullet\text{NO}_2$), dinitrogen trioxide (N₂O₃), and ONOO⁻) can also induce oxidative modifications of protein residues including Cys thiols (Figure 5). Similar to O₂^{-•}, $\bullet\text{NO}$ is a relatively unreactive radical and preferentially reacts with other radical species and with metals. By reacting with O₂^{-•}, $\bullet\text{NO}$ generates ONOO⁻. Besides binding to heme-containing proteins (395), $\bullet\text{NO}$ is involved in a covalent modification of protein Cys termed S-nitrosylation (575). This reversible modification does not directly involve $\bullet\text{NO}$ and three major mechanisms have been proposed to account for S-nitrosothiol (–SNO) formation (575). The reaction of $\bullet\text{NO}$ with transition metals of metalloproteins yields unstable metal-nitroxyl complexes that can then transfer the NO moiety to a Cys residue that generally belongs to the same protein

16

(Figure 5). Alternatively, $\bullet\text{NO}_2$, which is spontaneously generated by the reaction of $\bullet\text{NO}$ with molecular oxygen, can induce the one-electron oxidation of Cys thiolates (Figure 5). This reaction leads to the formation of thiyl radicals that can undergo radical-radical combination with $\bullet\text{NO}$ to yield S-nitrosothiols. S-nitrosothiols formation can also be generated by the nitrosating compound N_2O_3 that is spontaneously formed by the radical reaction between $\bullet\text{NO}$ and $\bullet\text{NO}_2$ (107,395). N_2O_3 can subsequently transfer its nitrosonium group (^+NO) to proteins or low-molecular weight thiolates generating S-nitrosothiols and releasing NO_2^- .

Due to its high intracellular concentration (1-5 mM, (156,373,440)) GSH might be a primary target of N_2O_3 -dependent nitrosylation yielding GSNO (Figure 6). This molecule along with S-nitrosylated proteins can transfer the NO moiety to another Cys in a process termed trans-nitrosylation (Figure 5). Within cells, the equilibrium between GSH and GSNO controls the level of S-nitrosylation in some proteins at least (Figure 6) (43,580). TRXs efficiently reduce GSNO *in vitro* ((369); Zaffagnini et al., personal communication) and catalyze protein denitrosylation of specific targets *in vivo* (262). However, TRX-dependent reduction of GSNO or protein-SNO releases a nitroxyl (HNO) that is highly reactive and still able to interact with Cys residues (49). To date, the foremost enzyme known to control the intracellular concentration of GSNO is GSNOR (300,575) (see Section II.C.4.).

The sensitivity of a particular Cys thiolate to trans-nitrosylation seems to depend on different factors including Cys reactivity, the accessibility to NO donors and the local Cys microenvironment (e.g. acid-base motif and hydrophobic residues) (129,153,304,320,469,579). In general, trans-nitrosylation is considered not only as a prominent mechanism of protein S-nitrosylation but also as a mechanism that allows propagating the NO signal far away from the site of $\bullet\text{NO}$ production (395). Compared to sulfenic acids, nitrosothiols cannot further react with oxidants but can generate sulfenic acids by spontaneous hydrolysis (Figure 5) or alternatively, form disulfides in the presence of protein or GSH thiolates (Figure 5).

Peroxynitrite (ONOO^-) and its protonated form (ONOOH) are highly reactive non-radical species that can cause oxidation of several protein residues including Cys, methionine, tryptophan and tyrosine. The most relevant peroxynitrite-mediated reaction is tyrosine nitration but its physiological relevance in signaling pathways still requires further

confirmation. Similar to $\bullet\text{OH}$, the reaction of ONOO^- with protein Cys yields thiyl radicals (Figure 5) (113,486) but other oxidation products such as sulfenic acids are also generated (Figure 5) (584).

II.C.4. GSNO reductase controls the level of nitrosothiols in plants

GSH can efficiently reduce protein S-nitrosothiols (181,433,575). However, although this non-enzymatic reaction restores reduced proteins, it also generates GSNO (Figure 6), which can further react with reactive Cys thiols yielding *de novo* S-nitrosothiols (97,575). Consequently, GSH by acting as an efficient reducing system can also promote further S-nitrosylation *via* GSNO. To date, the foremost enzyme known to control the intracellular concentration of GSNO is GSNOR (300,551,575). This enzyme is highly conserved in most bacteria and all eukaryotes including plants (303). GSNOR belongs to the class III alcohol dehydrogenase family and catalyzes the reduction of GSNO using NADH as an electron donor (268,271,303). The effective contribution of GSNOR in degrading GSNO relies on its catalytic ability to reduce GSNO into glutathione sulfenamide (GSNH_2), which spontaneously forms GSSG and NH_3 in the presence of GSH (Figure 6). Consequently, GSNOR acts as a specific scavenging system for GSNO and indirectly controls the extent of GSNO-dependent protein S-nitrosylation.

In plants, the role of GSNOR in S-nitrosothiols metabolism was demonstrated by Loake and colleagues (139). *Arabidopsis* mutants that do not express GSNOR (*gsnor*) have more low molecular weight nitrosothiols (*e.g.* GSNO) and high-molecular weight nitrosothiols (*e.g.* S-nitrosylated proteins). The function of GSNOR was also associated to various physiological processes including pathogen response, thermotolerance, plant growth, flowering, hypocotyl elongation and germination, and resistance to cell death. Whether these effects are also mediated by S-nitrosylation, however, still need to be clearly established (139,272,281,300,443).

The activity of plant GSNOR itself has been recently reported to be altered by redox modifications (Figure 6). *Arabidopsis* and poplar GSNOR were found to undergo S-nitrosylation *in vivo* under conditions of increased endogenous NO availability (83,162). Intriguingly, this modification causes partial inhibition of GSNOR activity (162,193). More recently, AtGSNOR was also found to be negatively affected by *in vitro* treatment with H_2O_2 or exposure of *Arabidopsis* plants to paraquat (268). Altogether, these evidences

suggest that the transient inhibition of plant GSNOR by oxidative modifications might reinforce NO signaling by favoring GSNO accumulation (193,268,300).

II.C.5. RSS-dependent redox modifications of protein thiols

The prototypical inorganic RSS is H₂S, which is the most stable RMS with a half-life in the minute time-scale (485). Based on its chemical properties (pK_{a1} = 7 and pK_{a2} = 12-15; (80,343)), H₂S can easily dissociate under physiological conditions and it is therefore assumed that H₂S pools mainly include H₂S and HS⁻. In plants, the involvement of H₂S as a signaling molecule is receiving growing attention because of its ability to interact with proteins and possibly with other RMS (16,17,79). Given its nucleophilic properties, H₂S can scavenge reactive intermediates including [•]NO, O₂^{-•}, ONOO⁻, or H₂O₂, suggesting that it can play protective effects against oxidative stress (249,534). However, a biological relevance for this activity is largely speculative because of its limited reactivity compared to GSH and its intracellular concentration, which is considered low (174,249,485). With proteins, H₂S can interact with some heme groups but also with Cys residues in a process called persulfidation. This oxidative modification consists in the conversion of a protein Cys into a persulfide (-S-SH) and it is suggested to modulate protein functions (259,361,392,393) by increasing the nucleophilicity of the Cys (106,392). Noteworthy, this reaction can involve both Cys thiolates and oxidatively-modified Cys intermediates like sulfenic acids (395). Although persulfidation has been proposed as a new key player in redox signaling, the underlying mechanisms are poorly understood and the physiological relevance of H₂S-related mechanisms in plants is still largely unknown.

Three major mechanisms for protein persulfidation have been postulated (Figure 7), none of which involves a direct reaction between H₂S and Cys residues (249,505). The first two mechanisms involve a nucleophilic attack of H₂S on oxidized protein Cys, either present as sulfenic acid or engaged in disulfide bonds (*i.e.* intra/inter or mixed disulfide) (Figure 7). However, disulfide-mediated persulfide formation is uncertain mainly because H₂S is a poor reductant compared to GSH and this reaction may proceed very slowly *in vivo* (70,395). Another possibility is that alternative intermediate Cys oxoforms (*e.g.* S-nitrosothiols or sulfenylamides) can react with H₂S yielding persulfides. The third mechanism involves the ROS-mediated oxidation of H₂S to H₂S_n (n=2 or higher) which can

subsequently undergo a nucleophilic attack by a protein thiolate to give rise to a persulfide (Figure 7).

Similar to nitrosothiols and sulfenic acids, persulfides contain two electrophilic centers and can react with another protein thiol yielding a disulfide or facilitating trans-persulfidation (Figure 7). The latter route is reminiscent to trans-nitrosylation and is likely to be highly protein specific (395).

II.C.6. S-glutathionylation as a special type of disulfide formation

Disulfide bond formation is the best-characterized Cys-based redox modification. It consists in the covalent bonding between two Cys residues belonging to the same or different polypeptides. Besides the well-known role of TRXs in dithiol-disulfide interchange reactions (see Introduction) (Figure 8A), disulfide formation may also involve RMS. One possible route relies on the primary oxidation of a Cys to sulfenic acid or S-nitrosothiol, followed by thiol condensation with an additional Cys (Figure 8A; see paragraphs I.3.1 and I.3.3, respectively).

Protein S-glutathionylation has emerged as a widespread oxidative modification involved in the modulation of protein function but also in the protection of protein Cys from irreversible oxidation (*i.e.* sulfinic and sulfonic acid formation) (572,574). As already mentioned, one potential mechanism of protein S-glutathionylation is the condensation of GSH with an intermediately oxidized Cys (*i.e.* sulfenic acid or S-nitrosothiol; see sections II.C.1 and II.C.3, respectively). The electrophilic nature of these oxidative intermediates favor the nucleophilic attack of GSH thiolates leading to the formation of protein mixed-disulfides (Figure 8B).

Another mechanism of protein S-glutathionylation involves a thiol-disulfide exchange between GSSG and a protein Cys thiolate (Figure 8B). Typically, this reaction proceeds very slowly and is supposed to be thermodynamically prevented by the high GSH/GSSG ratios of most plant subcellular compartments (see Section VI) (155,157,458). Nevertheless, we cannot exclude *a priori* the possibility that specific proteins might undergo GSSG-dependent glutathionylation being highly sensitive to limited fluctuations of the glutathione redox pool. Plastidial GRXS12 for instance is glutathionylated *in vitro* at GSH/GSSG ratios of 10^2 – 10^3 that fully prevent the glutathionylation of other targets like cytoplasmic GAPDH (36,573).

As an alternative to GSSG, protein glutathionylation can occur in the presence of GSNO (Figure 8B). This molecule can allow the formation of S-nitrosothiols but can also transfer its GS-moiety to a target Cys. The structural features controlling one reaction over another are still uncertain and are likely related to the local environment surrounding the target Cys residue. GRXS12 is an example of a protein that is glutathionylated by GSNO, rather than nitrosylated (573).

Finally, in addition to non-enzymatic mechanisms, protein glutathionylation might also be catalyzed by specific oxidoreductases (Figure 8B). This was shown for human GRX2 that appears to promote protein S-glutathionylation following a reaction mediated by either GSSG or GS[•] radical (38,163). Both mechanisms rely on the formation of glutathionyl-GRX intermediates and the ability of GRX to transfer the glutathionyl-adduct to an acceptor protein thiolate in a trans-glutathionylation reaction. To date, no evidence suggests the ability of plant GRXs to catalyze such reactions *in vivo*. However, a remarkable example of enzyme-assisted glutathionylation occurring in plants involves the genetically encoded probe roGFP2 fused to human GRX1 (GRX1-roGFP2; (333,458)). This chimeric protein has been developed to monitor the glutathione redox state and its functioning is specifically related to reversible trans-glutathionylation reactions between the probe and GRX1.

III. REDOX PROTEOMICS: METHODOLOGICAL PRINCIPLES AND FUTURE DEVELOPMENTS IN THE PLANT FIELD

Despite the latest improvements of mass spectrometry (MS) in terms of sensitivity and resolution over the last decade, direct analysis of redox-modified proteins remains highly challenging. As shown in Figure 9 (see also Section II), more than ten thiol-based redox PTMs are currently known (101,182,395). Due to their lability, their low stoichiometry and their possible interchange during sample processing as exemplified in Figure 9 (black and gray boxes corresponding to primary and secondary modifications), the redox proteomics field has to face different biochemical, methodological and instrumental challenges to get insights about the *in vivo* dynamics of redox PTMs. In complex systems, redox proteomic strategies currently rely on the differential labeling of Cys according to their modification state followed by MS analyses at the peptide level after an affinity enrichment step.

Non-targeted quantitative strategies, such as OxICAT (283,470) and OxiTMT (474) were developed to determine oxidation levels of hundreds of Cys upon oxidative treatments. To

date, these approaches have been applied to quantitatively identify oxidative-prone Cys in the marine diatom *P. tricornutum* (436) and the cyanobacteria *Synechocystis* sp. PCC 6803 (194). In this latter organism, 20 to 40% of proteins were found to contain oxidized Cys in the dark. Nevertheless, these strategies are unable to distinguish which reversible redox PTM is at the origin of the modification of the Cys. In this section, we will focus on approaches trapping selectively the different reversible redox PTMs with a special emphasis on their advantages, drawbacks and limitations, and their use in photosynthetic organisms.

III.A. Thioredoxome

Two main proteomic strategies have been employed to identify hundreds of proteins containing disulfide bonds reduced by TRX (56,299). The first and most common approach takes advantage of the ability of a monocysteinic TRX variant (Figure 10), where the C-terminal active site Cys is replaced by serine or alanine, to covalently bind oxidized target proteins (for the mechanism, see Section V). The monocysteinic TRX is most often grafted on a chromatographic resin and TRX-bound targets are eluted with a chemical reductant like dithiothreitol (DTT). This type of column has been applied to numerous protein extracts from the cyanobacterium *Synechocystis* sp. PCC 6803 (298,402,404) and also different photosynthetic eukaryotes (6,24,27,28,32,187,208,227,285,317,319,353,543,552,565). This approach has several drawbacks. First, it lacks specificity as several TRX classes (*f*, *m*, *y*, *h*) immobilized to the resin retain the same targets while they have distinct specificities in solution at more diluted conditions (see Section IV). This may be due to the high concentration of TRX or to peculiar properties of the monocysteinic variants (339). Moreover, depending on the washing conditions, proteins interacting with TRX targets may be eluted together with genuine TRX targets thereby increasing false-positive rates. Nevertheless, the major drawback of the column approach is that it only identifies the target protein whereas the exact Cys targeted by TRX remains unknown.

The second main strategy, named “reductome” approach, is based on the *in vitro* reconstitution of the enzymatic TRX system (NADPH, NADPH:TRX reductase and TRX) within a cell-free protein extract followed by labeling of newly exposed Cys with fluorescent (311,559), radioactive (318) or biotinylated probes (317) (Figure 10). This

strategy was applied to total or subcellular soluble protein extracts from different land plants (6,26,27,208,311,312,325,542,543,558). Biotinylated tags allow enrichment of Cys-containing peptides by affinity purification and allow identification of TRX-targeted Cys, a major advantage of the reductome approach. Unfortunately, to increase the number and diversity of targets, the *in vitro* reduction has to be performed using relatively high TRX concentration for which isoform specificity is mostly lost. Therefore, the lack of specificity is common to both the affinity column and reductome approaches. The two approaches are complementary as the targets identified only partially overlap (317,405,543).

Recently, quantitative adaptations of the reductome approach were developed for MS analyses based on chemical labeling with cleavable Isotope-Coded Affinity Tag reagents (cICAT) (205,206) or with Cys-reactive Tandem Mass Tag (Cys-TMT) (588). The most recent study combined the column with the quantitative reductome approach to investigate the thioredoxome of the unicellular green alga *Chlamydomonas reinhardtii* and identified 1188 proteins and 1052 Cys regulated by TRX. The quantitative approach based on differential cICAT labeling allowed to decrease false positives by filtering out the noise due to incomplete thiol blocking of the protein extract and thereby retain only proteins that are effectively reduced by TRX (405). Nevertheless, the targets identified remain putative and the presence of a TRX-reduced disulfide bond needs to be confirmed experimentally. Some TRXs were also shown to function, on specific targets, as denitrosylase (41,42,46,487) and deglutathionylase (36,189,482). However, such activities should not impact the identification of TRX targets in both approaches as the vast majority of nitrosylated proteins are denitrosylated by GSH rather than TRX (44,388,433,580), and TRX targets were analyzed in conditions where S-nitrosylation and S-glutathionylation are limited or absent (350,571). Moreover, the reduction of S-nitrosylated or S-glutathionylated proteins by monocysteine TRX is considered to yield nitrosylated or glutathionylated TRX rather than mixed disulfide with the target (36,262,405). Finally, both the proteomic identification of already established TRX targets and the biochemical confirmation of targets previously identified by proteomics strongly support the reliability of proteomic approaches to identify TRX targets. Biochemically confirmed TRX targets previously identified by proteomic studies include at least 2-Cys PRX (187,353), phosphoglycerate kinase (349) magnesium chelatase CHLI subunit (232), β -amylase 1 (478), methionine

sulfoxide reductases (494,517), glucan water dikinase (342), uricase (130), and cytosolic NAD-MDH (212).

III.B. Nitrosylome

The identification and the quantification of S-nitrosothiols and S-nitrosylated proteins in biological samples remain highly challenging due to the lability of the –SNO bond (242) whose stability is strongly influenced by multiple factors including light, metals and reducing compounds such as GSH or TRXs. Such an instability of S-nitrosothiols precludes their direct detection by matrix-assisted laser desorption-ionization (MALDI) MS (250) and even by electrospray (ESI) MS (211) unless ionization parameters are carefully optimized (525). Therefore, high throughput analysis of nitrosylated proteins is based on indirect methods for which the NO moiety is replaced by a more stable tag that allows an enrichment step.

Most studies rely on the Biotin Switch Technique (BST) developed in 2001 (241) which was the first approach allowing detection and identification of S-nitrosylated proteins at the proteome scale (Figure 10). This method consists in the replacement of the NO moiety of S-nitrosylated Cys residues by a disulfide-bonded biotin tag in a three step process: (i) initial blocking of unmodified Cys thiols under denaturing conditions; (ii) “specific” reduction of –SNOs by ascorbate; (iii) labeling of the nascent thiols with the biotinylating reagent N-[6-(biotinamido)hexyl]-3'-(2'-pyridyldithio)-propionamide (Biotin-HPDP). The replacement of the –SNO moiety by a disulfide bonded biotin tag allows detection of previously S-nitrosylated proteins by immunoblotting or purification by avidin-based affinity chromatography and DTT elution for MS-based identification (301). Many variants of the original BST approach have been proposed such as the –SNO site identification (SNOSID) approach which includes a trypsin digestion step before enrichment (210) or the –SNO resin-assisted capture (SNO-RAC) method which takes advantage of a thiol-reactive resin for capturing nascent thiols after ascorbate reduction (Figure 10) (152). The two methods allow identification of both the modified proteins and the modified Cys. The BST was applied to a wide range of photosynthetic organisms (reviewed in (269,420,463,575)) and allowed identifying nitrosylated proteins in different organs and subcellular compartments (73,385,389,463), in mutant lines (229,296), and in plants exposed to exogenous NO donors (301,350,389) or affected by biotic (20,432) or abiotic stresses

(1,64,136,217,296,421,462,463,491,492,512). The most extensive studies identified 492 proteins and 392 sites in *Chlamydomonas reinhardtii* cells subjected to a 15 minutes GSNO treatment (350) and 926 proteins and 1195 sites in *Arabidopsis* Col-0 and KO mutants for GSNOR (*gsnor1-3* lines; (229)).

Despite its popularity, BST is a very difficult technique with inherent limitations and biases that are not sufficiently taken into account. A major drawback relies in the identification of false positives due to incomplete blocking and loss of targets due to spontaneous denitrosylation during sample handling. Moreover, the specificity of the ascorbate-dependent reduction step is difficult to establish unambiguously toward either disulfide bonds (105), or byproducts of reactions of classical thiol blocking agents with other species such as sulfenic acids (426). Overall, the signal to noise ratio is low and variable due to differences in biological material, growth conditions, experimental design, sample handling, instrument setup, and bioinformatic data analysis. This strongly decreases the reproducibility and sensitivity of the method.

Several quantitative BST approaches allowing quantification of nitrosylation levels have been proposed. They are based on the combination of BST with chemical labeling strategies such as ICAT or related molecules (136,167,388,421), Cys-TMT (359), iodo-TMT (422) or isobaric tag for relative and absolute quantification (iTRAQ) using the SNO-RAC method (152), stable isotope labeling with amino acids in cell culture (SILAC) (593) or label-free spectral counting (589). Such quantitative approaches will certainly improve the confidence into data generated by BST-based studies and allow uncoupling protein levels from nitrosylation levels. We believe that a method more reliable than BST is probably required for analysis nitrosylation at a dynamic level. More direct and promising approaches based on direct capture of S-nitrosocysteine residues have been proposed but need further confirmation of their potential for quantitative proteomic studies (129,135,520).

III.C. Glutathionylome

Proteomic analysis of S-glutathionylated proteins has been initially performed using radiolabeling of the glutathione pool in cell cultures in the presence of ³⁵S-cysteine and protein synthesis inhibitors (Figure 10). Radiolabeled proteins are visualized by fluorography after separation on 2D gels. The spots disappearing in the presence of

reducing agent, which correspond to S-glutathionylated proteins, are then identified by MS. Originally developed for human cells (160), this method allowed identification of 25 proteins in *Chlamydomonas reinhardtii* (340) but proved unsuccessful in *Arabidopsis* due to low levels of radiolabeling (126). This method has numerous drawbacks: (i) the protein synthesis inhibitors perturb cell physiology; (ii) this method cannot distinguish S-glutathionylated proteins (protein-SSG) from other forms of S-thiolation such as S-cysteinylation; (iii) it is limited by the necessity to perform 2D gels; (iv) it can only be used with cell cultures, thereby precluding studies on whole plants, (v) it can only detect proteins undergoing glutathionylation during treatment excluding proteins already glutathionylated under basal conditions, and (vi) finally it precludes high-throughput identification of glutathionylated sites.

An alternative method is based on biotinylated glutathione (BioGSH/BioGSSG) or the membrane permeant biotinylated glutathione ethyl ester (BioGEE) (Figure 10). The presence of the biotin tag allows detection of S-glutathionylated proteins by immunoblotting or enrichment by affinity chromatography. The latter can be coupled to MS for identification of not only S-glutathionylated proteins but also S-glutathionylated Cys if proteins are trypsin-digested before enrichment, as in the SNOSID approach (see paragraph II.2). The major drawback of such methods is that proteins are not S-glutathionylated by the cellular GSH itself but by an exogenous, sterically different molecule. The presence of the biotin tag on the glutathione molecule might perturb the function of glutathione-dependent enzymes and especially GRXs (Zaffagnini et al., personal communication). Another drawback, shared with the ³⁵S labeling method, is that proteins glutathionylated under basal conditions are not detected. Originally used in mammals (483), this approach allowed identification of more than 70 S-glutathionylated proteins in *Arabidopsis* (126,236), 225 proteins and 56 S-glutathionylation sites in *Chlamydomonas* (571) and 349 proteins and 145 sites in *Synechocystis* sp. PCC 6803 (76).

Several additional methods have been employed but not yet used in photosynthetic organisms. Commercial anti-glutathione antibodies which can be useful for analysis of isolated proteins lack specificity and sensitivity, precluding application for high-throughput proteomics. S-glutathionylation can also be studied using an adaptation of the BST where the reduction step is performed with GRXs instead of ascorbate (Figure 10)

(175,209,253,297). This approach has roughly the same drawbacks as the BST. In addition, the blocking of free thiols under denaturing conditions is difficult to combine with the enzymatic reduction of S-glutathionylated proteins by the GRX system (NADPH, glutathione reductase, GRX; see Section V) that has to be performed in the absence of detergents.

Overall, despite the fact that S-glutathionylation is more stable than S-nitrosylation, the methods currently employed have numerous caveats and drawbacks and the development of new approaches is most probably required for proteome-wide quantitative analysis of glutathionylation. A “chemobiology” approach based on click chemistry (417) may be possible since biosynthesis of a click analogue of glutathione seems experimentally feasible (141,254,445,446). Such approaches have proven very efficient for proteomic analysis of S-palmitoylation (323,592), N-myristoylation (545) or glycosylation (292,496).

III.D. Sulfenylome

Proteomic analysis of sulfenic acids follows two major strategies that are based on either chemical or genetically encoded probes (4,413,554). Current chemical probes are mostly based on 1,3-carbonyl scaffold such as the cyclic dimedone (5,5-dimethyl-1,3-cyclohexanedione) (198,424). At physiological pH, dimedone is in equilibrium with its enolic form which itself performs a nucleophilic attack on sulfenic acid. Dimedone tagged peptides can be detected by MS and due to the generated mass increase, the involved Cys can be easily characterized. Nevertheless, dimedone has limited application for complex samples as it lacks a functional group for enrichment. Therefore, molecules harboring a dimedone conjugated with a fluorescent tag (DCP-Rho and DCP-FL series) or a biotin tag (DCP-Bio series) have been developed (Figure 10) (77,415). These probes have proven efficient but the presence of a bulky tag may alter cell permeability or prevent interaction with sulfenic acids that are not fully solvent accessible (413,466).

Recently, small biorthogonal probes derived from dimedone have been developed such as DAz-1/DAz-2 (289) and DYn-1/DYn-2 (396). These probes can be biotinylated through click chemistry allowing enrichment of sulfenylated peptides. Used at lower concentrations than the classical dimedone, they are non-toxic and do not influence the intracellular redox balance (396,555). Analysis of sulfenylated Cys with dimedone-based probes is compatible with classical quantitative MS-based strategies such as iTRAQ or TMT, which

introduce reporter tags on tryptic peptides. Another way consists in synthesizing light and heavy isotope-coded forms of DYn-2 (556). Such a strategy allowed identification, in human cells, of 1000 sulfenylated Cys in 700 proteins (555). Despite their selectivity, these probes suffer from poor reaction kinetics under physiological conditions compared to biological reactions of sulfenic acids (197). New probes with faster reaction rates are therefore being considered to further expand our ability to monitor the sulfenome (198,199,302,416). Biotinylated strained bicyclo[6.1.0]nonyne derivatives appear promising tools as they show reaction rates two orders of magnitude higher than dimedone even at low concentrations (μM range) (416).

The second approach is based on the yeast transcription factor Yap-1 which naturally interacts with the sulfenic acid formed on the Orp1 protein through formation of a transient mixed-disulfide (Figure 10) (116,544). An engineered monocysteinic His-tagged version of Yap1 has been developed and shown to covalently trap sulfenylated proteins in *E. coli* (489) and *S. cerevisiae* (490). The major advantage of this type of probe is that their reaction kinetics is, at least theoretically, faster than dimedone-based chemical probes (4). Moreover, since they are genetically encoded they can be controlled through genetic circuits and can be targeted to explore the sulfenylome of diverse subcellular compartments. Yap1-based methods also have several drawbacks including a low efficiency that may be linked to *in vivo* reduction of Yap1-target mixed disulfides and, a selectivity-bias due to the Yap1-protein backbone and its steric effects.

In photosynthetic organisms, few studies addressed the question of the sulfenylated proteome *in vivo*. A combination of DCP-Bio and Yap1 probe allowed identification of 91 proteins in *Medicago truncatula* and 20 in its symbiont *Sinorhizobium meliloti* (381). More recently, the YAP1 probe was combined with a tandem affinity purification tag to detect 97 sulfenylated proteins in *Arabidopsis* cell suspensions under H_2O_2 stress (527). The DYn-2 probe was also recently employed in *Arabidopsis* and allowed identification of 226 sulfenylated proteins (3). Interestingly, a low overlap (17%) was observed between the two *Arabidopsis* sulfenylomes obtained by the same groups suggesting that both approaches are highly complementary.

III.E. Persulfidome

Persulfides exhibit a reactivity similar to thiols rendering their analysis at a proteome scale challenging. Some BST-based proteomic strategies aiming at unravelling persulfidation in complex samples have been recently developed. In the pioneering method, free thiols are blocked by methyl methanethiosulfonate (MMTS) whereas unblocked persulfides are subsequently biotinylated by HPDP-Biotin before enrichment by avidin-based affinity chromatography (361). Nevertheless, the assumed selectivity of the strong thiol-alkylating agent MMTS is questionable as it was shown to react indifferently with thiols and persulfides (390). Another approach combines initial blocking of all free thiols and persulfides with N-ethyl maleimide (NEM), DTT reduction and labeling of nascent thiols with NEM-biotin (511). This strategy should be used with care as many proteins can undergo multiple DTT-reducible redox PTMs (186,405).

A more innovative proteomic approach, called Tag-switch, allows persulfide biotinylation without the use of any reductant (585). In this strategy, both thiols and persulfides are first blocked with the alkylating reagent methylsulfonyl benzothiazole (MSBT) but only the activated disulfide bond of MSBT-derivatized persulfides are able to react in a second step with the biotinylated electrophile methyl cyanoacetate (Figure 10). After enrichment using avidin-based affinity purification, persulfidated proteins are eluted under non-selective denaturing conditions that may lead to contaminations with proteins tightly bound to avidin such as endogenously biotinylated proteins. Another issue is linked to the selectivity of the Tag-switch approach as methyl cyanoacetate can cross-react with other forms of protein oxidations (sulfenic acid, sulfenylamide, carbonyls) (585).

The last strategy recently developed consists in the direct alkylation of persulfidated proteins with biotinylated cysteine alkylating reagents (127,165). In this case, both persulfides and thiol groups are indiscriminately biotinylated and persulfidated proteins retained on avidin affinity columns are specifically eluted in the presence of DTT. Nevertheless, to avoid that true persulfidated proteins remain linked to the column due to the presence of other biotinylated surface-exposed cysteines in their sequence, low concentration (50 μ M range) of biotinylated alkylating reagents should be employed as these conditions are known to promote alkylation of hyper-reactive thiols such as persulfides and thiolates rather than thiols (165,530). The persulfide site identification

approach, which is equivalent to the SNOSID approach, circumvents these pitfalls by identifying persulfidated peptides and thus cysteines instead of proteins (165). Moreover, it remains compatible with classical quantitative MS techniques to compare persulfidomes (307).

In photosynthetic organisms, data about protein persulfidation are limited. Only two studies attempted to characterize the persulfidome in the model plant *A. thaliana*. By using either the pioneering approach (17) or the Tag-switch assay (16), these studies allowed the identification of 106 and 2015 persulfidated proteins, respectively. These proteins are localized in different subcellular compartments but mainly reside in chloroplasts and cytoplasm (65%) and are involved in a wide variety of pathways and processes suggesting that persulfidation may be an important thiol switching mechanism as other redox PTMs in photosynthetic organisms.

III.F. The Cys proteome: a complex dynamic network

Before the advent of omics strategies, research in cell signaling has been conducted using ingenious analytical approaches. It is becoming clear now that proteomes are so intricate that we cannot understand the cellular functional organization using only a reductionist approach studying a limited number of cellular components. This is especially relevant for redox signaling which coordinate large numbers of redox elements involved in a multitude of pathways and cellular processes to allow resistance and adaptation to environmental challenges (182). This Cys proteome can be considered as an interface between the functional genome and the external environment (183). This highly dynamic network probably involves spatial and temporal regulation of multiple interconnected redox PTMs on hundreds of protein thiols with flexible reactivities (395,414,530). Therefore, global approaches are required to fully understand the entire molecular complexity of redox signaling pathways and their links with numerous pathophysiological features. Among global approaches, MS-based strategies have benefited lately from tremendous technological improvements, and are now ready to face the challenge of comprehensive and quantitative proteomic approaches at the level of protein expression, protein interactions or PTMs (372).

Combinations of multiple redox PTMs act as a cellular network rather than as insulated elements. Understanding the organization of these networks will require to unravel the

determinants of the specificity of the diverse redox PTMs for proteins and Cys. Indeed, it remains unclear whether multiple redox PTMs occur on a limited number of proteins containing reactive Cys or if each modification targets a distinct redox network. Recently, the identity of redox-modified Cys belonging to proteins undergoing at least two different redox PTMs (among targets of TRX, S-glutathionylation and S-nitrosylation) were compared in *Chlamydomonas* (405). This analysis revealed that 86% of these cysteines were modified by only one type of redox modification. This comparison indicates, on one hand, that the Cys proteome does not represent a subset of highly reactive cysteines that are modified indiscriminately and highlights, on the other hand, a strikingly high specificity of each modification for distinct Cys residues (405). A similar high specificity with a limited overlap between Cys targeted by multiple PTMs was also reported in human and mouse (186,289). These results indicate that the Cys proteome does not represent a small subset of highly reactive Cys that are modified through indiscriminate interaction with the molecules they encounter but represent a complex system of redox PTMs that are specific toward distinct interconnected protein networks (405).

The complexity of the network likely provides the robustness and specificity required to allow simple molecules such as ROS, RNS and RSS to play a signaling role. This redox network is presumably a major component of signal integration and constitutes the molecular signature of the ROS/RNS/RSS crosstalk whose importance in cell signaling has been recognized (158,161,191,347,471).

Understanding this complex network will require to determine the stoichiometry and dynamics of multiple redox PTMs under diverse physiological conditions or in different genetic backgrounds, and at different time scales. This should be favored in the future by the development of sensitive and accurate redox quantitative MS approaches combined with the development of new chemospecific probe molecules (554). These chemical probes will have to (i) be specific for a given modification with no interference with other biological molecules, (ii) be compatible with quantitative MS, (iii) be non-toxic and membrane permeable to allow *in situ* or *in vivo* labeling, (iv) be highly sensitive to allow detection of low abundant proteins or low levels of modifications, (v) allow efficient enrichment methods using *e.g.* click chemistry, and (vi) exhibit fast reaction rates compatible with the half-life and reactivity of the species studied. New types of

modifications may also become amenable to proteomic analysis with the development of new probes such as NO-Bio, a recent biotin-tagged probe for proteomic analysis of sulfinic acids (306). Future redox proteomic studies will have to take advantage of isotope-coded multiplex reagents such as tandem mass tags to monitor multiple modifications or multiple samples simultaneously. Progress in the sensitivity of MS instruments and proteomic methods will allow analyses on limited amounts of biological samples and thus foster the development of single cell redox proteomic approaches to decipher the redox signaling network rather than unravel averaged redox signals from multiple cells. In other words, temporal quantitative redox proteomics on limited number of cells is certainly the grail that will allow us to discriminate redox modifications events from noise and thus shed light on the functioning of the redox network.

In addition, computational structural genomic approaches will be required to integrate the Cys proteome at the structural level. Finally, besides redox PTMs, the integration of the signal implicates a myriad of other molecules and processes acting at multiple levels (326). In photosynthetic organisms, several redox PTMs are linked to signaling pathways controlled by hormones (140,262,497,522,528,567) or calcium (506) and in mammals, nitrosylation was shown to interfere with signaling processes mediated by phosphorylation, ubiquitylation, sumoylation, acetylation or palmitoylation (214). Therefore, a strong effort is required to integrate redox networks with other signaling pathways and to analyze their impacts on the cellular responses at multiple levels. This will certainly be crucial to unravel how environmental challenges are encoded into a biochemical signal than can be exploited to trigger the appropriate responses in terms of localization, duration and intensity, at the genome, transcriptome, proteome and metabolome level to allow adaptation and survival.

IV. THE REMARKABLE DIVERSITY OF REDOXINS IN PHOTOSYNTHETIC ORGANISMS

IV.A. A general introduction on plant TRX superfamily (redoxins)

The TRX superfamily encompasses several protein families (notably TRXs, GRXs, protein disulfide isomerases (PDI) and glutathione-S-transferases (GSTs)), the members of which have in common a specific structural arrangement named the TRX fold (see Section V) and often a typical XCXXC/S signature containing the redox active Cys pair.

The number of PDI genes found in plant genomes is comparable to the one in mammals and higher than the one in fungi (465). For the TRX, GRX and GST gene families, algae and terrestrial plants have an expanded number of representatives, which is explained in part by the existence of additional classes (87,100,274,286,287,336). Hence, in the next subsections, we will focus our attention on the remarkable diversity found in TRX and GRX families, describing their subcellular distribution and how comparative genomics led to a rather exhaustive and refined classification of these genes/proteins and to a better understanding of their evolution.

IV.B. Classification and evolution of redoxins and their reductases

TRXs and GRXs were initially defined by quite strict signatures *e.g.* WC[G/P]PC and YCP[F/Y]C respectively, but the sequencing of numerous genomes pointed to the existence of a large variety of other combinations. These variations are usually still compatible with an oxidoreductase activity, although some are associated with the capacity to bind Fe-S clusters as observed initially for GRXC1 which possesses a slightly divergent YCGYC active site signature and then with several other GRXs (441). In the PDI family, the majority of plant isoforms possess a WCGHC signature, but variations also appeared in some representatives (465). There is no such universal signature for GSTs and actually only a very few of them have conserved both Cys. An important number has even lost the first catalytic Cys that has been replaced by a serine. This has led to a change in the type of activity catalyzed by GSTs. Those that kept the catalytic Cys have glutathione-removing activities whereas those possessing a serine have glutathione-conjugating activities, this residue serving for the activation of the thiol group of the glutathione molecule. Besides, GSTs have a particular structural arrangement with the existence of an all-helical domain fused at the C-terminus of the TRX domain. We invite the reader to refer to the following reviews for detailed information about phylogenomic analyses of PDIs (287,465) and GSTs possessing the catalytic Cys (274). From now, this section will uniquely focus on the TRX and GRX systems that primarily control the RMS-dependent PTMs of protein Cys.

IV.B.1. Phylogenetic and sequence diversity within the TRX and TRX reductase families

The TRX family is split into 21 well-defined classes including the NADPH-TRX reductase C (NTRC) fusion proteins that contain a TRX domain and a TRX reductase domain (Table 1 and Figure 11). Some TRX family members can unequivocally be distinguished by the

active site signature and domain organization. Typical TRX isoforms (TRX *f*, *m*, *x*, *y*, *z*, *o*, and *h* classes) are formed by a single domain with regular WCGPC or WCPPC active site signatures corresponding to the one found in ancestral TRXs (Figure 11). In addition, there are larger proteins that contain either two or more TRX domains (chloroplast drought-induced stress protein of 32 kDa, CDSP32 or nucleoredoxins, NRX) or a TRX domain fused to a domain with other functions (TRX reductase domain in NTRC, tetratricopeptide repeat domain in tetratricopeptide domain-containing TRXs (TDXs) (Figure 11). The active site signatures of the TRX domain(s) are also usually regular or with little variations. In CDSP32, the first domain has lost the Cys whereas the signature of the C-terminal domain is of the HCGPC type (Figure 11). Among NRXs, three groups can be distinguished. In NRX1 and NRX3 members, both TRX domains have generally WCGPC or WCPPC active site signatures whereas in NRX2 members, only the C-terminal domain conserved the Cys and the consensus signature has significantly diverged being of the [W/R]C[L/A]P[C/G] form (Figure 11). The C-terminal TRX domains in NTRC and TDX have a TCGPC and WCGPC signature, respectively (Figure 11). Finally, there are atypical TRXs formed by a single domain and divergent active site motifs: CLOT (WCPDC), HCF164 (WCEVC), TRX-like1 (most often WCRVC), TRX-like2 (WCRKC), TRX-lilium1 (GCGGC), TRX-lilium2 (WC[G/A]SC), TRX-lilium3 (SCGSC), TRX *s* (no conserved signature) and TRX CxxS (often WC[M/I]PS) which are included in the TRX *h* class (Figure 11). Lilium-type TRXs are also known as atypical Cys histidine-rich TRXs (ACHT, (110,111,133)) because they contain several conserved Cys and histidine residues outside the active site. These chloroplast atypical TRXs are proposed to play a role in the inactivation of light-activated redox targets (see Section VII). It is worth mentioning that HCF164 possesses an N-terminal anchoring domain to the thylakoid membrane (Figure 11). The TRX *s* class is not presented in Table 1 because it is only found in some *leguminosae*. There are four members in *Medicago truncatula* (428) and they likely possess specific functions for the establishment of symbiotic interactions between plants and bacteria of the rhizobia genus. Interestingly, the TRX *s1* is secreted into the microsymbiont although it seems that it derived from plastidial TRX *m* (428). Therefore, it may be that the plastid targeting sequence evolved into a secretory signal.

When considering two angiosperms, the dicot *Arabidopsis thaliana* and the monocot *Oryza sativa*; a lycophyte, the fern *Selaginella moellendorffii*; a bryophyte, the moss

Physcomitrella patens; a green alga, *Chlamydomonas reinhardtii* and a cyanobacterium, *Synechocystis* sp. PCC 6803, the minimal TRX equipment in photosynthetic organisms, as found in this cyanobacterium and conserved in all other organisms, appears to be formed by 4 members belonging to the HCF164, TRX *m*, TRX *x*, and TRX *y* types (Table 1) (87). This number increases to 20 in *C. reinhardtii* with the appearance of TRX *f*, *h*, *o*, *z*, CDSP32, CLOT, TRX-like, TRX-lilium, NRX and NTRC. Another increase occurred in terrestrial plants, both non-vascular (mosses) and vascular (ferns and angiosperms) ones. So far, in land plants, the lowest and highest numbers of reported TRXs have been found in *S. moellendorffii* (22 isoforms, Table 1) and in *Eucalyptus grandis* (45 isoforms) (412). This rise is mostly linked to duplications within existing classes, as the sole innovation specific to angiosperms is the TDX class that contains one or two members. These substantial differences in the TRX content among terrestrial plants are appealing although some cautions may be needed for recent, automatically annotated genomes.

Why the evolution positively selected complexity in the plant TRX system (on average in the human genome one TRX-coding gene is found for every 10,000 protein-coding genes versus 1350 protein-coding genes in *Arabidopsis*) is unknown. Reasonably more than a single evolutionary cause has contributed to positive selection. In fact, it is generally accepted that in plants several physiological processes are under the control of the TRX-mediated redox mechanisms. Whether as a result of the sessile lifestyle of photosynthetic organisms or due to the greater permissiveness to genome doubling events as well as arising from the existence of three evolutionary distinct genomes (nuclear, mitochondrial and plastid genome) inside a cell, plant TRX system is indeed more complex and versatile than that of prokaryotes (*e.g.* bacteria) and heterotrophic organisms (*e.g.* animal and fungi).

On the contrary, there are only minimal variations concerning the TRX reductases (TRs) along the green lineage (Table 1). The FTR is composed by a catalytic and a variable subunit (Figure 12), which is, by definition, difficult to identify based on sequence homology. Hence, concentrating on the FTR catalytic subunit, all analyzed genomes contain a single gene except *P. patens* which has two (Table 1). Concerning NTRs, there is usually a single NTRC isoform and 1 to 2 NTRA/B members (Table 1, Figure 11 and Figure 12). A large number of NTRA/B genes (six) is found in the genome of *Quercus robur* but the

same caution as before applies for this first assembled genome version (412). One particularity is the presence of a mammalian-type NAPDH-TRX reductase in some green algae such as *C. reinhardtii* (239). These are remnant selenoproteins common to many eukaryotes but not terrestrial plants, since they lost the system for selenocysteine insertion.

The subcellular localization of most *Arabidopsis* TRXs and TRs has been determined experimentally. The mitochondrion is likely the less rich compartment containing only TRXs *o* and a TRX *h2* in some organisms as poplar and *Arabidopsis* (172,275,330). They should be maintained reduced via NTRA or NTRB, both isoforms having been detected although NTRB may be more abundant (425). Both TRXs *o1* and *o2* show double localization, the former in mitochondria and nucleus, the latter in mitochondria and cytoplasm (118,171). Both NTRA/B are also found in the cytoplasm whereas NTRA may also be in the nucleus (316,425). In these compartments, they might reduce a certain number of cytoplasmic TRXs (Clot, TRX-like 1, TRX *h1*, *h3* to *h8*, TRX CxxS1, TDX) and nuclear proteins (NRX1, NRX2 and NRX3) (85,316) but also some membrane-bound TRXs (TRX *h9*, TRX CxxS2) owing to the existence of N-terminal glycine and Cys residues promoting membrane anchoring through N-myristoylation and palmitoylation, respectively (330,507). The employed reduction system has not been validated for all of them but TRX CxxS and TRX *h9* (or TRX *h4* in poplar) use a GSH/GRX system (173,264,330). Besides, a myristoylated glycine in *A. thaliana* TRX *h7* and TRX *h8* promotes their attachment to the ER/Golgi endomembrane system (507). An orthologous tobacco TRX *h* is secreted which raises the question of its reduction (247).

The chloroplast possesses by far the largest TRX equipment. In *A. thaliana*, there are 20 TRXs taking into account NTRC (52,61,92,110,288,330,468). All regular/typical TRXs (*i.e.* TRX *m*, *f*, *x*, *y*, *z*) are reduced by FTR (87,564) and some of them, such as TRX *z*, may be reduced by NTRC as well (563). It is not yet clear how CDSP32 is recycled upon oxidation whereas poplar TRX-Like 2.1 and TRX-Lilium2 were shown to be reduced by a GSH system (85). ACHT1/4 were proposed to be reduced by TRX-regulated ADP-glucose pyrophosphorylase, thereby contributing to its downregulation (133) (see Section VII). HCF164 is attached to thylakoids, likely facing the luminal side (288) and would relay the

reducing equivalents from stromal TRXs into the lumen (352), where proteins regulated by disulfide formation are present (475).

As far as their reducing activity is concerned, TRX *m* and *f* reduce disulfides on several metabolic targets, including enzymes of the CB cycle, oxidative pentose phosphate pathway, starch metabolism, ATP synthase and malate valve (68,92,200,349,367,478-480). TRX *x* and *y*, together with CDSP32 and ACHT1/4 are more specific for antioxidant enzymes, *e.g.* PRXs and methionine sulfoxide reductases (93,111,124,147,164,225,494,495).

IV.B.2. Phylogenetic and sequence diversity within the GRX family

The GRX family can be split into six classes (see below for further details; Figure 13). Class I and II are shared by eukaryotes and cyanobacteria (Table 1). Class III and IV are specific to eukaryotes (Table 1 and Figure 13). Classes V and VI to cyanobacteria though they are not present in *Synechocystis* sp. PCC 6803 (Table 1 and Figure 13). Therefore, both photosynthetic eukaryotes and cyanobacteria contain GRXs belonging to up to four classes (eukaryotes: class I, II, III, IV; cyanobacteria: class I, II, V, VI). As for the TRX family, members of these GRX classes differ notably by their active site signature and domain organization (Figure 13). The nomenclature established previously using *A. thaliana* members relies on the presence of a Cys or a serine at the last position of the active site signature (439). Therefore, they were named from GRXC1 to C14 and from GRXS1 to S17 albeit AtGRXS13 possesses a CPLG motif and at the time, the two class IV members (see below) were not included. The presence of a residue different from Cys or serine at the last position is also observed in a limited number of GRX members in some other species (*e.g.* *Oryza sativa* or *Sorghum bicolor*).

Except for the specific case of the PRX-GRX fusion proteins found in some cyanobacteria, class I GRX isoforms (GRXC1-C5, GRXS12 and cyanobacterial GRX I) are formed by a single domain with a quite regular YC[P/S/G][Y/F]C active site signature with some exceptions as GRXC5 (WCSYC) and GRXS12 (WCSYS) (Figure 13). The phylogenetic analysis reveals that cyanobacterial and algal GRXs form independent clades whereas terrestrial plants can be further divided into GRXC1/C2, GRXC3/C4 and GRXC5/S12 subgroups (Figure 13), and these subgroups also differ in their biochemical and redox properties (100-102,104,573).

Only two class I isoforms are found in model non-photosynthetic organisms such as *E. coli* and *H. sapiens*, but four in *S. cerevisiae*.

The class II GRXs are typified by their extremely conserved CGFS signature. They can be also further divided into four subclasses (GRXS14, S15, S16 and S17) in eukaryotic photosynthetic organisms according in particular to the existence of multidomain proteins whereas cyanobacterial GRX II isoforms systematically grouped independently (Figure 13). The GRXS14 and S15 members are only formed by a single GRX domain, as are cyanobacterial orthologs (Figure 13). The GRXS16 and S17 have a modular organization (Figure 13). The former possesses an N-terminal domain with some similarity with a certain type of endonuclease and the latter is formed by an N-terminal TRX-like domain with a distorted active site signature fused to one to three GRX domains. It is extremely interesting to point out how the GRXS17 fusion appeared and evolved during evolution. Indeed, haptophytes such as *Emiliania huxleyi* have isoforms with only one GRX domain, heterokonts and green algae with two GRX domains, sequenced mosses (*P. patens* and *Sphagnum fallax*), liverwort (*Marchantia polymorpha*) and fern (*S. moellendorffii*) possesses isoforms with two and/or three GRX domains, and gymnosperms (*Picea abies*) and angiosperms have isoforms with three GRX domains (100). Since GRXS16 prototypes are specific to the green lineage, only one to three class II isoforms are found in model non-photosynthetic organisms, one in *E. coli*, three in *S. cerevisiae* and two in *H. sapiens*.

The class III GRXs are characterized by the presence of two adjacent Cys forming CCxC, CCxS or CCxG signatures (Figure 13). They are uniquely found in terrestrial plants, ranging from 2 isoforms in *P. patens* to 24 in *P. trichocarpa* (100,412). The expansion of class III GRXs in angiosperms occurred mainly through paleopolyploidy duplications shortly after the monocot-eudicot split (201) and then proceeded by species-specific duplication leading to the existence of multiple tandem duplication.

The class IV GRXs (also referred to as GRX-like) are only present in terrestrial plants and they are rarely represented by more than two isoforms in a given species. These proteins have a particular domain organization with the presence of a long N-terminal extension followed by a GRX domain with a quite divergent active site signature (though green algal ancestors have CPYC/CPHC motifs), and two additional domains with unknown function, named DEP (domain found in Dishweller, Egl10 and Pleckstrin) and DUF547 (domain of

unknown function 547) (Figure 13). There are in fact two clades, the first containing sequences with a NCRD[C/S] signature, the second comprising sequences with a GCE[E/D]C signature.

As mentioned above, the class V and VI GRXs are found uniquely in cyanobacteria but not in all of them. They are for instance absent in *Synechocystis* sp. PCC 6803 and thus not included in Table 1. On the contrary, a few species have both of them (100). Members of class V are formed by a GRX domain with a highly conserved CPWG followed by a C-terminal extension predicted to form three to five transmembrane domains (Figure 13). Members of class VI are formed by an N-terminal DUF296 domain, followed by a C-terminal GRX domain with a CPW[C/S] signature (Figure 13). From the presence of this DUF296 domain in proteins that contain AT-hook motifs and the conservation of metal-binding histidines, it is predicted that these proteins have DNA-binding properties.

When considering the same set of representative organisms as before, the basal common GRX equipment in photosynthetic organisms as found in *Synechocystis* sp. PCC 6803 is formed by three members, two belonging to the class I and one to the class II (Table 1). This number increases to seven in *C. reinhardtii* because of duplications occurring for class II GRXs and of the appearance of class IV GRXs (Table 1). Another increase occurred in non-vascular plants (mosses) and in ferns with further duplications occurring for class II GRXs and with the appearance of class III GRXs (Table 1). Finally, the class III GRX has strongly expanded in seed plants, from 9 in *Carica papaya* to 24 in *P. trichocarpa* (Figure 13) (201,412). To date, in terrestrial plants, the lowest and highest numbers of reported GRXs are found in *P. patens* (15 isoforms) and in *P. trichocarpa* (38 isoforms), respectively (Table 1) (412).

The subcellular localization of many poplar and *Arabidopsis* GRXs has been determined experimentally. First, it is important to point out that there might be a single GRX in mitochondria, which is the class II GRXS15 (30,351). This is extremely surprising because it has no or extremely poor oxidoreductase activity (39,351) while there is an intense GSH-dependent metabolism in this compartment suggesting that a catalyst of protein deglutathionylation is required. In chloroplasts, there are three GRXs in most photosynthetic organisms, GRXS12 (class I) and GRXS14 and S16 (class II) (30,104). A variation is observed in brassicaceae including *A. thaliana* due to existence of the close

GRXS12 paralog, GRXC5, and in algae, because they have only the two class II GRXs (102,104,284). It is again surprising that there is no class I GRX with regular GSH-dependent activity in algal plastids. The fourth class II GRX, GRXS17, is found both in the cytoplasm and in the nucleus as do GRXC1 and C2 and most class III GRXs (30,228,263,366,431,441,549,550,553). In fact, there are still some uncertainties about several class III GRXs, for which the targeting has not been experimentally verified or which have N-terminal extensions (104,439). Interestingly, GRXC3 and C4 have also short N-terminal extensions, which may represent either a signal peptide for secretion or a membrane-anchoring sequence.

In conclusion, the genomic and phylogenetic analyses indicate that the TRX and GRX families constitute a largely diversified group of proteins in plants with numerous plant-specific isoforms or classes, which appeared during evolution whereas this expansion/diversification did not occur in bacterial, fungal and animal kingdoms. Although this classification is quite robust, relying on the use of specific motifs for protein identification (for instance the presence of glutathione-binding residues in the case of the GRX family) (100), one could wonder whether all these proteins adopt a TRX fold and have oxidoreductase activity. Hence, having systematic activity and structural information for isoforms belonging to each class would be mandatory in assessing to which extent the electrostatic surfaces are crucial in determining the specificity of TRXs and GRXs towards their targets as proposed in the case of *E. coli* PAPS reductase (48). This may provide clues to refine the classification on an activity/structure basis. Besides and this is not detailed at all in previous paragraphs, the presence of extra-Cys residues in some specific GRXs or TRXs is known to interfere with their activity and recycling. To cite only two examples, some TRX *h* having an additional Cys at position 4 become dependent on GSH and GRX instead of NTR (264), and the glutathionylation of Cys67 of *A. thaliana* TRX *f1* inactivates the protein preventing its regeneration by FTR (338). Finally yet importantly, besides the punctual changes in key amino acids, many proteins have additional domains, the function of which is often not yet determined although it could considerably affect their localizations, protein-protein interactions or activities. It would be expected that these protein innovations modify for instance the set of partner proteins. In this regard, it is interesting to see the intricate relationship between class III GRXs and TGA transcription

factors, sustaining the role of these GRXs in plant stress response and development (notably floral development) (201).

V. STRUCTURES AND CATALYTIC MECHANISMS OF REDOXINS

V.A. The TRX-fold and the structural determinants of redoxin reactivity

The TRX fold, common to all TRXs and GRXs, is composed by a central core made by a four to five stranded mixed beta-sheet, flanked by three to four α -helices (Figure 14A and 14B). The residues forming the typical CXXC/S signature containing the catalytic Cys are positioned at the N-terminus of one of the α -helices. Another important structural feature of the TRX superfamily members is the presence of an invariant cis-Pro residue that is found about 40 amino acids on the C-terminal side of the CXXC/S motif and, in the tridimensional structures, faces the catalytic Cys in the active site. This fold was firstly identified in the crystal structure of oxidized *E. coli* TRX1 (224). Since then, several structures of TRXs and GRXs from different photosynthetic organisms have been solved (Table 2).

The catalytic site containing the redox active Cys is located in a hydrophobic region quite exposed to the solvent. The thiol group of the first Cys of the generic $C_NX_1X_2C_C/S$ signature (where C_N and C_C are the N-terminal and C-terminal Cys, respectively), is accessible and can easily react with disulfides or possibly other forms of oxidized thiols on the target proteins (Figure 14A and 14B). On the contrary, the thiol of the second Cys, substituted by serine in some GRX classes (see Section IV and Figure 13), is buried and surrounded by hydrophobic residues. The reactivity of the N-terminal Cys is mainly determined by the pK_a of its thiol group (see Section II) ranging from 4.0 to 5.0 in GRX (102,104,573) and from 6.3 to 7.1 in TRX ((434), Zaffagnini et al., personal communication), indicating partial or complete deprotonation of the N-terminal Cys at physiological pHs. In spite of their acidic Cys, neither TRX nor GRX are particularly prone to oxidation by H_2O_2 , confirming that other factors come into play in the thiolate to sulfenic acid conversion ((508,573), Zaffagnini et al., personal communication). On the other hand, the C-terminal active site Cys, which may be absent or not essential for activity in GRX, shows a pK_a that may even be higher than that of free Cys and therefore should be relatively unreactive ((88), Zaffagnini et al., personal communication). Nevertheless, the C-terminal Cys of TRX is involved in the thiol-disulfide exchange reaction. The mechanism proposed for *E. coli* TRX (89) predicts that a

buried and highly conserved aspartic residue (Asp26 in *E. coli* TRX) works as an acceptor for the proton released by the C-terminal thiol when it attacks the N-terminal Cys bonded with the target protein (see below) (65,329).

The low pK_a of the N-terminal Cys of both TRXs and GRXs is chiefly determined by a hydrogen bond network, whereas the contribution of the helix macrodipole is negligible (150,435). Crystallographic investigations showed that the N-terminal Cys thiolate is often stabilized by hydrogen bonds with residues belonging to the catalytic sequence $C_NX_1X_2C_C/S$. For example, in barley TRX *h1* (PDB ID 2VM1; (314)) the sulfur atom of the N-terminal Cys40 is involved in a double hydrogen bond with the sulfhydryl group and the backbone amide group of the C-terminal Cys (Cys43; Figure 14C). The lower pK_a value of the N-terminal Cys in GRX like *Arabidopsis* GRXC5 was explained by an additional, third H-bond with the backbone amide group of the X_2 residue, that further stabilizes the N-terminal thiolate (Figure 14D) (104). A similar hydrogen bond network could not be established in most TRX active sites due to the presence of a proline in the X_2 position (150).

V.B. TRX and GRX: mechanisms of disulfide reduction

Although the large superfamily of TRXs include members that do not appear to be redox active, TRXs and GRXs can be considered anyway typical reducing agents for disulfide bonds. The TRX system is older than the GRX system in evolutionary terms (171,335) and it is more efficient in reducing protein disulfides even under severe oxidative stress ensuring a reduced environment in the cell. On the other hand, GRXs are more versatile being able to reduce protein disulfides compensating if necessary TRXs, but also glutathione-mixed disulfides. Reduced GRXs are regenerated mainly by GSH and in a few cases by TRX reductases (*i.e.* FTR, NTR), depending on the redox potential and catalytic mechanism of the specific GRX (145,246,578). Instead, TRXs are mainly reduced by TRX reductases (FTR, NTR), but a small subgroup of plant TRXs *h* is uniquely reduced by the GSH/GRX system (see Section IV.B.1; (173,264,330)).

In the catalytic mechanism of TRXs, the exposed N-terminal Cys of the active site $C_NX_1X_2C_C$ signature performs a nucleophilic attack on the disulfide of the target protein forming a mixed disulfide bond with the target protein itself (Figure 15A). Then, the free C-terminal Cys becomes reactive (deprotonated) thanks to the proton accepting role of a conserved

nearby Asp and attacks the N-terminal sulfur atom involved in the mixed disulfide, generating oxidized TRXs and reduced target proteins (Figure 15A). The reaction is reversible and its equilibrium is determined by the redox potentials of both TRXs and target proteins (92,93,222,223,322,478-480). The midpoint redox potential of TRX *f* and *m* is about -290 mV at pH 7 (223,339) and several target proteins show midpoint redox potentials that differ from that of these TRXs by less than ± 30 mV (92,93,222,223,322,478-480), suggesting that fluctuations in TRX redox state may effectively translate in fluctuations of target protein redox states and *viceversa*. An exception to this general view is constituted by Liliu/ACHT atypical TRXs that possess redox potential about 50 mV less negative than typical TRX *f* or *m* (85,110). Indeed these TRXs have been proposed to shuttle electrons from reduced AGPase to 2-Cys PRX in the presence of H₂O₂, possibly constituting a pathway of downregulation of chloroplast starch biosynthesis under low-light intensity. A similar role of TRX in the oxidation of reduced chloroplast targets might be expected for TRX *y* that on one side is less reducing than TRX *f* and *m* (93), and on the other hand is a good reductant for 2-Cys PRX (93,124).

Though typical of TRXs, the dithiol oxidoreductase mechanism just described is also shared by some GRXs (166,578). Most GRXs, however, are specialized in protein deglutathionylation. In this reaction, the N-terminal catalytic Cys of GRXs attacks the disulfide of the glutathionylated protein, releases the reduced peptide and becomes itself glutathionylated (Figure 15B). Afterwards, a second GSH molecule reduces back the glutathionylated thiol of GRX (60,379) generating GSSG (Figure 15B), in turn reduced to GSH by NADPH and glutathione reductase (GR) all together forming the GSH/GRX reducing system (100,574). The C-terminal Cys of GRXs when present is not involved in this mechanism, which is therefore called monothiol mechanism. The monothiol mechanism requires a single Cys on GRX (the N-terminal of the active site signature) but two glutathione molecules, one bound to the target protein and one free (39). This mechanism may be used both by class I GRX with a single Cys in the active site or having also the second one (see Section IV.B.2.), although it is not part of the catalytic cycle. An example of GRX utilizing a monothiol mechanism for deglutathionylation is poplar GRXS12 found in chloroplasts with a WCSYS active site sequence, unique to plants (102,573).

Some GRXs such as GRX3 from *Chlamydomonas* (578) use instead a dithiol mechanism for deglutathionylation (Figure 15C). In this mechanism, the deglutathionylation of the target protein occurs like in the monothiol mechanism. However, the glutathionylated GRX is then deglutathionylated by a second protein Cys that generates an internal disulfide and releases the GSH (Figure 15C). Depending on the GRX isoform, the second Cys may or may not belong to the active site. The latter is the case of GRX3 from *Chlamydomonas*, a chloroplast class II GRX whose internal disulfide is very efficiently reduced by FTR, thus constituting a potential link between deglutathionylation and photosynthesis (335,578).

Unlike TRXs, some plant GRXs (GRXC1, GRXC5, GRXS14-S17) have been identified as Fe-S cluster binding proteins ligating [2Fe-2S] clusters (30,142,233,351,441). While the Fe-S clusters bound to class I GRXs (GRXC1 and GRXC5) may modulate GRX activity (the holoforms are inactive) under oxidative stress conditions for instance, class II GRX (GRXS14-S17) are involved in Fe-S cluster biosynthesis and assembly in specific cell compartments (103).

V.C. Structural basis of TRX/target interaction and specificity

A detailed comparison of the crystal structures of two plastidial TRXs from the same organism (spinach TRX *f* and TRX *m*) showed that in spite of a quite similar overall structure (rmsd 1.2 Å for 102 superimposed C_α atoms; (65)), they show a different distribution of charges around the active site, with TRX *f* being characterized by a positive region that is less prominent in TRX *m*. In addition, TRX *f* active site is more flexible and the Trp45, the residue preceding the N-terminal Cys, can adopt different conformations. It is plausible that these features contribute to the different specificities shown by these two TRXs toward their targets. Indeed, although many tested targets may be reduced *in vitro* by either TRX *f* or *m*, in some cases a strong specificity for TRX *f* was documented ((339) and references therein).

The crystal structure of TRX/target complexes provide further information on the interaction between plant TRXs and their targets. One study investigated the complex between barley TRX *h2* and barley alpha-amylase/subtilisin inhibitor (BASI) (313). The interface area between the two proteins is quite small (762 Å²). TRX *h2* recognizes the target by interacting with the exposed Cys (Cys148) with which it forms the mixed disulfide bond, and two preceding residues (Asp146, Trp147). This short peptide of BASI which is

solvent exposed and free of intermolecular contacts, forms van der Waals interactions and three backbone-backbone hydrogen bonds with two TRX residues (Met88 and Ala106) both belonging to loop regions. Therefore, the TRX *h2* active site portion (Trp45-Cys46-Gly47-Pro48) plus two additional segments (Ala87-Met88-Pro89 and Val104-Gly105-Ala106) form the so called “substrate recognition loop motif”, which is also conserved in several other TRXs, but also in some GSTs, few PDIs and different proteins as cytochrome c (313). A similar motif is also observed in the co-crystal structure of the *E. coli* 3'-phosphoadenosine-5'-phosphosulfate reductase covalently bound to *E. coli* TRX1 (78).

VI. GENETICALLY ENCODED SENSORS FOR DETECTION OF REDOX COUPLES *IN VIVO*

VI.A. Detection of RMS and antioxidants in plant cells

Biochemical techniques have been largely applied to study RMS and the redox status of the most important antioxidant pools in plant cells or tissues (375,376). In most cases, these are still the only methods available allowing analysis of the general redox state of antioxidant molecules like ascorbate and glutathione in whole tissues or subcellular compartments (157). Data on the subcellular concentrations of ascorbate and glutathione in plant tissues were also obtained by immunogold electron microscopy, a technique that cannot distinguish between reduced and oxidized forms (582,583). TRX isoforms, for which the subcellular distribution is usually known, were quantified by proteomic methods and their redox state under light and dark conditions examined by redox western blots (564). Unfortunately, in most cases biochemical assays require tissue homogenization which, on one side, may dramatically reduce the sensitivity of the analysis and, on the other, can introduce artefacts due to the sample manipulation. Since both RMS and antioxidants are unevenly distributed in different subcellular compartments, the meaning of biochemical determinations of concentrations and redox states in raw extracts is intrinsically limited, independently from the precision of the measurements.

To overcome these problems, in the last 15 years, biologists have started to use new *in vivo* technologies which rely on the use of genetically encoded sensors that enable a real-time monitoring of the dynamics of chemical species and redox couples (333,458). While this approach has greatly increased the precision and the flexibility of the measurements that can be performed *in vivo*, the availability of genetically encoded sensors is still

restricted to few chemical species and redox couples. Technical developments are urgently needed for expanding the palette of sensors to a larger number of redox compounds.

VI.B. Genetically encoded sensors for glutathione

In the redox field, the most commonly used genetically encoded sensors are RxYFP, roGFP1 and roGFP2 that are based on modified yellow (YFP) or green (GFP) fluorescent proteins (128,333,386,458). In these modified versions of the GFP- or YFP-based sensors, two Cys residues have been inserted in adjacent β -strands on the surface of the protein β -barrel making the protein able to make a disulfide in a cellular context (333,458). The Cys residues, being positioned in close proximity to the chromophore, can form a disulfide bond that causes a structural change influencing the light absorption and fluorescence of the sensor (Figure 16A).

To reveal the formation or reduction of the disulfide bond, it is required to perform a ratiometric imaging by dual and sequential excitation of the sensor, usually with violet (~405 nm) and blue (~488 nm) light (Figure 16A). The emitted fluorescence is then acquired in a 505-540 nm window. Specifically, the disulfide-induced structural change of the fluorescent sensor has the effect of changing the quantum yield (QY) of its two main absorption peaks with an opposite trend: the QY at 405 nm increases, whereas the QY at 488 nm decreases, hence leading to a ratiometric response. The ratio of the light emitted after excitation at 405 and 488 nm (briefly, the 488/405 nm ratio) provides a direct readout of disulfide bond formation in the sensor population. The higher the 488/405 nm ratio is, the higher the oxidation of the sensor (*i.e.* the percentage of sensor molecules bearing the disulfide). Most importantly, such ratio can be monitored in real time and *in vivo* with different grades of resolution depending on the system used for the acquisition (*e.g.* wide-field and confocal microscopy or a fluorescent-based plate reader).

The field of application of the system depends on whether the sensor *in vivo* equilibrates with one or more redox couples such that it can be used to measure the redox state of these couples. The sensors of the roGFP family show midpoint redox potentials (E^0_{roGFP}) between -260 and -290 mV and are proposed to provide an accurate determination of the redox potential of glutathione (E_{GSH}) *in vivo* (331,387,459). This implies that glutathione is assumed to equilibrate with the sensor *in vivo*. Since the midpoint redox potential of glutathione is less negative (E^0_{GSH} -240 mV), the roGFP sensors are intrinsically more

adapted to measure highly reduced than oxidized glutathione redox states. Moreover, since GSH dimerizes upon oxidation ($\text{GSSG} + 2 \text{e}^- + 2\text{H}^+ \rightarrow 2 \text{GSH}$), the E_{GSH} depends on the $[\text{GSH}]^2/[\text{GSSG}]$ ratio. In other words, it depends on both the GSH/GSSG ratio and the total concentration of GSH plus GSSG. Therefore, glutathione redox potentials estimated by the roGFP cannot be translated into GSH/GSSG ratios unless the total concentration of GSH+GSSG is known (157).

Key advantages of the ratiometric nature of these sensors are manifold. First, the sensor readout is largely independent on their concentration in the cell. Second, the ratiometric feature of the sensors allows for the correction of focus changes or moving artefacts when samples are imaged by microscopy. Third, by using different promoters, they can be specifically expressed in different tissues and engineered for their targeting to different subcellular compartments or to modify their properties. Considering all these features, these redox genetically encoded sensors have been shown to be suitable for deriving information on redox conditions prevailing in the cell in different plant species, different cell types as well as different subcellular compartments.

Concerns about the specificity of the roGFP for glutathione have long been debated. Peroxidases like yeast Orp1 and mammalian GPX4 appear to oxidize roGFP2 directly in response to H_2O_2 in HeLa cells, suggesting that the roGFP redox state may be influenced by other factors than glutathione (203). In fact, roGFP is not oxidized by H_2O_2 *in vitro* but is rapidly oxidized by H_2O_2 *in vivo*. Whether this effect is mediated by glutathione or peroxidases is difficult to tell. Anyway, even if different compounds obviously influence the roGFP redox state *in vivo* it is still possible that roGFP and glutathione reciprocally equilibrate under any condition. As briefly discussed below, experimental evidence acquired so far supports this hypothesis.

The first work reporting the expression of a redox sensor in plants was published in 2006 (244) in a study where the roGFP1 was expressed in the cytoplasm and mitochondria of *Arabidopsis thaliana* and performed oxidation and reduction treatments with H_2O_2 and DTT (244). This pioneering work showed the possibility to monitor dynamically subcellular redox changes by measuring in real time the sensor fluorescent emission ratio. By carrying out a calibration curve, it was possible to convert the sensor ratios into redox potentials showing that in mitochondria the E_{roGFP} was more reduced than in the cytoplasm (-362 mV

and -318 mV, respectively). Soon after the development of the rYFP and roGFP sensors and their first applications in animals and plants, it clearly emerged that both redox sensors equilibrated predominantly with glutathione (331,387,459) and that equilibration *in vivo* was accelerated by GRXs which mediated the thiol-disulfide exchange between glutathione and the redox sensor (458). A confirmation of this came in 2007 when Meyer and co-workers expressed the roGFP2 sensor in *Arabidopsis* (GFP2 is an enhanced variant of GFP1, see below). Also in this case the roGFP2 reversibly responded to redox changes induced by incubation with H₂O₂ or DTT and, more important, the sensor was severely oxidized in mutants with reduced levels of glutathione and in wild-type plants in which the glutathione content was depleted by treatments with an inhibitor of glutathione biosynthesis (L-buthionine-sulfoximine, BSO) (332). Soon after another work confirmed these results in *Arabidopsis* leaves (459). The fact that different laboratories with different imaging techniques, wide-field vs confocal microscopy, obtained similar results pointed out the reliability of the roGFP measurements. In addition, Schwarzländer and co-workers showed that, *in vivo*, roGFP1 had a lower dynamic range and was less photostable than roGFP2. Hence, the use of roGFP2 instead of roGFP1 was recommended (458).

As the equilibrium between roGFPs and glutathione was suspected to be mediated by GRXs *in vivo*, it was reasoned that the availability of endogenous GRXs might limit the fast equilibration between glutathione and the sensor. To overcome this problem, human GRX1 was fused to the roGFP2 (202). This new GRX1-roGFP2 was expressed and tested in plants such as *A. thaliana* and tobacco and in the phytopathogenic fungus *Botrytis cinerea* (132,216,328). In *Botrytis*, a side by side comparison of GRX1-roGFP2 and roGFP2 revealed that the oxidation of GRX1-roGFP2 was slightly faster than roGFP2, thereby sustaining the hypothesis that GRX could facilitate the equilibrium between glutathione and the sensor (216). The functional interaction between glutathione and GRX1-roGFP2 is proposed to involve first the glutathionylation of GRX1 by GSSG, then the internal transglutathionylation of roGFP2 by GRX1, followed by the formation of the disulfide in the roGFP2 (Figure 16B). All steps are reversible (Figure 16B). Note that roGFPs do not contain acidic/reactive Cys, therefore its glutathionylation can proceed via GRX1-dependent transglutathionylation with no requirement of H₂O₂ and transient sulfenic acid formation (see

Section II.C6 and Figure 8). Neither GRX1 nor roGFP2 are expected to react with H₂O₂ directly.

Altogether, the results obtained with different redox sensors based on roGFP1/2 expressed in different subcellular compartments of different organisms under physiological conditions show that the sensors are always highly reduced in mitochondria, nuclei, peroxisomes, chloroplasts and cytoplasm and highly oxidized in the ER lumen (458). Interestingly, the picture changes in stress conditions. For example, drought stress causes oxidation of roGFP1 in the cytoplasm of *Arabidopsis* (E_{GSH} shifted from -311 mV to -302 mV) with reversion to control values after re-watering (248). Strong oxidation of cytoplasmic roGFP2 was also observed in the root tip of *Arabidopsis* seedlings treated with cadmium (515) and in wounded *Arabidopsis* leaves (40,332). In the latter case, an oxidation wave propagating from the wound area preceded a reduction wave in the opposite direction, suggesting a systemic signaling response as previously hypothesized for ROS waves (346). Technically, the *in vivo* monitoring of the GSH/GSSG status in real time offered an unprecedented spatial and temporal resolution which may be difficult, if not impossible, to reach with other techniques.

The oxidation of cytoplasmic roGFP2 was also reported in *Arabidopsis* and tobacco leaves infected with the avirulent pathogen *Pseudomonas syringae* DC3000 (328). The mitochondrial version of roGFP1 and roGFP2 sensors were oxidized in response to heat stress, cadmium and darkness (437,458,460). Dark-induced roGFP2 oxidation occurred also in plastids, peroxisomes and cytoplasm, but in all cases with a different and slower timing than in mitochondria (437), suggesting that mitochondria may represent the origin of the oxidative stress in the dark occurring during the senescence program. In chloroplasts, treatments with electron transport inhibitors (3-(3,4-dichlorophenyl)-1,1-dimethylurea, DCMU; 2,5-Dibromo-6-isopropyl-3-methyl-1,4-benzoquinone, DBMIB) led to stromal roGFP2 oxidation and, in the same organelle, increased formation of stromules (53). The effect is interesting since stromules were shown to play a role in oxidative signaling (66).

As expected for a sensor sensing the glutathione redox potential, roGFP2 was also found more oxidized in *Arabidopsis* mutants (*rml1*, (8); *cad2*, (332)) in which the total glutathione content is strongly diminished (62,514), and in mutants of glutathione reductase (*gr1*, *gr2*) in which the GSH/GSSG is more oxidized (324,569).

VI.C. Other redox sensors

The high sensitivity of thiol peroxidases, including PRXs, for H_2O_2 was exploited to develop a redox sensor with different specificity than roGFP variants. PRXs bear an extremely reactive catalytic Cys that forms a sulfenic acid upon reaction with H_2O_2 . The sulfenic acid is then resolved by a second Cys forming a disulfide. Although in the common catalytic cycle of PRXs, the disulfide is reduced by TRX or GRX, some PRXs harbor an intrinsic and powerful capacity to act as H_2O_2 -dependent protein thiol oxidases when they are recruited into proximity of oxidizable target proteins (203). Hence, the idea of fusing the yeast glutathione peroxidase-like protein Orp1 to the roGFP2 to get an H_2O_2 sensor came (203). However, this probe cannot be considered as a strict H_2O_2 sensor as the roGFP2-Orp1 is on one side oxidized by H_2O_2 , but on the other is likely to be reduced *in vivo* by TRXs that have been shown to directly reduce Orp1 (458). Different from the GRX1-roGFP2 probe whose oxidation by GSSG and reduction by GSH is reversible, the oxidation of the catalytic Cys of Orp1 by H_2O_2 is not reversed by water ((508); sulfenic acids are not easily reduced by water), such that roGFP2-Orp1 cannot equilibrate with the H_2O_2/H_2O redox couple. As a matter of fact, the redox state of roGFP-Orp1 is not only influenced by the level of the oxidant (H_2O_2), but also by the reductants, GRXs and TRXs. This makes the sensor unsuitable to determine absolute H_2O_2 levels (458). Nevertheless, the roGFP2-Orp1 expressed in *Drosophila* showed a different redox state from GRX1-roGFP2 during development and aging (5), suggesting that both sensors provide different information. The roGFP2-Orp1 sensor has been recently used in *Arabidopsis*, revealing that in guard cells treatment with H_2S determines its oxidation via activation of NADPH oxidase (H_2O_2 production) (461).

Other relevant redox couples important for redox homeostasis in plants are represented by nicotinamide adenine dinucleotides. *In vivo* monitoring of NADH/NAD⁺ ratios was attempted by combining a bacterial NADH-binding protein and a fluorescent protein variant, creating a genetically encoded fluorescent biosensor of the cytoplasmic NADH/NAD⁺ redox state, named Peredox (231). The functionality of Peredox was demonstrated in mammalian cells showing that it efficiently reported the cytoplasmic NADH/NAD⁺ ratio and that it was sensitive to exogenous administration of lactate and pyruvate (231). Such sensor was also employed in the fungus *Ustilago maydis* to monitor

cytoplasmic NAD redox dynamics (213). More recently, a new ratiometric, pH-resistant, genetically encoded fluorescent indicator for NADPH (iNap) was also generated (493). The iNap sensors have been used to monitor NADPH fluctuations during the activation of macrophage cells or wound response *in vivo* (493). Up to now there are no reports showing the functionality of such NAD(P)(H) sensors in plant cells.

VII. REDOX PLANT PHYSIOLOGY *IN VIVO*

As outlined above, plants organize a multiplicity of different low-molecular weight redox couples and redox proteins to regulate cellular redox homeostasis. Whereas research in the past mainly focused on the characterization of these components during *in vitro* studies, recent progress has been made to resolve the organization and biological significance of this complex redox network *in planta*. In the following section, we will review the emerging roles of this regulatory network in integrating photosynthesis, growth, development and stress responses of plants to cope with fluctuating environmental conditions.

VII.A. Redox regulation of light acclimation: the FTR-TRX system and light-responsive control of photosynthesis within the chloroplast

Sunlight represents the source of energy for photosynthesis and plant growth. However, photosynthetic cells have to manage strong fluctuations in light intensities that can occur very rapidly in nature. This requires sensitive and rapid light acclimation mechanisms to maintain photosynthetic performance and chloroplast functions in a dynamic manner and to avoid the generation of potentially harmful ROS.

One pathway to transfer light signals to chloroplast target enzymes is provided by the FDX-TRX system (54). It involves sequential transfer of reducing power from photosynthetic light reactions via FDX and FTR to five different TRX classes (*f*, *m*, *x*, *y* and *z*), which activate specific sets of stromal and thylakoid proteins by reducing their regulatory disulfides (Figure 17) (564).

Comparative studies using sets of recombinant purified TRX isoforms and target proteins revealed functional specificities of the different classes of TRXs for their targets *in vitro* (92,322,500,562). TRXs belonging to *f*- and *m*-classes revealed metabolic functions in activating enzymes of the CB cycle, starch synthesis, redox export via the malate valve and ATP synthesis, whereas isoforms belonging to the *x* and *y* classes revealed antioxidative

functions in providing reducing power to PRXs. For a comprehensive overview on the TRX target proteins and their regulatory specificities for different TRX isoforms identified during *in vitro* studies see (171).

Although until recently most of our knowledge on the functional diversity of chloroplast TRXs relied on *in vitro* studies, a boost of genetic studies in the last years specifically in *Arabidopsis* led to a rapid increase in our knowledge on their roles *in vivo*. As outlined in Section IV, the plant genome contains a complex gene family of TRXs, with up to 21 different TRX classes, including 7 classes containing typical TRXs because of their conserved active site signature and single domain structure. Typical TRXs from five classes reside in *Arabidopsis* chloroplasts, with different isoforms (TRXs *f*1-2, *m*1-4, *x*, *y*1-2 and *z*). The chloroplasts contain also several atypical TRX isoforms that are often little studied with respect to typical ones. A quantification of the protein levels of typical TRX isoforms showed that TRXs *f* and *m* are the major isoforms, accumulating to 22 and 69% of the total level of typical TRXs in the chloroplast stroma, respectively (383). For the sake of simplicity, when not otherwise specified, the term TRX will be used for typical TRXs in the following text.

Arabidopsis mutants deficient in TRX *f*1 (lacking 70-90% of total TRX *f* proteins) or with combined deficiencies of TRXs *f*1 and *f*2 (TRX*f* null mutants) revealed that *f*-class TRXs are important for the rapid activation of carbon metabolism and photosynthesis in response to light. During rapid dark-light transitions, TRX *f* deficiency led to delayed and incomplete reduction and activation of the CB cycle enzyme FBPase and RubisCO activase, retarded light activation of CB cycle activity and transient inhibition of photosynthetic electron transport, whereas thermal dissipation of the absorbed light energy by non-photochemical quenching (NPQ) was transiently increased (363,383,498,501,562). This shows a role of TRX *f* in short-term light adjustment of photosynthetic carbon fixation to optimize photosynthetic efficiency. Deficiency of TRX *f* also led to an incomplete photoreduction of the small subunit of the key starch synthetic enzyme AGPase resulting in decreased starch accumulation during the day, providing evidence for a role of TRX *f* in regulating diurnal starch turnover in response to dark-light alterations (363,498,500). Interestingly, despite the complete lack of *f*-class TRXs, FBPase and RubisCO activase became partially reduced during illumination (363,382,562) indicating functional compensation by other classes of

TRXs or thiol-reduction systems (see below). In line with this, silencing of TRX *f* did not substantially affect overall rates of photosynthetic carbon fixation and plant growth under long-day conditions, whereas there were only slight growth retardations under short-days or very low light intensities (363,498).

TRXs of the *m*-class have more diverse *in vivo* functions than TRX *f*. Earlier studies documented a role of the very low abundant TRX *m3* in symplastic permeability and meristem development (45), see also below). On the other hand, more recent reports revealed photosynthetic functions for the relatively high abundant TRXs *m1*, *m2* and *m4*, each representing approx. 23% of the total stromal TRX (99,383,501,523). For TRX *m4* a role in the regulation of cyclic photosynthetic electron transport was revealed (99), whereas TRXs *m1* and *m2* were found to participate in the rapid light-activation of NADP-MDH (501) involved in the export of excess reducing equivalents from the chloroplast *via* the malate valve to prevent photoinhibition (447). This indicates that TRXs *m1*, *m2* and *m4* are important to balance the chloroplast ATP/NADPH ratio for optimized photosynthesis. *Arabidopsis* double mutants with combined deficiencies of TRXs *m1* and *m2* showed wild-type growth and photosynthesis under constant light conditions, but photosynthetic parameters were strongly modified in fluctuating light environments with rapidly alternating low and high light intensities (501). Combined silencing of TRXs *m1* and *m2* led to lower photosynthetic efficiency in high light, but surprisingly had the opposite effect in the low light periods. This indicates that TRXs *m1* and *m2* are involved in dynamic acclimation of photosynthesis, being essential for full activation of photosynthesis in the high-light peaks by rapid induction of the malate valve to prevent photoinhibition, whereas there is a trade-off in photosynthetic efficiency during the low-light phases of fluctuating light (501). The reason for the higher photosynthetic efficiency of the TRX*m1m2* mutants in low light is unclear and requires further investigation.

Interestingly, multiple silencing of TRX *m1*, TRX *m2* and TRX *m4* in triple *Arabidopsis* mutants led to more severe phenotypes, depending on the extent of the decrease in total TRX *m* protein (383,523). A decrease in TRX *m* protein to approx. 30% of the level found in wild-type plants led to incomplete photo-reduction of FBPase and SBPase from the CB cycle and NADP-MDH from the malate valve in response to light, resulting in decreased CO₂ assimilation rates, inhibition of photosynthetic electron transport and substantial

retardations in plant growth under constant light conditions (383). When compared with TRXf1f2 mutants (see above), this reveals a high level of redundancy of *f*- and *m*-class TRXs in the light activation of the CB cycle and photosynthesis being operational *in vivo*, which is unexpected given the predominant role of *f*-class TRXs in regulating enzymes of the CB cycle as proposed by *in vitro* studies (171). When the total amount of TRX *m* proteins was decreased to less than 15% of the level found in wild-type plants, mutant plants displayed very severe growth defects, pale green leaves, strongly decreased PSII activity and impaired PSII assembly (383,523). In line with this, triple silencing of TRXs *m1*, *m2* and *m4* in transgenic *Arabidopsis* led to a decrease in chlorophyll accumulation and in the redox status and activity of Mg-protoporphyrin IX methyltransferase (CHLM), which catalyzes the second step in the chlorophyll synthesizing Mg branch of the tetrapyrrol pathway in the chloroplast (108). Interestingly, studies in pea revealed that simultaneous silencing of TRX *f* and *m* genes is required to decrease the *in vivo* redox status of the Mg chelatase CHLI subunit (CHLI), catalyzing the first step of the Mg branch, as well as chlorophyll content and photosynthetic capacity (309). While interpretation of *in vivo* results is complicated by the fact that genetic removal of part of the TRX pool is likely to affect the redox state of the remnants, overall, these studies suggest redundant roles of *f*- and *m*-class TRXs in, both, rapid light activation of photosynthetic metabolism and more long-term light regulation of the biosynthesis of photosynthetic machineries.

Arabidopsis mutants deficient in the less abundant TRXs *x* or *y* showed wild-type phenotypes, despite their proposed roles in reduction of 2-Cys PRX and PRX Q for peroxide detoxification based on *in vitro* studies (280,419). This indicates functional compensation by other chloroplast TRX systems *in vivo* (see below). In contrast to this, deficiency of the low abundant TRX *z* led to an albino phenotype with impaired photoautotrophic growth and disturbed chloroplast development, similar to mutants of chloroplast gene expression (18). In confirmation to this, TRX *z* was found to act as an essential structural component of the plastid-encoded RNA polymerase complex and proposed to be important for the light-dependent expression of photosynthetic genes in the chloroplast. However, the role of TRX *z* in this context seems to be independent of its redox activity (535) and the *in vivo* pathways leading to its reduction are currently unclear (563) because the *Arabidopsis* isoform does not seem to be reduced by FTR *in vitro* (51) unlike poplar counterpart (86).

Further studies will be necessary to elucidate the role of TRX z in the chloroplast dithiol/disulfide network.

VII.B. Redox-regulation of light acclimation: chloroplast NTRC, 2-Cys PRXs and photosynthetic performance under low light

In addition to the light-dependent FDX-TRX system described above, the more recently discovered NTRC forms a separate thiol reduction cascade in the chloroplast stroma, combining both NTR and TRX activities on a single polypeptide (Figure 17) (468). Unlike FTR, NTRC receives its reducing potential from NADPH and provides electrons to target proteins via its own TRX domain (47). Biochemical and genetic studies established a major role of NTRC in reducing 2-Cys PRXs involved in the scavenging of H₂O₂ within the chloroplast (409,563). Comparative studies using *Arabidopsis* mutants deficient in NTRC and TRX x identified NTRC as the primary electron donor for 2-Cys PRXs *in vivo*, providing a redox buffer to keep this enzyme in a reduced state for antioxidant functions in the light as well as in the dark (419). Although these studies suggested that NTRC operated as a separate thiol-reduction system independently of light, recent work provided *in vivo* evidence for additional functions of NTRC in the light-dependent regulation of photosynthetic metabolism and thylakoid energy transduction similar to the FDX-TRX system. In *Arabidopsis* mutants, deficiency of NTRC led to incomplete photo-reduction of regulatory disulfides in enzymes involved in chlorophyll biosynthesis (CHLI, CHLM and glutamyl-transfer RNA reductase1, GluTR1; (407,429)), starch biosynthesis (AGPase; (498)), CB cycle (FBPase, SBPase and phosphoribulokinase (PRK) (371,382,498,563)), ATP synthesis (γ -subunit of CF1-ATP synthase (69,371)) and NADPH export (NADP-MDH; (501)) in response to dark-light transitions, resulting in impaired chlorophyll accumulation (429,468), starch turnover ((290,498), CO₂ assimilation (498), photosynthetic light-energy utilization (69,364,371,498,501) and plant growth (290,364,498). For most of these parameters, silencing and overexpression of NTRC led to opposing effects, indicating that NTRC is limiting for CO₂ fixation, photosynthetic efficiency and growth in wild-type *Arabidopsis* plants (371) and may be a promising target for biotechnological strategies to improve crops (370). The role of NTRC to optimize photosynthetic efficiency is specifically relevant under constant (69,364) and fluctuating low light intensities (69,501). When light availability is limiting, NADPH-dependent NTRC allows efficient redox-activation of proton-

coupled ATP synthase, leading to lower acidification of the thylakoid lumen and lower energy dissipation by NPQ resulting in a more efficient utilization of available light energy for photosynthesis and growth (69,364). In confirmation to this notion, blocking of NPQ in the *ntrc* mutant background led to partial recovery of photosynthetic performance and growth, indicating that NTRC promotes photosynthesis by regulating NPQ (364). Under rapidly alternating low and high light intensities, NTRC is indispensable to ensure the full range of dynamic responses of NPQ to optimize photosynthesis and maintain growth in fluctuating light environments occurring frequently in nature (501).

VII.C. Redox-regulation of light acclimation: cooperation of FTR-TRX and NADPH-NTRC systems for photoautotrophic growth

The participation of NTRC in the light activation of enzymes known to be regulated by the FDX-TRX system suggests that chloroplast redox regulation depends on the cross talk between both thiol-redox systems *in vivo*. To dissect the relationship of NTRC with the other TRXs, recent studies investigated *Arabidopsis* mutants with combined deficiencies of NTRC and TRXs. When the deficiency of NTRC was combined with those of TRX *f1/2* (382,498) or TRX *x* (382), double/triple mutants showed severe growth retardation phenotypes, almost abolished light activation of FBPase from the CB cycle, severely impaired CO₂ assimilation, starch turnover, photosynthetic efficiency and chlorophyll accumulation, whereas single mutants were hardly affected. Severe growth retardation and severely impaired chlorophyll synthesis were also revealed when NTRC deficiency was combined with deficiencies of TRXs *m1*, *m2* and *m4* in quadruple mutants (108). A double mutant combining the deficiency of NTRC and of the catalytic subunit of FTR was not viable under photoautotrophic conditions (563). This suggests that NADPH dependent NTRC acts concertedly with diverse other classes of TRXs of the light dependent FDX-TRX system in photosynthetic redox regulation, with TRXs *f1/2*, *m1/2/4* and *x* showing a high degree of functional redundancy. A cooperation of both thiol-reduction loops is therefore indispensable to sustain light acclimation of photosynthetic metabolism, photosynthetic efficiency and photoautotrophic growth of plants.

Different mechanisms have been proposed to explain the functional integration of NTRC and FDX/TRX systems. The phenotypic recovery of the *ntrc Arabidopsis* mutant by overexpression of redox-inactive forms of NTRC together with bimolecular fluorescence

complementation (BiFC) assay based protein-protein interaction studies provided evidence that NTRC physically interacts with the FDX-TRX system and its targets *in vivo* (371). However, the functional role of this interaction is still unclear. *In vitro* studies show that NTRC is very inefficient in reducing TRXs *f1*, *f2*, *m1*, *m4*, *x* and *y1* (51,563) and is not able to reduce the regulatory disulfides of the TRX target enzymes FBPase, SBPase and NADP-MDH directly (382,563). This puts forward indirect effects to explain why light activation of the CB cycle and export of excess reducing equivalents require NTRC. Recent studies show that decreased levels of 2-Cys PRX suppress the phenotype of the *ntrc* single and *ntrc-trxf1-trxf2* triple *Arabidopsis* mutants, indicating that FDX-TRX and NTRC redox systems are integrated via the redox balance of 2-Cys PRX (408). As NTRC is the major system to provide electrons for the reduction of 2-Cys PRXs (419,563), it will indirectly maintain the reducing capacity of the pool of FDX-TRXs (408) and restrict re-oxidation of their targets via an oxidation loop involving H₂O₂, oxidized 2-Cys PRX and the atypical TRXs ACHT1/4 (111,133,371) and TRXL2 (561) to finally increase the reduction state of disulfides in target proteins of the FDX-TRX system (Figure 17).

VII.D. Redox-regulation of light acclimation: integration of redox signals at the cellular level

In addition to intraorganellar crosstalk of redox systems within the chloroplast, light acclimation of photosynthesis also requires interorganellar redox communication (380,449). During acclimation to fluctuating light intensities, chloroplasts communicate information by retrograde signaling to the nucleus, leading to rapid changes in the transcription of nuclear genes coding for proteins involved in light harvesting, electron transport, stromal metabolism and antioxidant systems to balance input of light energy with photosynthetic capacity (122,184). There is *in vivo* evidence that H₂O₂ acts as an important retrograde signal in this response sensing excess excitation energy in the chloroplast rather than being a toxic byproduct of aerobic metabolism (134,159,345). Elevated light leads to increased reduction of oxygen to superoxide radicals at the acceptor side of PSI, leading to increased production of H₂O₂ via superoxide dismutase within the chloroplast (134,355). The elevated level of H₂O₂ is subsequently transferred from the chloroplast into the nucleus (50,134,355), where it leads to induced expression of high light responsive nuclear genes (134,510) via redox sensitive transcription factors (473). As

H₂O₂ movement from chloroplast to nucleus does not involve the cytoplasm (134), its transfer most likely involves a close physical association of the two organelles (464) allowing efficient aquaporin-mediated transmembrane diffusion (50), or the formation of stromules as direct stroma-filled interorganelar connections (53). In confirmation, stromule formation between chloroplasts and nucleus is specifically increased in response to light and chloroplast ROS production (53). This retrograde signaling pathway will (i) be attenuated by light-dependent reductive signals mediated by chloroplast TRXs and NTRC, which will diminish the production of H₂O₂ by decreasing acceptor limitation at PSI (501), (ii) increase the scavenging of H₂O₂ by activation of PRXs in the chloroplast stroma (563), and (iii) restrict the transport of H₂O₂ to the nucleus by inhibiting stromule formation (53). This is consistent with recent studies on *Arabidopsis* mutants with combined deficiencies of chloroplast 2-Cys PRXs and APXs revealing increased H₂O₂ levels and up-regulation of H₂O₂-responsive marker genes in the nucleus (22).

Interorganelar redox signaling also involves the exchange of reducing equivalents via metabolite shuttles, including the triose-P/3PGA shuttle at the chloroplast envelope (518) and the malate/oxaloacetate shuttles at the chloroplast (260,447), mitochondrial (447) and peroxysomal (219) envelopes/membranes. This allows high light acclimation responses at the cellular level by sensing acceptor limitation at PSI via an increase in the chloroplast NADPH/NADP⁺ ratio, which is transmitted to cytoplasm, mitochondria and peroxisomes via a combination of the different redox shuttles. Recent studies suggested that this redox signaling system affects light acclimation responses by (i) translational inhibition of photosynthetic gene expression via TRX-*h* dependent regulation of denitrosylation of the repressor protein NAB1 in the cytoplasm (46), (ii) inhibition of protein uptake into chloroplasts via redox-regulation of chloroplast envelope translocons (29,586), (iii) inhibition of catalase in peroxisomes to modulate H₂O₂ signaling responses (219), and (iv) dissipation of excess reducing equivalents via alternative oxidase in mitochondria (149,566) probably involving regulation by mitochondrial TRXs (109) to prevent an over-reduction of the photosystems in the chloroplast (malate valve) and to modulate ROS responses. Although direct evidence for the light dependency of mitochondrial TRXs is largely lacking, there is *in vivo* evidence that the malate valve can act in the reverse direction by transmitting mitochondrial redox signals to the chloroplasts,

leading to redox-regulation of chloroplast metabolism (71) and import of chloroplast precursor proteins (586) via alterations in the chloroplast NADPH/NADP⁺ ratio. This implies crosstalk of chloroplast, cytoplasmic and mitochondrial TRX systems to integrate redox signals at the cellular level. Further work is required to resolve the network of interorganellar redox-communication and the *in vivo* roles of its components, ensuring photosynthetic light acclimation and redox balancing at the cellular level.

VII.E. Redox control of abiotic and biotic stress responses: integration of multiple signaling pathways

In addition to its role in light acclimation of photosynthesis, redox regulation is also involved in the control of various abiotic and biotic stress responses. As reviewed recently, ROS and RNS play critical and integrative roles in multiple stress signaling (34,377,472), controlling pathogen defense (282,450) and abiotic stress tolerance of plants (Figure 17) (138,423). The complexity in ROS responses to various environmental stimuli is attributable to the intrinsic chemical properties of different ROS species, different sites and mechanisms of ROS production, the spatial and temporal coordination of ROS signals and their integration with other signals related to metabolites, antioxidants, redoxins, hormones and genetic control elements (reviewed in (34,218,251,341,374,377,423)). In this context, different subcellular sites of ROS production may define specificity in signaling (341,377). ROS are produced in the apoplast by activation of plasmalemma RBOHs (484) or cell wall peroxidases (315) and in chloroplasts (123), peroxisomes (115) and mitochondria (230), as a byproduct of aerobic metabolism (see Section II). It is proposed that specific sets of environmental stress conditions, such as pathogen infection, ozone, UV-B, excess irradiation, salinity, drought, temperature or low oxygen, will result in specific subcellular ROS, RNS and redox signatures that will in turn lead to the activation of specific defense and acclimation responses (90,119,403,423). However little is known on the underlying mechanisms allowing subcellular changes in ROS and RNS levels to be sensed and the signal being transduced to specific downstream response elements (158,377,423). In yeast and *Chlamydomonas*, the induction of autophagy in response to numerous stress conditions is associated with ROS production and is regulated by TRX-dependent activation of the ATG4 cysteine protease (398-401,406). In plants, recent studies indicate that defense responses to abiotic and biotic stresses involve an interplay between salicylic acid

(SA), ROS, RNS, GSH and TRXs (218,499). Different environmental stimuli lead to ROS production in different subcellular compartments which precedes SA signaling causing transcriptional reprogramming of gene expression (218). The ROS/SA interaction is modulated by GSH, which leads to increased SA production, whereas SA causes increased GSH levels and reducing power, which in turn is involved in ROS scavenging (131). Upon pathogen infection, ROS is produced in the apoplast (315) leading to elevated SA levels and a subsequent more reduced cellular redox state (or at least, glutathione redox state), which is sensed by the NPR1 protein, a master regulator of pathogenesis related (PR) gene expression (354). Redox regulation involves NTRA-dependent TRX *h5* leading to monomerization of the NPR1 oligomer in the cytoplasm to allow its translocation into the nucleus (487), where it activates the expression of PR genes via its interaction with TGA transcription factors, which are also modulated by redox conditions (262). In this context, TRX *h5* is facilitating NPR1 monomerization by catalyzing the direct reduction of intermolecular disulfide bonds linking the NPR1 monomers (487) and by denitrosylation of the regulatory Cys156 in antagonistic action to GSNO and NO (262).

A further cytoplasmic mediator of redox signal transduction is the highly conserved glyceraldehyde-3-phosphate dehydrogenase C (GAPC), a key glycolytic enzyme with important non-catalytic functions for various abiotic and biotic stress responses (reviewed in (220,557,577)). Plant GAPCs acts as common target proteins of ROS and RNS with their catalytic Cys being subjected to diverse reversible modifications, such as S-nitrosylation, sulfenylation and S-glutathionylation, which can be reversed/reduced by GSH, TRX, and GRX (36,46,102,166,575,577,580). During cadmium induced oxidative stress, NO accumulates and GAPC1 is translocated from the cytoplasm to the nucleus, where its role remains to be established (515). Whereas in mammalian cells nuclear relocalization of GAPC depends on nitrosylation of its catalytic Cys, mutation of this residue (Cys155) in *Arabidopsis* plants led to a stimulation of relocalization, rather than an inhibition (515).

With respect to transcription factors, group VII ethylene response factors (ERF-VII) have emerged as novel regulators of abiotic and biotic stress responses involved in oxygen- and NO-dependent signal transduction in plants (177,560). Molecular oxygen and NO lead to oxidation of the conserved N-terminal Cys of ERF-VIIs to Cys sulfinic and sulfonic acids facilitated by PCOs targeting ERF-VII proteins to the N-end rule pathway of proteasomal

degradation (176,178,179,294,531,533). This provides a sensing mechanism for oxygen and NO mediating ERF-VII degradation and reprogramming of gene expression (178,294,560), allowing an efficient regulation of central metabolic processes to optimize hypoxic resistance (394) and immune responses of plants (394,591). While the N-end rule pathway has emerged as an important regulator of environmental stress responses, further studies are necessary to identify N-end rule substrates beyond ERF-VII and their role in the plant signaling network (125,176).

Recent studies provide evidence for an emerging role of chloroplasts as integrators of plant stress signals specifically in plant immunity against pathogens (reviewed in (119,154,252,467)). Chloroplasts are important as sensors of available photosynthetic energy to fuel immune responses and serve as major production sites of pro-defense molecules such as phytohormones (including SA and jasmonic acid) and ROS providing retrograde signals to modulate nuclear gene expression and plant resistance to pathogens. This involves the chloroplast redox status as a major regulator of defense responses (Figure 17). Manipulation of ROS build-up in chloroplasts by expression of a plastid-targeted flavodoxin (411), silencing of FTR (295), deficiency of NTRC and PRX (234,235) and depletion of chloroplast forms of glutathione peroxidases-like, GPXL1 and GPXL7 (75), led to changes in the expression of pathogenesis related genes and pathogen resistance in diverse plant species. Although the interplay between plastidial and extra-plastidial ROS sources during plant immunity is still unclear (341), the specificity of chloroplast ROS signaling may be attributable to pathogen-induced formation of stromules, providing physical connections to transport ROS and other pro-defense molecules from the chloroplast directly to the nucleus (66). This will allow the transport of chloroplast derived signaling proteins such as NRIP1 involved in pathogen recognition (67) or WHIRLY1 involved redox sensing (154) to the nucleus to trigger PR gene expression. As NTRC acts a master regulator of chloroplast redox homeostasis (408) it will affect pathogen related responses by modulating H₂O₂ production via 2-Cys PRXs (234) and light dependent stromule formation (53).

GRXs, represented by members belonging to four different classes in terrestrial plants (see Section IV), are also emerging as important redox-active players of plant responses to stress. For example, GRXS12 positively correlates with brassinosteroid accumulation and

antioxidant responses under chilling conditions in tomato plants (548). Although poplar GRXS12 is very active in protein deglutathionylation *in vitro* (573), the relevance of this activity *in vivo* is still unknown. Class II GRXs are best known for their role in Fe-S cluster biogenesis (30,351,481) but they are also implied in stress responses. Class II GRXS14 levels correlate with plant tolerance to abiotic stress conditions in *Arabidopsis* (81,427) and tomato (195). Plants with altered class II GRXS17 expression were found to be tolerant to drought, oxidative and heat stresses (82,546,547). Recently, GRXS17 was found associated with components of the cytoplasmic Fe-S cluster assembly pathway and to be demanded for a proper response to iron deficiency stress (233). Members of class III, namely GRXC7 and GRXC8 (ROXY1 and ROXY2, respectively), participate in pathogen responses, overexpressing lines being hyper-susceptible to the infection of the necrotrophic pathogen *Botrytis cinerea* with a concomitant accumulation of H₂O₂ (526). Interestingly, plants impaired in class III GRXS13 are less susceptible to *B. cinerea* infection (273). Transgenic plants with reduced level of GRXS13 and GRXC9 showed increased levels of superoxide radical and reduced tolerance to high light and methyl viologen treatments (278). Overexpression of class III GRXC7 and class I GRXC2 confers increased arsenic tolerance allowing reduced accumulation of this metal pollutant in both seeds and shoot tissues (513). In general, plant *grx* mutant analyses point to a positive role of GRXs of any class in different biotic and abiotic stress responses *in vivo*. Mechanistic models of their function, however, are still largely hypothetical.

VII.F Redox regulation of plant development: integration of redox signals into molecular networks of developmental control

An increasing number of reports in the literature indicate redox regulation of growth and development as an emerging field in plant biology. This is summarized in many excellent recent reviews documenting emerging roles of oxidation (oxygen, ROS, RNS) and reduction signals (TRX, GSH, GRX) in the regulation of the whole plant developmental cycle interfacing with signaling pathways involving phytohormones and transcription factors (95,377,438,451,452,504). There is evidence for the role of ROS, GSH, GRX and TRX in controlling the development of root and shoot apical meristems. ROS production by mitochondria (568) and plasmalemma located NADPH oxidases (245) together with GRXS17 (263) and ABPH2 (553) are involved in the regulation of transcription factors to

determine meristem size and maintenance. Plastid-located TRX *m3* (45) and plasma membrane-associated TRX *h9* (330) allow cell-to-cell communication and meristem function. Extra-plastidic NTRA/NTRB and GSH (33), and chloroplastic TRXs and NTRC (261,382) are involved in auxin and redox signaling regulating meristem development. These mechanisms may also influence cell cycle progression and cell differentiation, which are associated to oscillations in cellular redox state involving bursts of H₂O₂ and subsequent import of GSH into the nucleus, regulating transcription factors through reversible Cys reduction/oxidation via nuclear TRXs (63,120,121). Thiol-based regulatory mechanisms are also involved in the molecular networks controlling floral development with GSH and class III GRX proteins regulating petal (549) and anther development and pollen formation (357) by interacting with TGA transcription factors in the nucleus (118). While research into hypoxia usually emphasized the response to changes in external oxygen supply during stress responses, there is recent evidence for developmental transitions in the oxygen status of meristems and reproductive plant organs (reviewed in (170,509)), while conversely local hypoxic conditions may contribute to regulate developmental processes in plants (94,293,451). Establishment of internal hypoxic environments will contribute to developmental regulation by maintaining reducing conditions in specific plant tissues. In this context, hypoxia arising naturally within growing anther tissue acts as a positional cue to set germ cell fate (255). Changes in oxygen concentrations may also contribute to plant development by affecting the stability of ERF-VII transcription factors via the N-end rule pathway. As published recently, the N-end rule pathway controls multiple functions during shoot and leaf development (188), probably via its function to sense gaseous signals like oxygen and NO (179,294). This may partly involve regulation of ERF-VII by protein degradation, as *Arabidopsis* plants overexpressing N-end rule insensitive forms of ERF-VII displayed changes in leaf development (180,394) and photomorphogenesis (2). During leaf development, maturation of chloroplasts regulates transition from cell proliferation to cell expansion (14). Chloroplast development is regulated by NTRC and FDX-TRXs (382) leading to changes in the production of oxidation signals such as oxygen, NO and ROS that will control the transition in leaf development by acting as retrograde signals (Figure 17) (14). During cell expansion the transcription factor

KUODA1 inhibits the expression of cell-wall peroxidases, lowering the levels of apoplastic ROS to restrict cell wall tightening and promote growth (308).

VII.G. Redox regulation in plant physiology: a brief conclusion

There is a balance of oxidation and reduction signals integrating photosynthesis, development and stress responses allowing plants to cope with fluctuating changes in their biotic and abiotic environment. This involves intra-organellar crosstalk of redox systems as well as redox communication within and between cells. In this context, NTRC acts as an important hub to control the redox balance between oxidation and reduction pathways within the chloroplast of C3 plants, thereby influencing retrograde signals such as ROS to control light acclimation, abiotic and biotic stress responses and plant development. There is also an emerging role of gaseous signals such as oxygen and NO, which modulate proteasomal degradation of proteins containing an N-terminal Cys via the N-end rule pathway. While research into hypoxia usually emphasized stress responses, there are also developmental transitions in the oxygen status, which conversely contribute to the regulation of plant development. Further studies are needed to dissect this complex redox signaling network and its integration with other signals related to metabolites, antioxidants, redoxins, phytohormones and genetic control elements.

VIII. CONCLUDING REMARKS AND FUTURE PERSPECTIVES

The importance and pervasiveness of redox regulation and signaling in plant biology has currently reached a level that probably Bob Buchanan and collaborators could not even vaguely imagine when they first discovered the principles of TRX-mediated regulation of photosynthetic metabolism in plants more than 50 years ago. This comprehensive review tries to account for the fact that we now know that redox regulation involves not only one but many different types of PTMs of protein Cys, different RMS, a large number of redoxins (TRXs, GRXs, and NTRC), and an enormous number of protein targets belonging to virtually every metabolic or signaling pathway and located in virtually every subcellular compartment, either of photosynthetic and non-photosynthetic plant cells. As a result, redox homeostasis infiltrates all aspects of plant physiology. The recent development of plant redox biology has provided the material of this comprehensive review, but also opened many questions that need to be answered in the future.

Combination of traditional biochemical approaches and redox proteomics is showing that redox-regulated proteins are organized in complex networks that we are just beginning to understand. A large part of the redox targets that have been identified by proteomics still have to be analyzed in order to understand the effect, if any, of the redox modification. Moreover, most of our knowledge is derived from non-quantitative studies performed under conditions that favor the redox modification of the proteome. We have little information of the real status of the redox proteome under different physiological or pathological conditions and even for the best characterized targets, we rarely know which is the relative abundance of the redox-modified proteins in the cell. To this end, quantitative proteomic methods are being developed and will allow determining the stoichiometry and dynamics of multiple redox PTMs in few or even a single cell, under diverse physiological conditions and time scales. The final goal will be to understand, besides the pervasiveness, the relevance of redox regulation and signaling for plant physiology, thereby digging below the surface that we have just started to scratch.

Beyond quantitative proteomics, a field of redox biology that will hopefully grow more and more in the future regards the genetically encoded redox sensors. At the moment, we have powerful tools to determine the dynamics of the glutathione redox state. Other important redox players (NADPH, ascorbate, TRXs, GRXs, RMS) are still waiting to be assayed *in vivo* by similar methods. In the absence of accurate information on their localization, dynamics and redox state, we will hardly get a comprehensive picture of how redox homeostasis influence plant's life. Basic research and genetic engineering will have a fundamental role in the development of new genetically encoded sensors, and the continuous improvement of fluorescent microscopy imaging techniques will likely provide further support to this field in the future.

Structural biology is also promising to contribute significantly to our global understanding of plant redox homeostasis. Once discovered that plants contain tens of different redoxins coexisting in the same subcellular compartment which, in the same time, also contains hundreds of proteins potentially targeted by different redox PTMs, we still have only a vague idea of which are the principles that govern specificity in all possible interactions. Such principles will be derived from computational analyses of atomic structures of interacting partners and redox-modified proteins. Our available repertoire of complex

structures is still limited in number. Solving the tridimensional structure of large complexes of interacting proteins proved difficult in the past because of the intrinsic limitations in obtaining crystals of sufficient quality for X-ray diffraction analysis, but cryo-electron microscopy techniques allow to by-pass the crystallization step and permit to unravel large complex structures at atomic resolution.

At the end, what we really would like to know best is how redox regulation and signaling works in the context of plant physiology. Whereas past research into redox regulation was mainly focused on biochemical studies, a recent boost of genetic studies elucidated the organization and biological significance of the redox network *in planta*. These recent studies have fully confirmed the original model of light-dependent regulation of the CB cycle as mediated by TRXs, but have also opened new fields of research and new levels of understanding.

Results from reverse genetic studies clearly indicate that redox regulatory and signaling pathways contain multiple branches and interconnections. Although reverse genetic approaches are the most powerful way to currently demonstrate the function of a protein *in vivo*, complex networks may hinder a clear-cut interpretation of the results. This is particularly true when a hub element of the network, like for example a TRX, is knocked out. Indeed, TRX knock out mutants are likely to show pleiotropic effects. Moreover, the crosstalk between redox signaling pathways requires the combination of different knock out mutations in order to obtain a reliable interpretation of the emerging phenotypes.

Besides the master redox regulators, also the targets should be investigated *in vivo* and mutagenic approaches specifically directed to the redox-active Cys are arguably the best way to tackle this problem. Also, this approach has its own limitation and in some cases, the substitution of a single Cys was found to affect protein stability *in vivo* besides redox regulation, thereby significantly complicating the emerging picture (204,476). Nevertheless, this approach seems promising and will possibly be boosted by genome editing techniques that are becoming available. Overall, we firmly believe that the integration of *in vitro* biochemical data with *in vivo* physiological evidence will provide the strongest basis to a general understanding of plant redox homeostasis.

Fifty years after germination, thiol-based redox biology in photosynthetic organisms has developed into a deeply rooted, well-established plant that grows and expands its foliage in all directions: it is still in its infancy but the future looks bright and full of opportunities.

ACKNOWLEDGEMENTS

The author MZ gratefully acknowledges supporting of its work from the University of Bologna (Alma Idea Grant). PG thanks the Deutsche Forschungsgemeinschaft (SFB-TR 175 B02) for funding. The authors thank Dr. Stephan Wagner, Prof. Bruce Morgan, and Prof. Markus Schwarzländer for providing original for Figure 16 (panel A).

REFERENCES

1. Abat JK, Deswal R. Differential modulation of S-nitrosoproteome of *Brassica juncea* by low temperature: change in S-nitrosylation of Rubisco is responsible for the inactivation of its carboxylase activity. *Proteomics* 9: 4368-80, 2009.
2. Abbas M, Berckhan S, Rooney Daniel J, Gibbs Daniel J, Vicente Conde J, Sousa Correia C, Bassel George W, Marín-de la Rosa N, León J, Alabadí D, Blázquez Miguel A, Holdsworth Michael J. Oxygen Sensing Coordinates Photomorphogenesis to Facilitate Seedling Survival. *Curr Biol* 25: 1483-88, 2015.
3. Akter S, Huang J, Bodra N, De Smet B, Wahni K, Rombaut D, Pauwels J, Gevaert K, Carroll K, Van Breusegem F, Messens J. DYn-2 Based Identification of Arabidopsis Sulfenomes. *Mol Cell Proteomics* 14: 1183-200, 2015.
4. Akter S, Huang J, Waszczak C, Jacques S, Gevaert K, Van Breusegem F, Messens J. Cysteines under ROS attack in plants: a proteomics view. *J Exp Bot* 66: 2935-44, 2015.
5. Albrecht SC, Barata AG, Grosshans J, Teleman AA, Dick TP. In vivo mapping of hydrogen peroxide and oxidized glutathione reveals chemical and regional specificity of redox homeostasis. *Cell Metab* 14: 819-29, 2011.
6. Alkhalfioui F, Renard M, Vensel WH, Wong J, Tanaka CK, Hurkman WJ, Buchanan BB, Montrichard F. Thioredoxin-linked proteins are reduced during germination of *Medicago truncatula* seeds. *Plant Physiol* 144: 1559-79, 2007.
7. Aller I, Meyer AJ. The oxidative protein folding machinery in plant cells. *Protoplasma* 250: 799-816, 2013.
8. Aller I, Rouhier N, Meyer AJ. Development of roGFP2-derived redox probes for measurement of the glutathione redox potential in the cytosol of severely glutathione-deficient *rml1* seedlings. *Front Plant Sci* 4: 506, 2013.
9. Alvarez C, Calo L, Romero LC, Garcia I, Gotor C. An O-acetylserine(thiol)lyase homolog with L-cysteine desulfhydrase activity regulates cysteine homeostasis in *Arabidopsis*. *Plant Physiol* 152: 656-69, 2010.
10. Alvarez C, Garcia I, Moreno I, Perez-Perez ME, Crespo JL, Romero LC, Gotor C. Cysteine-generated sulfide in the cytosol negatively regulates autophagy and modulates the transcriptional profile in *Arabidopsis*. *Plant Cell* 24: 4621-34, 2012.

11. Alvarez C, Garcia I, Romero LC, Gotor C. Mitochondrial sulfide detoxification requires a functional isoform O-acetylserine(thiol)lyase C in *Arabidopsis thaliana*. *Mol Plant* 5: 1217-26, 2012.
12. Anderson LE. Activation of pea leaf chloroplast sedoheptulose 1,7-diphosphate phosphatase by light and dithiothreitol. *Biochem Biophys Res Commun* 59: 907-13, 1974.
13. Anderson LE, Lim TC. Chloroplast glyceraldehyde 3-phosphate dehydrogenase: light-dependent change in the enzyme. *FEBS Lett* 27: 189-91, 1972.
14. Andriankaja M, Dhondt S, De Bodt S, Vanhaeren H, Coppens F, De Milde L, Mühlenbock P, Skiryicz A, Gonzalez N, Beemster Gerrit TS, Inzé D. Exit from Proliferation during Leaf Development in *Arabidopsis thaliana*: A Not-So-Gradual Process. *Dev Cell* 22: 64-78, 2012.
15. Armstrong DA. Applications of pulse radiolysis for the study of short-lived sulphur species. In: *Sulfur-centered reactive intermediates in chemistry and biology*. Springer; 1990. pp. 121-134.
16. Aroca A, Benito JM, Gotor C, Romero LC. Persulfidation proteome reveals the regulation of protein function by hydrogen sulfide in diverse biological processes in *Arabidopsis*. *J Exp Bot* 68: 4915-27, 2017.
17. Aroca A, Serna A, Gotor C, Romero LC. S-sulfhydration: a cysteine posttranslational modification in plant systems. *Plant Physiol* 168: 334-42, 2015.
18. Arsova B, Hoja U, Wimmelbacher M, Greiner E, Üstün Ş, Melzer M, Petersen K, Lein W, Börnke F. Plastidial Thioredoxin z Interacts with Two Fructokinase-Like Proteins in a Thiol-Dependent Manner: Evidence for an Essential Role in Chloroplast Development in *Arabidopsis* and *Nicotiana benthamiana*. *Plant Cell* 22: 1498-1515, 2010.
19. Asard H, Barbaro R, Trost P, Berczi A. Cytochromes b561: ascorbate-mediated trans-membrane electron transport. *Antioxid Redox Signal* 19: 1026-35, 2013.
20. Astier J, Besson-Bard A, Lamotte O, Bertoldo J, Bourque S, Terenzi H, Wendehenne D. Nitric oxide inhibits the ATPase activity of the chaperone-like AAA+ ATPase CDC48, a target for S-nitrosylation in cryptogein signalling in tobacco cells. *Biochem J* 447: 249-60, 2012.

21. Astier J, Gross I, Durner J. Nitric oxide production in plants: an update. *J Exp Bot*, 2017.
22. Awad J, Stotz HU, Fekete A, Krischke M, Engert C, Havaux M, Berger S, Mueller MJ. 2-cysteine peroxiredoxins and thylakoid ascorbate peroxidase create a water-water cycle that is essential to protect the photosynthetic apparatus under high light stress conditions. *Plant Physiol* 167: 1592-603, 2015.
23. Baier D, Latzko E. Properties and regulation of C-1-fructose-1,6-diphosphatase from spinach chloroplasts. *Biochim Biophys Acta* 396: 141-8, 1975.
24. Balmer Y, Koller A, del Val G, Manieri W, Schürmann P, Buchanan BB. Proteomics gives insight into the regulatory function of chloroplast thioredoxins. *Proc Natl Acad Sci U S A* 100: 370-5, 2003.
25. Balmer Y, Vensel WH, Cai N, Manieri W, Schürmann P, Hurkman WJ, Buchanan BB. A complete ferredoxin/thioredoxin system regulates fundamental processes in amyloplasts. *Proc Natl Acad Sci U S A* 103: 2988-93, 2006.
26. Balmer Y, Vensel WH, DuPont FM, Buchanan BB, Hurkman WJ. Proteome of amyloplasts isolated from developing wheat endosperm presents evidence of broad metabolic capability. *J Exp Bot* 57: 1591-602, 2006.
27. Balmer Y, Vensel WH, Hurkman WJ, Buchanan BB. Thioredoxin target proteins in chloroplast thylakoid membranes. *Antioxid Redox Signal* 8: 1829-34, 2006.
28. Balmer Y, Vensel WH, Tanaka CK, Hurkman WJ, Gelhaye E, Rouhier N, Jacquot JP, Manieri W, Schürmann P, Droux M, Buchanan BB. Thioredoxin links redox to the regulation of fundamental processes of plant mitochondria. *Proc Natl Acad Sci U S A* 101: 2642-7, 2004.
29. Balsera M, Soll J, Buchanan BB. Redox extends its regulatory reach to chloroplast protein import. *Trends Plant Sci* 15: 515-21, 2010.
30. Bandyopadhyay S, Gama F, Molina-Navarro MM, Gualberto JM, Claxton R, Naik SG, Huynh BH, Herrero E, Jacquot JP, Johnson MK, Rouhier N. Chloroplast monothiol glutaredoxins as scaffold proteins for the assembly and delivery of [2Fe-2S] clusters. *EMBO J* 27: 1122-33, 2008.

31. Baniulis D, Hasan SS, Stofleth JT, Cramer WA. Mechanism of enhanced superoxide production in the cytochrome b(6)f complex of oxygenic photosynthesis. *Biochemistry* 52: 8975-83, 2013.
32. Bartsch S, Monnet J, Selbach K, Quigley F, Gray J, von Wettstein D, Reinbothe S, Reinbothe C. Three thioredoxin targets in the inner envelope membrane of chloroplasts function in protein import and chlorophyll metabolism. *Proc Natl Acad Sci U S A* 105: 4933-8, 2008.
33. Bashandy T, Guilleminot J, Vernoux T, Caparros-Ruiz D, Ljung K, Meyer Y, Reichheld J-P. Interplay between the NADP-Linked Thioredoxin and Glutathione Systems in Arabidopsis Auxin Signaling. *Plant Cell* 22: 376-91, 2010.
34. Baxter A, Mittler R, Suzuki N. ROS as key players in plant stress signalling. *J Exp Bot* 65: 1229-40, 2014.
35. Bechtold U, Rabbani N, Mullineaux PM, Thornalley PJ. Quantitative measurement of specific biomarkers for protein oxidation, nitration and glycation in Arabidopsis leaves. *Plant J* 59: 661-71, 2009.
36. Bedhomme M, Adamo M, Marchand CH, Couturier J, Rouhier N, Lemaire SD, Zaffagnini M, Trost P. Glutathionylation of cytosolic glyceraldehyde-3-phosphate dehydrogenase from the model plant *Arabidopsis thaliana* is reversed by both glutaredoxins and thioredoxins in vitro. *Biochem J* 445: 337-47, 2012.
37. Bedhomme M, Zaffagnini M, Marchand CH, Gao XH, Moslonka-Lefebvre M, Michelet L, Decottignies P, Lemaire SD. Regulation by glutathionylation of isocitrate lyase from *Chlamydomonas reinhardtii*. *J Biol Chem* 284: 36282-91, 2009.
38. Beer SM, Taylor ER, Brown SE, Dahm CC, Costa NJ, Runswick MJ, Murphy MP. Glutaredoxin 2 catalyzes the reversible oxidation and glutathionylation of mitochondrial membrane thiol proteins: implications for mitochondrial redox regulation and antioxidant DEFENSE. *J Biol Chem* 279: 47939-51, 2004.
39. Begas P, Liedgens L, Moseler A, Meyer AJ, Deponte M. Glutaredoxin catalysis requires two distinct glutathione interaction sites. *Nat Commun* 8: 14835, 2017.

40. Beneloujaephajri E, Costa A, L'Haridon F, Metraux JP, Binda M. Production of reactive oxygen species and wound-induced resistance in *Arabidopsis thaliana* against *Botrytis cinerea* are preceded and depend on a burst of calcium. *BMC Plant Biol* 13: 160, 2013.
41. Benhar M. Nitric oxide and the thioredoxin system: a complex interplay in redox regulation. *Biochim Biophys Acta* 1850: 2476-84, 2015.
42. Benhar M, Forrester MT, Hess DT, Stamler JS. Regulated protein denitrosylation by cytosolic and mitochondrial thioredoxins. *Science* 320: 1050-4, 2008.
43. Benhar M, Forrester MT, Stamler JS. Protein denitrosylation: enzymatic mechanisms and cellular functions. *Nat Rev Mol Cell Biol* 10: 721-32, 2009.
44. Benhar M, Thompson JW, Moseley MA, Stamler JS. Identification of S-nitrosylated targets of thioredoxin using a quantitative proteomic approach. *Biochemistry* 49: 6963-9, 2010.
45. Benitez-Alfonso Y, Cilia M, Roman AS, Thomas C, Maule A, Hearn S, Jackson D. Control of *Arabidopsis* meristem development by thioredoxin-dependent regulation of intercellular transport. *Proc Natl Acad Sci U S A* 106: 3615-20, 2009.
46. Berger H, De Mia M, Morisse S, Marchand CH, Lemaire SD, Wobbe L, Kruse O. A Light Switch Based on Protein S-Nitrosylation Fine-Tunes Photosynthetic Light Harvesting in *Chlamydomonas*. *Plant Physiol* 171: 821-32, 2016.
47. Bernal-Bayard P, Hervas M, Cejudo FJ, Navarro JA. Electron Transfer Pathways and Dynamics of Chloroplast NADPH-dependent Thioredoxin Reductase C (NTRC). *J Biol Chem* 287: 33865-72, 2012.
48. Berndt C, Schwenn JD, Lillig CH. The specificity of thioredoxins and glutaredoxins is determined by electrostatic and geometric complementarity. *Chem Sci* 6: 7049-7058, 2015.
49. Bianco CL, Toscano JP, Bartberger MD, Fukuto JM. The chemical biology of HNO signaling. *Arch Biochem Biophys* 617: 129-136, 2017.
50. Bienert GP, Chaumont F. Aquaporin-facilitated transmembrane diffusion of hydrogen peroxide. *Biochim Biophys Acta* 1840: 1596-604, 2014.

51. Bohrer AS, Massot V, Innocenti G, Reichheld JP, Issakidis-Bourguet E, Vanacker H. New insights into the reduction systems of plastidial thioredoxins point out the unique properties of thioredoxin z from Arabidopsis. *J Exp Bot* 63: 6315-23, 2012.
52. Broin M, Cuine S, Eymery F, Rey P. The plastidic 2-cysteine peroxiredoxin is a target for a thioredoxin involved in the protection of the photosynthetic apparatus against oxidative damage. *Plant Cell* 14: 1417-32, 2002.
53. Brunkard JO, Runkel AM, Zambryski PC. Chloroplasts extend stromules independently and in response to internal redox signals. *Proc Natl Acad Sci U S A* 112: 10044-9, 2015.
54. Buchanan BB. The Path to Thioredoxin and Redox Regulation in Chloroplasts. *Annu Rev Plant Biol* 67: 1-24, 2016.
55. Buchanan BB, Balmer Y. Redox regulation: a broadening horizon. *Annu Rev Plant Biol* 56: 187-220, 2005.
56. Buchanan BB, Holmgren A, Jacquot JP, Scheibe R. Fifty years in the thioredoxin field and a bountiful harvest. *Biochim Biophys Acta* 1820: 1822-9, 2012.
57. Buchanan BB, Kalberer PP, Arnon DI. Ferredoxin-activated fructose diphosphatase in isolated chloroplasts. *Biochem Biophys Res Commun* 29: 74-9, 1967.
58. Buchanan BB, Schürmann P, Kalberer PP. Ferredoxin-activated fructose diphosphatase of spinach chloroplasts. Resolution of the system, properties of the alkaline fructose diphosphatase component, and physiological significance of the ferredoxin-linked activation. *J Biol Chem* 246: 5952-9, 1971.
59. Buey RM, Arellano JB, Lopez-Maury L, Galindo-Trigo S, Velazquez-Campoy A, Revuelta JL, de Pereda JM, Florencio FJ, Schurmann P, Buchanan BB, Balsera M. Unprecedented pathway of reducing equivalents in a diflavin-linked disulfide oxidoreductase. *Proc Natl Acad Sci U S A* 114: 12725-12730, 2017.
60. Bushweller JH, Billeter M, Holmgren A, Wüthrich K. The nuclear magnetic resonance solution structure of the mixed disulfide between Escherichia coli glutaredoxin (C14S) and glutathione. *J Mol Biol* 235: 1585-97, 1994.
61. Cain P, Hall M, Schröder WP, Kieselbach T, Robinson C. A novel extended family of stromal thioredoxins. *Plant Mol Biol* 70: 273-81, 2009.

62. Cairns NG, Pasternak M, Wachter A, Cobbett CS, Meyer AJ. Maturation of arabidopsis seeds is dependent on glutathione biosynthesis within the embryo. *Plant Physiol* 141: 446-55, 2006.
63. Calderon A, Ortiz-Espin A, Iglesias-Fernandez R, Carbonero P, Pallardo FV, Sevilla F, Jimenez A. Thioredoxin (Trxo1) interacts with proliferating cell nuclear antigen (PCNA) and its overexpression affects the growth of tobacco cell culture. *Redox Biol* 11: 688-700, 2017.
64. Camejo D, Romero-Puertas Mdel C, Rodriguez-Serrano M, Sandalio LM, Lazaro JJ, Jimenez A, Sevilla F. Salinity-induced changes in S-nitrosylation of pea mitochondrial proteins. *J Proteomics* 79: 87-99, 2013.
65. Capitani G, Markovic-Housley Z, DelVal G, Morris M, Jansonius JN, Schürmann P. Crystal structures of two functionally different thioredoxins in spinach chloroplasts. *J Mol Biol* 302: 135-54, 2000.
66. Caplan Jeffrey L, Kumar Amutha S, Park E, Padmanabhan Meenu S, Hoban K, Modla S, Czymmek K, Dinesh-Kumar Savithramma P. Chloroplast Stromules Function during Innate Immunity. *Dev Cell* 34: 45-57, 2015.
67. Caplan JL, Mamillapalli P, Burch-Smith TM, Czymmek K, Dinesh-Kumar SP. Chloroplastic protein NRIP1 mediates innate immune receptor recognition of a viral effector. *Cell* 132: 449-62, 2008.
68. Cardi M, Zaffagnini M, De Lillo A, Castiglia D, Chibani K, Gualberto JM, Rouhier N, Jacquot J-P, Esposito S. Plastidic P2 glucose-6P dehydrogenase from poplar is modulated by thioredoxin m-type: Distinct roles of cysteine residues in redox regulation and NADPH inhibition. *Plant Sci* 252: 257-66, 2016.
69. Carrillo LR, Froehlich JE, Cruz JA, Savage L, Kramer DM. Multi-level regulation of the chloroplast ATP synthase: The chloroplast NADPH thioredoxin reductase C (NTRC) is required for redox modulation specifically under low irradiance. *Plant J* 87: 654-63, 2016.
70. Cavallini D, Federici G, Barboni E. Interaction of proteins with sulfide. *Eur J Biochem* 14: 169-74, 1970.

71. Centeno DC, Osorio S, Nunes-Nesi A, Bertolo ALF, Carneiro RT, Araujo WL, Steinhauser M-C, Michalska J, Rohrmann J, Geigenberger P, Oliver SN, Stitt M, Carrari F, Rose JKC, Fernie AR. Malate Plays a Crucial Role in Starch Metabolism, Ripening, and Soluble Solid Content of Tomato Fruit and Affects Postharvest Softening. *Plant Cell* 23: 162-84, 2011.
72. Chacinska A, Pfannschmidt S, Wiedemann N, Kozjak V, Sanjuan Szklarz LK, Schulze-Specking A, Truscott KN, Guiard B, Meisinger C, Pfanner N. Essential role of Mia40 in import and assembly of mitochondrial intermembrane space proteins. *Embo J* 23: 3735-46, 2004.
73. Chaki M, Shekariesfahlan A, Ageeva A, Mengel A, von Toerne C, Durner J, Lindermayr C. Identification of nuclear target proteins for S-nitrosylation in pathogen-treated Arabidopsis thaliana cell cultures. *Plant Sci* 238: 115-26, 2015.
74. Chamizo-Ampudia A, Sanz-Luque E, Llamas A, Ocana-Calahorro F, Mariscal V, Carreras A, Barroso JB, Galvan A, Fernandez E. A dual system formed by the ARC and NR molybdoenzymes mediates nitrite-dependent NO production in Chlamydomonas. *Plant Cell Environ* 39: 2097-107, 2016.
75. Chang CCC, Ślesak I, Jordá L, Sotnikov A, Melzer M, Miszalski Z, Mullineaux PM, Parker JE, Karpińska B, Karpiński S. Arabidopsis Chloroplastic Glutathione Peroxidases Play a Role in Cross Talk between Photooxidative Stress and Immune Responses. *Plant Physiol* 150: 670-83, 2009.
76. Chardonnet S, Sakr S, Cassier-Chauvat C, Le Maréchal P, Chauvat F, Lemaire SD, Decottignies P. First proteomic study of S-glutathionylation in cyanobacteria. *J Proteome Res* 14: 59-71, 2015.
77. Charles RL, Schroder E, May G, Free P, Gaffney PR, Wait R, Begum S, Heads RJ, Eaton P. Protein sulfenation as a redox sensor: proteomics studies using a novel biotinylated dimedone analogue. *Mol Cell Proteomics* 6: 1473-84, 2007.
78. Chartron J, Shiao C, Stout CD, Carroll KS. 3'-Phosphoadenosine-5'-phosphosulfate Reductase in Complex with Thioredoxin: A Structural Snapshot in the Catalytic Cycle. *Biochemistry* 46: 3942-3951, 2007.

79. Chen J, Wu FH, Wang WH, Zheng CJ, Lin GH, Dong XJ, He JX, Pei ZM, Zheng HL. Hydrogen sulphide enhances photosynthesis through promoting chloroplast biogenesis, photosynthetic enzyme expression, and thiol redox modification in *Spinacia oleracea* seedlings. *J Exp Bot* 62: 4481-93, 2011.
80. Chen KY, Morris JC. Kinetics of oxidation of aqueous sulfide by oxygen. *Environmental science & technology* 6: 529-37, 1972.
81. Cheng NH, Liu JZ, Brock A, Nelson RS, Hirschi KD. AtGRXcp, an Arabidopsis chloroplastic glutaredoxin, is critical for protection against protein oxidative damage. *J Biol Chem* 281: 26280-8, 2006.
82. Cheng NH, Liu JZ, Liu X, Wu Q, Thompson SM, Lin J, Chang J, Whitham SA, Park S, Cohen JD, Hirschi KD. Arabidopsis monothiol glutaredoxin, AtGRXS17, is critical for temperature-dependent postembryonic growth and development via modulating auxin response. *J Biol Chem* 286: 20398-406, 2011.
83. Cheng T, Chen J, Ef AA, Wang P, Wang G, Hu X, Shi J. Quantitative proteomics analysis reveals that S-nitrosoglutathione reductase (GSNOR) and nitric oxide signaling enhance poplar defense against chilling stress. *Planta* 242: 1361-90, 2015.
84. Chibani K, Saul F, Didierjean C, Rouhier N, Haouz A. Structural snapshots along the reaction mechanism of the atypical poplar thioredoxin-like2.1. *FEBS Lett* 592: 1030-1041, 2018.
85. Chibani K, Tarrago L, Gualberto JM, Wingsle G, Rey P, Jacquot J-P, Rouhier N. Atypical thioredoxins in poplar: the glutathione-dependent thioredoxin-like 2.1 supports the activity of target enzymes possessing a single redox active cysteine. *Plant Physiol* 159: 592-605, 2012.
86. Chibani K, Tarrago L, Schürmann P, Jacquot JP, Rouhier N. Biochemical properties of poplar thioredoxin z. *FEBS Lett* 585: 1077-81, 2011.
87. Chibani K, Wingsle G, Jacquot JP, Gelhaye E, Rouhier N. Comparative genomic study of the thioredoxin family in photosynthetic organisms with emphasis on *Populus trichocarpa*. *Mol Plant* 2: 308-22, 2009.
88. Chivers PT, Prehoda KE, Volkman BF, Kim B-M, Markley JL, Raines RT. Microscopic pK a values of *Escherichia coli* thioredoxin. *Biochemistry* 36: 14985-14991, 1997.

89. Chivers PT, Raines RT. General acid/base catalysis in the active site of Escherichia coli thioredoxin. *Biochemistry* 36: 15810-15816, 1997.
90. Choudhury FK, Rivero RM, Blumwald E, Mittler R. Reactive oxygen species, abiotic stress and stress combination. *Plant J* 90: 856-867, 2017.
91. Cobessi D, Tete-Favier F, Marchal S, Azza S, Branlant G, Aubry A. Apo and holo crystal structures of an NADP-dependent aldehyde dehydrogenase from Streptococcus mutans. *J Mol Biol* 290: 161-73, 1999.
92. Collin V, Issakidis-Bourguet E, Marchand C, Hirasawa M, Lancelin JM, Knaff DB, Miginiac-Maslow M. The Arabidopsis plastidial thioredoxins: new functions and new insights into specificity. *J Biol Chem* 278: 23747-52, 2003.
93. Collin V, Lamkemeyer P, Miginiac-Maslow M, Hirasawa M, Knaff DB, Dietz KJ, Issakidis-Bourguet E. Characterization of plastidial thioredoxins from Arabidopsis belonging to the new γ -type. *Plant Physiol* 136: 4088-95, 2004.
94. Considine MJ, Diaz-Vivancos P, Kerchev P, Signorelli S, Agudelo-Romero P, Gibbs DJ, Foyer CH. Learning To Breathe: Developmental Phase Transitions in Oxygen Status. *Trends in Plant Science* 22: 140-153, 2017.
95. Considine MJ, Foyer CH. Redox regulation of plant development. *Antioxid Redox Signal* 21: 1305-26, 2014.
96. Copley SD, Novak WR, Babbitt PC. Divergence of function in the thioredoxin fold suprafamily: evidence for evolution of peroxiredoxins from a thioredoxin-like ancestor. *Biochemistry* 43: 13981-95, 2004.
97. Corpas FJ, Alche JD, Barroso JB. Current overview of S-nitrosoglutathione (GSNO) in higher plants. *Front Plant Sci* 4: 126, 2013.
98. Coudeville N, Thureau A, Hemmerlin C, Gelhaye E, Jacquot JP, Cung MT. Solution structure of a natural CPPC active site variant, the reduced form of thioredoxin h1 from poplar. *Biochemistry* 44: 2001-8, 2005.
99. Courteille A, Vesa S, Sanz-Barrio R, Cazale A-C, Becuwe-Linka N, Farran I, Havaux M, Rey P, Rumeau D. Thioredoxin m4 Controls Photosynthetic Alternative Electron Pathways in Arabidopsis. *Plant Physiol* 161: 508-20, 2013.
100. Couturier J, Jacquot JP, Rouhier N. Evolution and diversity of glutaredoxins in photosynthetic organisms. *Cell Mol Life Sci* 66: 2539-57, 2009.

101. Couturier J, Jacquot JP, Rouhier N. Toward a refined classification of class I dithiol glutaredoxins from poplar: biochemical basis for the definition of two subclasses. *Front Plant Sci* 4: 518, 2013.
102. Couturier J, Koh CS, Zaffagnini M, Winger AM, Gualberto JM, Corbier C, Decottignies P, Jacquot JP, Lemaire SD, Didierjean C, Rouhier N. Structure-function relationship of the chloroplastic glutaredoxin S12 with an atypical WCSYS active site. *J Biol Chem* 284: 9299-310, 2009.
103. Couturier J, Przybyla-Toscano J, Roret T, Didierjean C, Rouhier N. The roles of glutaredoxins ligating Fe-S clusters: Sensing, transfer or repair functions? *Biochim Biophys Acta* 1853: 1513-27, 2015.
104. Couturier J, Stroher E, Albetel AN, Roret T, Muthuramalingam M, Tarrago L, Seidel T, Tsan P, Jacquot JP, Johnson MK, Dietz KJ, Didierjean C, Rouhier N. Arabidopsis chloroplastic glutaredoxin C5 as a model to explore molecular determinants for iron-sulfur cluster binding into glutaredoxins. *J Biol Chem* 286: 27515-27, 2011.
105. Couvertier SM, Zhou Y, Weerapana E. Chemical-proteomic strategies to investigate cysteine posttranslational modifications. *Biochim Biophys Acta* 1844: 2315-30, 2014.
106. Cuevasanta E, Lange M, Bonanata J, Coitino EL, Ferrer-Sueta G, Filipovic MR, Alvarez B. Reaction of Hydrogen Sulfide with Disulfide and Sulfenic Acid to Form the Strongly Nucleophilic Persulfide. *J Biol Chem* 290: 26866-80, 2015.
107. Czapski G, Goldstein S. The role of the reactions of .NO with superoxide and oxygen in biological systems: a kinetic approach. *Free Radic Biol Med* 19: 785-94, 1995.
108. Da Q, Wang P, Wang M, Sun T, Jin H, Liu B, Wang J, Grimm B, Wang H-B. Thioredoxin and NADPH-dependent thioredoxin reductase C regulation of Tetrapyrrole Biosynthesis. *Plant Physiol* 175: 652-66, 2017.
109. Daloso DM, Mueller K, Obata T, Florian A, Tohge T, Bottcher A, Riondet C, Banat L, Carrari F, Nunes-Nesi A, Buchanan BB, Reichheld J-P, Araujo WL, Fernie AR. Thioredoxin, a master regulator of the tricarboxylic acid cycle in plant mitochondria. *Proc Natl Acad Sci U S A* 112: 1392-400, 2015.
110. Dangoor I, Peled-Zehavi H, Levitan A, Pasand O, Danon A. A small family of chloroplast atypical thioredoxins. *Plant Physiol* 149: 1240-50, 2009.

111. Dangoor I, Peled-Zehavi H, Wittenberg G, Danon A. A chloroplast light-regulated oxidative sensor for moderate light intensity in Arabidopsis. *Plant Cell* 24: 1894-906, 2012.
112. Danon A. Environmentally-induced oxidative stress and its signaling. In: *Photosynthesis*. Springer; 2012. pp. 319-330.
113. Davies MJ. Protein oxidation and peroxidation. *Biochem J* 473: 805-25, 2016.
114. Declercq JP, Evrard C, Clippe A, Stricht DV, Bernard A, Knoop B. Crystal structure of human peroxiredoxin 5, a novel type of mammalian peroxiredoxin at 1.5 Å resolution. *J Mol Biol* 311: 751-9, 2001.
115. Del Rio LA, Lopez-Huertas E. ROS Generation in Peroxisomes and its Role in Cell Signaling. *Plant Cell Physiol* 57: 1364-1376, 2016.
116. Delaunay A, Pflieger D, Barrault MB, Vinh J, Toledano MB. A thiol peroxidase is an H₂O₂ receptor and redox-transducer in gene activation. *Cell* 111: 471-81, 2002.
117. Delledonne M, Xia Y, Dixon RA, Lamb C. Nitric oxide functions as a signal in plant disease resistance. *Nature* 394: 585-8, 1998.
118. Delorme-Hinoux V, Bangash SA, Meyer AJ, Reichheld JP. Nuclear thiol redox systems in plants. *Plant Sci* 243: 84-95, 2016.
119. Delprato ML, Krapp AR, Carrillo N. Green Light to Plant Responses to Pathogens: The Role of Chloroplast Light-Dependent Signaling in Biotic Stress. *Photochem Photobiol* 91: 1004-11, 2015.
120. Diaz-Vivancos P, de Simone A, Kiddle G, Foyer CH. Glutathione--linking cell proliferation to oxidative stress. *Free Radic Biol Med* 89: 1154-64, 2015.
121. Diaz Vivancos P, Wolff T, Markovic J, Pallardo FV, Foyer CH. A nuclear glutathione cycle within the cell cycle. *Biochem J* 431: 169-78, 2010.
122. Dietz K-J. Efficient high light acclimation involves rapid processes at multiple mechanistic levels. *J Exp Bot* 66: 2401-14, 2015.
123. Dietz K-J, Turkan I, Krieger-Liszkay A. Redox- and Reactive Oxygen Species-Dependent Signaling into and out of the Photosynthesizing Chloroplast. *Plant Physiol* 171: 1541-50, 2016.
124. Dietz KJ. Peroxiredoxins in plants and cyanobacteria. *Antioxid Redox Signal* 15: 1129-59, 2011.

125. Dissmeyer N, Rivas S, Graciet E. Life and death of proteins after protease cleavage: protein degradation by the N-end rule pathway. *New Phytol*, 2017.
126. Dixon DP, Skipsey M, Grundy NM, Edwards R. Stress-induced protein S-glutathionylation in Arabidopsis. *Plant Physiol* 138: 2233-44, 2005.
127. Doka E, Pader I, Biro A, Johansson K, Cheng Q, Ballago K, Prigge JR, Pastor-Flores D, Dick TP, Schmidt EE, Arner ES, Nagy P. A novel persulfide detection method reveals protein persulfide- and polysulfide-reducing functions of thioredoxin and glutathione systems. *Sci Adv* 2: e1500968, 2016.
128. Dooley CT, Dore TM, Hanson GT, Jackson WC, Remington SJ, Tsien RY. Imaging dynamic redox changes in mammalian cells with green fluorescent protein indicators. *J Biol Chem* 279: 22284-93, 2004.
129. Doulias PT, Greene JL, Greco TM, Tenopoulou M, Seeholzer SH, Dunbrack RL, Ischiropoulos H. Structural profiling of endogenous S-nitrosocysteine residues reveals unique features that accommodate diverse mechanisms for protein S-nitrosylation. *Proc Natl Acad Sci U S A* 107: 16958-63, 2010.
130. Du H, Kim S, Nam KH, Lee MS, Son O, Lee SH, Cheon CI. Identification of uricase as a potential target of plant thioredoxin: Implication in the regulation of nodule development. *Biochem Biophys Res Commun* 397: 22-6, 2010.
131. Dubreuil-Maurizi C, Poinssot B. Role of glutathione in plant signaling under biotic stress. *Plant Signal Behav* 7: 210-2, 2012.
132. Dubreuil-Maurizi C, Vitecek J, Marty L, Branciard L, Frettinger P, Wendehenne D, Meyer AJ, Mauch F, Poinssot B. Glutathione deficiency of the Arabidopsis mutant pad2-1 affects oxidative stress-related events, defense gene expression, and the hypersensitive response. *Plant Physiol* 157: 2000-12, 2011.
133. Eliyahu E, Rog I, Inbal D, Danon A. ACHT4-driven oxidation of APS1 attenuates starch synthesis under low light intensity in Arabidopsis plants. *Proc Natl Acad Sci U S A* 112: 12876-81, 2015.
134. Exposito-Rodriguez M, Laissue PP, Yvon-Durocher G, Smirnoff N, Mullineaux PM. Photosynthesis-dependent H₂O₂ transfer from chloroplasts to nuclei provides a high-light signalling mechanism. *Nat Commun* 8: 49, 2017.

135. Faccenda A, Bonham CA, Vacratsis PO, Zhang X, Mutus B. Gold nanoparticle enrichment method for identifying S-nitrosylation and S-glutathionylation sites in proteins. *J Am Chem Soc* 132: 11392-4, 2010.
136. Fares A, Rossignol M, Peltier JB. Proteomics investigation of endogenous S-nitrosylation in Arabidopsis. *Biochem Biophys Res Commun* 416: 331-6, 2011.
137. Farmer EE, Mueller MJ. ROS-mediated lipid peroxidation and RES-activated signaling. *Annu Rev Plant Biol* 64: 429-50, 2013.
138. Farnese FS, Menezes-Silva PE, Gusman GS, Oliveira JA. When Bad Guys Become Good Ones: The Key Role of Reactive Oxygen Species and Nitric Oxide in the Plant Responses to Abiotic Stress. *Front Plant Sci* 7: 471, 2016.
139. Feechan A, Kwon E, Yun BW, Wang Y, Pallas JA, Loake GJ. A central role for S-nitrosothiols in plant disease resistance. *Proc Natl Acad Sci U S A* 102: 8054-9, 2005.
140. Feng J, Wang C, Chen Q, Chen H, Ren B, Li X, Zuo J. S-nitrosylation of phosphotransfer proteins represses cytokinin signaling. *Nat Commun* 4: 1529, 2013.
141. Feng S, Chen Y, Yang F, Zhang L, Gong Y, Adilijiang G, Gao Y, Deng H. Development of a Clickable Probe for Profiling of Protein Glutathionylation in the Central Cellular Metabolism of *E. coli* and *Drosophila*. *Chem Biol* 22: 1461-9, 2015.
142. Feng Y, Zhong N, Rouhier N, Hase T, Kusunoki M, Jacquot JP, Jin C, Xia B. Structural insight into poplar glutaredoxin C1 with a bridging iron-sulfur cluster at the active site. *Biochemistry* 45: 7998-8008, 2006.
143. Fermani S, Sparla F, Falini G, Martelli PL, Casadio R, Pupillo P, Ripamonti A, Trost P. Molecular mechanism of thioredoxin regulation in photosynthetic A2B2-glyceraldehyde-3-phosphate dehydrogenase. *Proc Natl Acad Sci U S A* 104: 11109-14, 2007.
144. Fermani S, Trivelli X, Sparla F, Thumiger A, Calvaresi M, Marri L, Falini G, Zerbetto F, Trost P. Conformational selection and folding-upon-binding of intrinsically disordered protein CP12 regulate photosynthetic enzymes assembly. *J Biol Chem* 287: 21372-83, 2012.

145. Fernandes AP, Fladvad M, Berndt C, Andresen C, Lillig CH, Neubauer P, Sunnerhagen M, Holmgren A, Vlamis-Gardikas A. A novel monothiol glutaredoxin (Grx4) from *Escherichia coli* can serve as a substrate for thioredoxin reductase. *J Biol Chem* 280: 24544-52, 2005.
146. Ferrer-Sueta G, Manta B, Botti H, Radi R, Trujillo M, Denicola A. Factors affecting protein thiol reactivity and specificity in peroxide reduction. *Chem Res Toxicol* 24: 434-50, 2011.
147. Finkemeier I, Goodman M, Lamkemeyer P, Kandlbinder A, Sweetlove LJ, Dietz KJ. The mitochondrial type II peroxiredoxin F is essential for redox homeostasis and root growth of *Arabidopsis thaliana* under stress. *J Biol Chem* 280: 12168-80, 2005.
148. Fischer BB, Hideg E, Krieger-Liszkay A. Production, detection, and signaling of singlet oxygen in photosynthetic organisms. *Antioxid Redox Signal* 18: 2145-62, 2013.
149. Florez-Sarasa I, Flexas J, Rasmusson AG, Umbach AL, Siedow JN, Ribas-Carbo M. In vivo cytochrome and alternative pathway respiration in leaves of *Arabidopsis thaliana* plants with altered alternative oxidase under different light conditions. *Plant Cell Environ* 34: 1373-83, 2011.
150. Foloppe N, Sagemark J, Nordstrand K, Berndt KD, Nilsson L. Structure, dynamics and electrostatics of the active site of glutaredoxin 3 from *Escherichia coli*: comparison with functionally related proteins1. *J Mol Biol* 310: 449-70, 2001.
151. Foresi N, Correa-Aragunde N, Parisi G, Calo G, Salerno G, Lamattina L. Characterization of a nitric oxide synthase from the plant kingdom: NO generation from the green alga *Ostreococcus tauri* is light irradiance and growth phase dependent. *Plant Cell* 22: 3816-30, 2010.
152. Forrester MT, Thompson JW, Foster MW, Nogueira L, Moseley MA, Stamler JS. Proteomic analysis of S-nitrosylation and denitrosylation by resin-assisted capture. *Nat Biotechnol* 27: 557-9, 2009.
153. Foster MW, Forrester MT, Stamler JS. A protein microarray-based analysis of S-nitrosylation. *Proc Natl Acad Sci U S A* 106: 18948-53, 2009.

154. Foyer CH, Karpinska B, Krupinska K. The functions of WHIRLY1 and REDOX-RESPONSIVE TRANSCRIPTION FACTOR 1 in cross tolerance responses in plants: a hypothesis. *Philosophical Transactions of the Royal Society B: Biological Sciences* 369: 20130226, 2014.
155. Foyer CH, Noctor G. Redox homeostasis and antioxidant signaling: a metabolic interface between stress perception and physiological responses. *Plant Cell* 17: 1866-75, 2005.
156. Foyer CH, Noctor G. Redox regulation in photosynthetic organisms: signaling, acclimation, and practical implications. *Antioxid Redox Signal* 11: 861-905, 2009.
157. Foyer CH, Noctor G. Ascorbate and glutathione: the heart of the redox hub. *Plant Physiol* 155: 2-18, 2011.
158. Foyer CH, Noctor G. Stress-triggered redox signalling: what's in pROspect? *Plant Cell Environ* 39: 951-64, 2016.
159. Foyer CH, Ruban AV, Noctor G. Viewing oxidative stress through the lens of oxidative signalling rather than damage. *Biochem J* 474: 877-883, 2017.
160. Fratelli M, Demol H, Puype M, Casagrande S, Eberini I, Salmona M, Bonetto V, Mengozzi M, Duffieux F, Miclet E, Bachi A, Vandekerckhove J, Gianazza E, Ghezzi P. Identification by redox proteomics of glutathionylated proteins in oxidatively stressed human T lymphocytes. *Proc Natl Acad Sci U S A* 99: 3505-10, 2002.
161. Frederickson Matika DE, Loake GJ. Redox regulation in plant immune function. *Antioxid Redox Signal* 21: 1373-88, 2014.
162. Frungillo L, Skelly MJ, Loake GJ, Spoel SH, Salgado I. S-nitrosothiols regulate nitric oxide production and storage in plants through the nitrogen assimilation pathway. *Nat Commun* 5: 5401, 2014.
163. Gallogly MM, Starke DW, Leonberg AK, Ospina SM, Mieyal JJ. Kinetic and mechanistic characterization and versatile catalytic properties of mammalian glutaredoxin 2: implications for intracellular roles. *Biochemistry* 47: 11144-57, 2008.
164. Gama F, Keech O, Eymery F, Finkemeier I, Gelhaye E, Gardestrom P, Dietz KJ, Rey P, Jacquot J-P, Rouhier N. The mitochondrial type II peroxiredoxin from poplar. *Physiol Plant* 129: 196-206, 2007.

165. Gao XH, Krokowski D, Guan BJ, Bederman I, Majumder M, Parisien M, Diatchenko L, Kabil O, Willard B, Banerjee R, Wang B, Bebek G, Evans CR, Fox PL, Gerson SL, Hoppel CL, Liu M, Arvan P, Hatzoglou M. Quantitative H₂S-mediated protein sulfhydration reveals metabolic reprogramming during the integrated stress response. *Elife* 4: e10067, 2015.
166. Gao XH, Zaffagnini M, Bedhomme M, Michelet L, Cassier-Chauvat C, Decottignies P, Lemaire SD. Biochemical characterization of glutaredoxins from *Chlamydomonas reinhardtii*: kinetics and specificity in deglutathionylation reactions. *FEBS Lett* 584: 2242-8, 2010.
167. Garcia-Santamarina S, Boronat S, Domenech A, Ayte J, Molina H, Hidalgo E. Monitoring in vivo reversible cysteine oxidation in proteins using ICAT and mass spectrometry. *Nat Protoc* 9: 1131-45, 2014.
168. Gascuel O. BIONJ: an improved version of the NJ algorithm based on a simple model of sequence data. *Molecular biology and evolution* 14: 685-695, 1997.
169. Gebicki S, Gebicki JM. Formation of peroxides in amino acids and proteins exposed to oxygen free radicals. *Biochem J* 289 (Pt 3): 743-9, 1993.
170. Geigenberger P. Response of plant metabolism to too little oxygen. *Curr Opin Plant Biol* 6: 247-56, 2003.
171. Geigenberger P, Thormählen I, Daloso DM, Fernie AR. The Unprecedented Versatility of the Plant Thioredoxin System. *Trends Plant Sci* 22: 249-62, 2017.
172. Gelhaye E, Rouhier N, Gérard J, Jolivet Y, Gualberto J, Navrot N, Ohlsson PI, Wingsle G, Hirasawa M, Knaff DB, Wang H, Dizengremel P, Meyer Y, Jacquot JP. A specific form of thioredoxin h occurs in plant mitochondria and regulates the alternative oxidase. *Proc Natl Acad Sci U S A* 101: 14545-50, 2004.
173. Gelhaye E, Rouhier N, Jacquot JP. Evidence for a subgroup of thioredoxin h that requires GSH/Grx for its reduction. *FEBS Lett* 555: 443-8, 2003.
174. Geng B, Yang J, Qi Y, Zhao J, Pang Y, Du J, Tang C. H₂S generated by heart in rat and its effects on cardiac function. *Biochem Biophys Res Commun* 313: 362-8, 2004.

175. Gergondey R, Garcia C, Marchand CH, Lemaire SD, Camadro JM, Auchere F. Modulation of the specific glutathionylation of mitochondrial proteins in the yeast *Saccharomyces cerevisiae* under basal and stress conditions. *Biochem J* 474: 1175-1193, 2017.
176. Gibbs DJ, Bailey M, Tedds HM, Holdsworth MJ. From start to finish: amino-terminal protein modifications as degradation signals in plants. *New Phytol* 211: 1188-94, 2016.
177. Gibbs DJ, Conde JV, Berckhan S, Prasad G, Mendiondo GM, Holdsworth MJ. Group VII Ethylene Response Factors Coordinate Oxygen and Nitric Oxide Signal Transduction and Stress Responses in Plants. *Plant Physiol* 169: 23-31, 2015.
178. Gibbs DJ, Lee SC, Isa NM, Gramuglia S, Fukao T, Bassel GW, Correia CS, Corbineau F, Theodoulou FL, Bailey-Serres J, Holdsworth MJ. Homeostatic response to hypoxia is regulated by the N-end rule pathway in plants. *Nature* 479: 415-8, 2011.
179. Gibbs DJ, Md Isa N, Movahedi M, Lozano-Juste J, Mendiondo GM, Berckhan S, Marin-de la Rosa N, Vicente Conde J, Sousa Correia C, Pearce SP, Bassel GW, Hamali B, Talloji P, Tome DF, Coego A, Beynon J, Alabadi D, Bachmair A, Leon J, Gray JE, Theodoulou FL, Holdsworth MJ. Nitric oxide sensing in plants is mediated by proteolytic control of group VII ERF transcription factors. *Mol Cell* 53: 369-79, 2014.
180. Giuntoli B, Shukla V, Maggiorelli F, Giorgi FM, Lombardi L, Perata P, Licausi F. Age-dependent regulation of ERF-VII transcription factor activity in *Arabidopsis thaliana*. *Plant Cell Environ*, 2017.
181. Giustarini D, Milzani A, Aldini G, Carini M, Rossi R, Dalle-Donne I. S-nitrosation versus S-glutathionylation of protein sulfhydryl groups by S-nitrosoglutathione. *Antioxid Redox Signal* 7: 930-9, 2005.
182. Go YM, Chandler JD, Jones DP. The cysteine proteome. *Free Radic Biol Med* 84: 227-245, 2015.
183. Go YM, Jones DP. Redox biology: interface of the exposome with the proteome, epigenome and genome. *Redox Biol* 2: 358-60, 2014.
184. Gollan PJ, Tikkanen M, Aro EM. Photosynthetic light reactions: integral to chloroplast retrograde signalling. *Curr Opin Plant Biol* 27: 180-91, 2015.

185. Gotor C, Alvarez C, Bermudez MA, Moreno I, Garcia I, Romero LC. Low abundance does not mean less importance in cysteine metabolism. *Plant Signal Behav* 5: 1028-30, 2010.
186. Gould NS, Evans P, Martinez-Acedo P, Marino SM, Gladyshev VN, Carroll KS, Ischiropoulos H. Site-Specific Proteomic Mapping Identifies Selectively Modified Regulatory Cysteine Residues in Functionally Distinct Protein Networks. *Chem Biol* 22: 965-75, 2015.
187. Goyer A, Haslekas C, Miginiac-Maslow M, Klein U, Le Maréchal P, Jacquot JP, Decottignies P. Isolation and characterization of a thioredoxin-dependent peroxidase from *Chlamydomonas reinhardtii*. *Eur J Biochem* 269: 272-82, 2002.
188. Graciet E, Walter F, O'Maoileidigh DS, Pollmann S, Meyerowitz EM, Varshavsky A, Wellmer F. The N-end rule pathway controls multiple functions during Arabidopsis shoot and leaf development. *Proc Natl Acad Sci U S A* 106: 13618-23, 2009.
189. Greetham D, Vickerstaff J, Shenton D, Perrone GG, Dawes IW, Grant CM. Thioredoxins function as deglutathionylase enzymes in the yeast *Saccharomyces cerevisiae*. *BMC Biochem* 11: 3, 2010.
190. Gross E, Sevier CS, Heldman N, Vitu E, Bentzur M, Kaiser CA, Thorpe C, Fass D. Generating disulfides enzymatically: reaction products and electron acceptors of the endoplasmic reticulum thiol oxidase Ero1p. *Proc Natl Acad Sci U S A* 103: 299-304, 2006.
191. Gross F, Durner J, Gaupels F. Nitric oxide, antioxidants and prooxidants in plant defence responses. *Front Plant Sci* 4: 419, 2013.
192. Gruber CW, Cemazar M, Heras B, Martin JL, Craik DJ. Protein disulfide isomerase: the structure of oxidative folding. *Trends Biochem Sci* 31: 455-64, 2006.
193. Guerra D, Ballard K, Truebridge I, Vierling E. S-Nitrosation of Conserved Cysteines Modulates Activity and Stability of S-Nitrosoglutathione Reductase (GSNOR). *Biochemistry* 55: 2452-64, 2016.
194. Guo J, Nguyen AY, Dai Z, Su D, Gaffrey MJ, Moore RJ, Jacobs JM, Monroe ME, Smith RD, Koppelaar DW, Pakrasi HB, Qian WJ. Proteome-wide light/dark modulation of thiol oxidation in cyanobacteria revealed by quantitative site-specific redox proteomics. *Mol Cell Proteomics* 13: 3270-85, 2014.

195. Guo Y, Huang C, Xie Y, Song F, Zhou X. A tomato glutaredoxin gene SIGRX1 regulates plant responses to oxidative, drought and salt stresses. *Planta* 232: 1499-509, 2010.
196. Gupta KJ, Fernie AR, Kaiser WM, van Dongen JT. On the origins of nitric oxide. *Trends Plant Sci* 16: 160-8, 2011.
197. Gupta V, Carroll KS. Sulfenic acid chemistry, detection and cellular lifetime. *Biochim Biophys Acta* 1840: 847-75, 2014.
198. Gupta V, Paritala H, Carroll KS. Reactivity, Selectivity, and Stability in Sulfenic Acid Detection: A Comparative Study of Nucleophilic and Electrophilic Probes. *Bioconjug Chem* 27: 1411-8, 2016.
199. Gupta V, Yang J, Liebler DC, Carroll KS. Diverse Redoxome Reactivity Profiles of Carbon Nucleophiles. *J Am Chem Soc* 139: 5588-5595, 2017.
200. Gutle DD, Roret T, Muller SJ, Couturier J, Lemaire SD, Hecker A, Dhalleine T, Buchanan BB, Reski R, Einsle O, Jacquot JP. Chloroplast FBPase and SBPase are thioredoxin-linked enzymes with similar architecture but different evolutionary histories. *Proc Natl Acad Sci U S A* 113: 6779-84, 2016.
201. Gutsche N, Thurow C, Zachgo S, Gatz C. Plant-specific CC-type glutaredoxins: functions in developmental processes and stress responses. *Biol Chem* 396: 495-509, 2015.
202. Gutsche M, Pauleau AL, Marty L, Brach T, Wabnitz GH, Samstag Y, Meyer AJ, Dick TP. Real-time imaging of the intracellular glutathione redox potential. *Nature Meth* 5: 553-9, 2008.
203. Gutsche M, Sobotta MC, Wabnitz GH, Ballikaya S, Meyer AJ, Samstag Y, Dick TP. Proximity-based protein thiol oxidation by H₂O₂-scavenging peroxidases. *J Biol Chem* 284: 31532-40, 2009.
204. Hadrich N, Hendriks JH, Kotting O, Arrivault S, Feil R, Zeeman SC, Gibon Y, Schulze WX, Stitt M, Lunn JE. Mutagenesis of cysteine 81 prevents dimerization of the APS1 subunit of ADP-glucose pyrophosphorylase and alters diurnal starch turnover in *Arabidopsis thaliana* leaves. *Plant J* 70: 231-42, 2012.

205. Hagglund P, Bunkenborg J, Maeda K, Finnie C, Svensson B. Identification of thioredoxin target disulfides using isotope-coded affinity tags. *Methods Mol Biol* 1072: 677-85, 2014.
206. Hagglund P, Bunkenborg J, Maeda K, Svensson B. Identification of thioredoxin disulfide targets using a quantitative proteomics approach based on isotope-coded affinity tags. *J Proteome Res* 7: 5270-6, 2008.
207. Hall A, Nelson K, Poole LB, Karplus PA. Structure-based insights into the catalytic power and conformational dexterity of peroxiredoxins. *Antioxid Redox Signal* 15: 795-815, 2011.
208. Hall M, Mata-Cabana A, Akerlund HE, Florencio FJ, Schroder WP, Lindahl M, Kieselbach T. Thioredoxin targets of the plant chloroplast lumen and their implications for plastid function. *Proteomics* 10: 987-1001, 2010.
209. Hamnell-Pamment Y, Lind C, Palmberg C, Bergman T, Cotgreave IA. Determination of site-specificity of S-glutathionylated cellular proteins. *Biochem Biophys Res Commun* 332: 362-9, 2005.
210. Hao G, Derakhshan B, Shi L, Campagne F, Gross SS. SNOSID, a proteomic method for identification of cysteine S-nitrosylation sites in complex protein mixtures. *Proc Natl Acad Sci U S A* 103: 1012-7, 2006.
211. Hao G, Gross SS. Electrospray tandem mass spectrometry analysis of S- and N-nitrosopeptides: facile loss of NO and radical-induced fragmentation. *J Am Soc Mass Spectrom* 17: 1725-30, 2006.
212. Hara S, Motohashi K, Arisaka F, Romano PG, Hosoya-Matsuda N, Kikuchi N, Fusada N, Hisabori T. Thioredoxin-h1 reduces and reactivates the oxidized cytosolic malate dehydrogenase dimer in higher plants. *J Biol Chem* 281: 32065-71, 2006.
213. Hartmann SK, Stockdreher Y, Wandrey G, Hosseinpour Tehrani H, Zambanini T, Meyer AJ, Buchs J, Blank LM, Schwarzlander M, Wierckx N. Online in vivo monitoring of cytosolic NAD redox dynamics in *Ustilago maydis*. *Biochim Biophys Acta*, 2018.
214. Held JM, Gibson BW. Regulatory control or oxidative damage? Proteomic approaches to interrogate the role of cysteine oxidation status in biological processes. *Mol Cell Proteomics* 11: R111 013037, 2012.

215. Heldt WH, Werdan K, Milovancev M, Geller G. Alkalization of the chloroplast stroma caused by light-dependent proton flux into the thylakoid space. *Biochim Biophys Acta* 314: 224-41, 1973.
216. Heller J, Meyer AJ, Tudzynski P. Redox-sensitive GFP2: use of the genetically encoded biosensor of the redox status in the filamentous fungus *Botrytis cinerea*. *Mol Plant Pathol* 13: 935-47, 2012.
217. Henard CA, Guarnieri MT, Knoshaug EP. The *Chlorella vulgaris* S-Nitrosoproteome under Nitrogen-Replete and -Deplete Conditions. *Front Bioeng Biotechnol* 4: 100, 2016.
218. Herrera-Vasquez A, Salinas P, Holuigue L. Salicylic acid and reactive oxygen species interplay in the transcriptional control of defense genes expression. *Front Plant Sci* 6: 171, 2015.
219. Heyno E, Innocenti G, Lemaire SD, Issakidis-Bourguet E, Krieger-Liszkay A. Putative role of the malate valve enzyme NADP-malate dehydrogenase in H₂O₂ signalling in *Arabidopsis*. *Philos Trans R Soc Lond B Biol Sci* 369: 20130228, 2014.
220. Hildebrandt T, Knuesting J, Berndt C, Morgan B, Scheibe R. Cytosolic thiol switches regulating basic cellular functions: GAPDH as an information hub? *Biol Chem* 396: 523-37, 2015.
221. Hind G, Nakatani HY, Izawa S. Light-dependent redistribution of ions in suspensions of chloroplast thylakoid membranes. *Proc Natl Acad Sci U S A* 71: 1484-8, 1974.
222. Hirasawa M, Ruelland E, Schepens I, Issakidis-Bourguet E, Miginiac-Maslow M, Knaff DB. Oxidation-reduction properties of the regulatory disulfides of sorghum chloroplast nicotinamide adenine dinucleotide phosphate-malate dehydrogenase. *Biochemistry* 39: 3344-50, 2000.
223. Hirasawa M, Schürmann P, Jacquot JP, Manieri W, Jacquot P, Keryer E, Hartman FC, Knaff DB. Oxidation-reduction properties of chloroplast thioredoxins, ferredoxin:thioredoxin reductase, and thioredoxin f-regulated enzymes. *Biochemistry* 38: 5200-5, 1999.
224. Holmgren A, Soderberg BO, Eklund H, Branden CI. Three-dimensional structure of *Escherichia coli* thioredoxin-S2 to 2.8 Å resolution. *Proc Natl Acad Sci U S A* 72: 2305-9, 1975.

225. Horling F, Lamkemeyer P, Konig J, Finkemeier I, Kandlbinder A, Baier M, Dietz KJ. Divergent light-, ascorbate-, and oxidative stress-dependent regulation of expression of the peroxiredoxin gene family in Arabidopsis. *Plant Physiol* 131: 317-25, 2003.
226. Hoshi T, Heinemann S. Regulation of cell function by methionine oxidation and reduction. *J Physiol* 531: 1-11, 2001.
227. Hosoya-Matsuda N, Motohashi K, Yoshimura H, Nozaki A, Inoue K, Ohmori M, Hisabori T. Anti-oxidative stress system in cyanobacteria. Significance of type II peroxiredoxin and the role of 1-Cys peroxiredoxin in *Synechocystis* sp. strain PCC 6803. *J Biol Chem* 280: 840-6, 2005.
228. Hou X, Hu W-W, Shen L, Lee LYC, Tao Z, Han J-H, Yu H. Global identification of DELLA target genes during Arabidopsis flower development. *Plant Physiol* 147: 1126-42, 2008.
229. Hu J, Huang X, Chen L, Sun X, Lu C, Zhang L, Wang Y, Zuo J. Site-specific nitrosoproteomic identification of endogenously S-nitrosylated proteins in Arabidopsis. *Plant Physiol* 167: 1731-46, 2015.
230. Huang S, Van Aken O, Schwarzlander M, Belt K, Millar AH. The Roles of Mitochondrial Reactive Oxygen Species in Cellular Signaling and Stress Response in Plants. *Plant Physiol* 171: 1551-9, 2016.
231. Hung YP, Albeck JG, Tantama M, Yellen G. Imaging cytosolic NADH-NAD(+) redox state with a genetically encoded fluorescent biosensor. *Cell Metab* 14: 545-54, 2011.
232. Ikegami A, Yoshimura N, Motohashi K, Takahashi S, Romano PG, Hisabori T, Takamiya K, Masuda T. The CHL1 subunit of Arabidopsis thaliana magnesium chelatase is a target protein of the chloroplast thioredoxin. *J Biol Chem* 282: 19282-91, 2007.
233. Inigo S, Durand AN, Ritter A, Le Gall S, Termathe M, Klassen R, Tohge T, De Coninck B, Van Leene J, De Clercq R, Cammue BP, Fernie AR, Gevaert K, De Jaeger G, Leidel SA, Schaffrath R, Van Lijsebettens M, Pauwels L, Goossens A. Glutaredoxin GRXS17 Associates with the Cytosolic Iron-Sulfur Cluster Assembly Pathway. *Plant Physiol* 172: 858-873, 2016.

234. Ishiga Y, Ishiga T, Ikeda Y, Matsuura T, Mysore KS. NADPH-dependent thioredoxin reductase C plays a role in nonhost disease resistance against *Pseudomonas syringae* pathogens by regulating chloroplast-generated reactive oxygen species. *PeerJ* 4: e1938, 2016.
235. Ishiga Y, Ishiga T, Wangdi T, Mysore KS, Uppalapati SR. NTRC and chloroplast-generated reactive oxygen species regulate *Pseudomonas syringae* pv. tomato disease development in tomato and *Arabidopsis*. *Mol Plant Microbe Interact* 25: 294-306, 2012.
236. Ito H, Iwabuchi M, Ogawa K. The sugar-metabolic enzymes aldolase and triose-phosphate isomerase are targets of glutathionylation in *Arabidopsis thaliana*: detection using biotinylated glutathione. *Plant Cell Physiol* 44: 655-60, 2003.
237. Jacques S, Ghesquiere B, De Bock PJ, Demol H, Wahni K, Willems P, Messens J, Van Breusegem F, Gevaert K. Protein Methionine Sulfoxide Dynamics in *Arabidopsis thaliana* under Oxidative Stress. *Mol Cell Proteomics* 14: 1217-29, 2015.
238. Jacques S, Ghesquiere B, Van Breusegem F, Gevaert K. Plant proteins under oxidative attack. *Proteomics* 13: 932-40, 2013.
239. Jacquot J-P, Eklund H, Rouhier N, Schürmann P. Structural and evolutionary aspects of thioredoxin reductases in photosynthetic organisms. *Trends Plant Sci* 14: 336-43, 2009.
240. Jacquot JP, Buchanan BB. Enzyme Regulation in C(4) Photosynthesis : purification and properties of thioredoxin-linked NADP-malate dehydrogenase from corn leaves. *Plant Physiol* 68: 300-4, 1981.
241. Jaffrey SR, Erdjument-Bromage H, Ferris CD, Tempst P, Snyder SH. Protein S-nitrosylation: a physiological signal for neuronal nitric oxide. *Nat Cell Biol* 3: 193-7, 2001.
242. Jagodnik J, Brosse A, Le Lam TN, Chiaruttini C, Guillier M. Mechanistic study of base-pairing small regulatory RNAs in bacteria. *Methods*, 2016.
243. Jeong W, Bae SH, Toledano MB, Rhee SG. Role of sulfiredoxin as a regulator of peroxiredoxin function and regulation of its expression. *Free Radic Biol Med* 53: 447-56, 2012.

244. Jiang K, Schwarzer C, Lally E, Zhang S, Ruzin S, Machen T, Remington SJ, Feldman L. Expression and characterization of a redox-sensing green fluorescent protein (reduction-oxidation-sensitive green fluorescent protein) in Arabidopsis. *Plant Physiol* 141: 397-403, 2006.
245. Jiao Y, Sun L, Song Y, Wang L, Liu L, Zhang L, Liu B, Li N, Miao C, Hao F. AtrbohD and AtrbohF positively regulate abscisic acid-inhibited primary root growth by affecting Ca²⁺ signalling and auxin response of roots in Arabidopsis. *J Exp Bot* 64: 4183-92, 2013.
246. Johansson C, Lillig CH, Holmgren A. Human mitochondrial glutaredoxin reduces S-glutathionylated proteins with high affinity accepting electrons from either glutathione or thioredoxin reductase. *J Biol Chem* 279: 7537-43, 2004.
247. Juárez-Díaz JA, McClure B, Vázquez-Santana S, Guevara-García A, León-Mejía P, Márquez-Guzmán J, Cruz-García F. A novel thioredoxin h is secreted in Nicotiana glauca and reduces S-RNase in vitro. *J Biol Chem* 281: 3418-24, 2006.
248. Jubany-Mari T, Alegre-Batlle L, Jiang K, Feldman LJ. Use of a redox-sensing GFP (c-roGFP1) for real-time monitoring of cytosol redox status in Arabidopsis thaliana water-stressed plants. *FEBS Lett* 584: 889-97, 2010.
249. Kabil O, Banerjee R. Redox biochemistry of hydrogen sulfide. *J Biol Chem* 285: 21903-7, 2010.
250. Kaneko R, Wada Y. Decomposition of protein nitrosothiols in matrix-assisted laser desorption/ionization and electrospray ionization mass spectrometry. *J Mass Spectrom* 38: 526-30, 2003.
251. Kangasjarvi S, Neukermans J, Li S, Aro EM, Noctor G. Photosynthesis, photorespiration, and light signalling in defence responses. *J Exp Bot* 63: 1619-36, 2012.
252. Kangasjärvi S, Tikkanen M, Durian G, Aro E-M. Photosynthetic light reactions – An adjustable hub in basic production and plant immunity signaling. *Plant Physiol Biochem* 81: 128-34, 2014.
253. Kehr S, Jortzik E, Delahunty C, Yates JR, 3rd, Rahlfs S, Becker K. Protein S-glutathionylation in malaria parasites. *Antioxid Redox Signal* 15: 2855-65, 2011.

254. Kekulandara DN, Samarasinghe KT, Munkanatta Godage DN, Ahn YH. Clickable glutathione using tetrazine-alkene bioorthogonal chemistry for detecting protein glutathionylation. *Org Biomol Chem*, 2016.
255. Kelliher T, Walbot V. Hypoxia triggers meiotic fate acquisition in maize. *Science* 337: 345-8, 2012.
256. Kieselbach T. Oxidative folding in chloroplasts. *Antioxid Redox Signal* 19: 72-82, 2013.
257. Kim MR, Khaleda L, Jung IJ, Kim JY, Lee SY, Cha J-Y, Kim W-Y. Overexpression of chloroplast-localized NADPH-dependent thioredoxin reductase C (NTRC) enhances tolerance to photo-oxidative and drought stresses in *Arabidopsis thaliana*. *J Plant Biol* 60: 175-80, 2017.
258. Kim SG, Chung JS, Sutton RB, Lee JS, Lopez-Maury L, Lee SY, Florencio FJ, Lin T, Zabet-Moghaddam M, Wood MJ, Nayak K, Madem V, Tripathy JN, Kim SK, Knaff DB. Redox, mutagenic and structural studies of the glutaredoxin/arsenate reductase couple from the cyanobacterium *Synechocystis* sp. PCC 6803. *Biochim Biophys Acta* 1824: 392-403, 2012.
259. Kimura H. Signaling molecules: hydrogen sulfide and polysulfide. *Antioxid Redox Signal* 22: 362-76, 2015.
260. Kinoshita H, Nagasaki J, Yoshikawa N, Yamamoto A, Takito S, Kawasaki M, Sugiyama T, Miyake H, Weber APM, Taniguchi M. The chloroplastic 2-oxoglutarate/malate transporter has dual function as the malate valve and in carbon/nitrogen metabolism. *Plant J* 65: 15-26, 2011.
261. Kirchsteiger K, Ferrandez J, Belen Pascual M, Gonzalez M, Javier Cejudo F. NADPH Thioredoxin Reductase C Is Localized in Plastids of Photosynthetic and Nonphotosynthetic Tissues and Is Involved in Lateral Root Formation in *Arabidopsis*. *Plant Cell* 24: 1534-1548, 2012.
262. Kneeshaw S, Gelineau S, Tada Y, Loake GJ, Spoel SH. Selective protein denitrosylation activity of Thioredoxin-h5 modulates plant Immunity. *Mol Cell* 56: 153-62, 2014.

263. Knuesting J, Riondet C, Maria C, Kruse I, Becuwe N, König N, Berndt C, Tourrette S, Guillemint-Montoya J, Herrero E, Gaymard F, Balk J, Belli G, Scheibe R, Reichheld JP, Rouhier N, Rey P. Arabidopsis glutaredoxin S17 and its partner, the nuclear factor Y subunit C11/negative cofactor 2alpha, contribute to maintenance of the shoot apical meristem under long-day photoperiod. *Plant Physiol* 167: 1643-58, 2015.
264. Koh CS, Navrot N, Didierjean C, Rouhier N, Hirasawa M, Knaff DB, Wingsle G, Samian R, Jacquot JP, Corbier C, Gelhaye E. An atypical catalytic mechanism involving three cysteines of thioredoxin. *J Biol Chem* 283: 23062-72, 2008.
265. Kolbert Z, Feigl G, Borde A, Molnar A, Erdei L. Protein tyrosine nitration in plants: Present knowledge, computational prediction and future perspectives. *Plant Physiol Biochem* 113: 56-63, 2017.
266. König J, Baier M, Horling F, Kahmann U, Harris G, Schürmann P, Dietz KJ. The plant-specific function of 2-Cys peroxiredoxin-mediated detoxification of peroxides in the redox-hierarchy of photosynthetic electron flux. *Proc Natl Acad Sci U S A* 99: 5738-43, 2002.
267. König J, Lotte K, Plessow R, Brockhinke A, Baier M, Dietz KJ. Reaction mechanism of plant 2-Cys peroxiredoxin. Role of the C terminus and the quaternary structure. *J Biol Chem* 278: 24409-20, 2003.
268. Kovacs I, Holzmeister C, Wirtz M, Geerlof A, Frohlich T, Romling G, Kuruthukulangarakoola GT, Linster E, Hell R, Arnold GJ, Durner J, Lindermayr C. ROS-Mediated Inhibition of S-nitrosoglutathione Reductase Contributes to the Activation of Anti-oxidative Mechanisms. *Front Plant Sci* 7: 1669, 2016.
269. Kovacs I, Lindermayr C. Nitric oxide-based protein modification: formation and site-specificity of protein S-nitrosylation. *Front Plant Sci* 4: 137, 2013.
270. Krieger-Liszkay A, Trebst A. Tocopherol is the scavenger of singlet oxygen produced by the triplet states of chlorophyll in the PSII reaction centre. *J Exp Bot* 57: 1677-84, 2006.

271. Kubienova L, Kopecny D, Tylichova M, Briozzo P, Skopalova J, Sebela M, Navratil M, Tache R, Luhova L, Barroso JB, Petrivalsky M. Structural and functional characterization of a plant S-nitrosoglutathione reductase from *Solanum lycopersicum*. *Biochimie* 95: 889-902, 2013.
272. Kwon E, Feechan A, Yun BW, Hwang BH, Pallas JA, Kang JG, Loake GJ. AtGSNOR1 function is required for multiple developmental programs in *Arabidopsis*. *Planta* 236: 887-900, 2012.
273. La Camera S, L'Haridon F, Astier J, Zander M, Abou-Mansour E, Page G, Thurow C, Wendehenne D, Gatz C, Métraux JP. The glutaredoxin ATGRXS13 is required to facilitate *Botrytis cinerea* infection of *Arabidopsis thaliana* plants. *Plant J* 68: 507-19, 2011.
274. Lallement P-A, Brouwer B, Keech O, Hecker A, Rouhier N. The still mysterious roles of cysteine-containing glutathione transferases in plants. *Front Pharmacol* 5: 192, 2014.
275. Laloi C, Rayapuram N, Chartier Y, Grienenberger JM, Bonnard G, Meyer Y. Identification and characterization of a mitochondrial thioredoxin system in plants. *Proc Natl Acad Sci U S A* 98: 14144-9, 2001.
276. Laloi C, Stachowiak M, Pers-Kamczyc E, Warzych E, Murgia I, Apel K. Cross-talk between singlet oxygen- and hydrogen peroxide-dependent signaling of stress responses in *Arabidopsis thaliana*. *Proc Natl Acad Sci U S A* 104: 672-7, 2007.
277. Lancelin JM, Guilhaudis L, Krimm I, Blackledge MJ, Marion D, Jacquot JP. NMR structures of thioredoxin m from the green alga *Chlamydomonas reinhardtii*. *Proteins* 41: 334-49, 2000.
278. Laporte D, Olate E, Salinas P, Salazar M, Jordana X, Holuigue L. Glutaredoxin GRXS13 plays a key role in protection against photooxidative stress in *Arabidopsis*. *J Exp Bot* 63: 503-15, 2011.
279. Latzko E, von Garnier R, Gibbs M. Effect of photosynthesis, photosynthetic inhibitors and oxygen on the activity of ribulose 5-phosphate kinase. *Biochem Biophys Res Commun* 39: 1140-4, 1970.

280. Laugier E, Tarrago L, Courteille A, Innocenti G, Eymery F, Rumeau D, Issakidis-Bourguet E, Rey P. Involvement of thioredoxin $\gamma 2$ in the preservation of leaf methionine sulfoxide reductase capacity and growth under high light. *Plant Cell Environ* 36: 670-82, 2013.
281. Lee U, Wie C, Fernandez BO, Feelisch M, Vierling E. Modulation of nitrosative stress by S-nitrosoglutathione reductase is critical for thermotolerance and plant growth in Arabidopsis. *Plant Cell* 20: 786-802, 2008.
282. Lehmann S, Serrano M, L'Haridon F, Tjamos SE, Metraux J-P. Reactive oxygen species and plant resistance to fungal pathogens. *Phytochemistry* 112: 54-62, 2015.
283. Leichert LI, Gehrke F, Gudiseva HV, Blackwell T, Ilbert M, Walker AK, Strahler JR, Andrews PC, Jakob U. Quantifying changes in the thiol redox proteome upon oxidative stress in vivo. *Proc Natl Acad Sci U S A* 105: 8197-202, 2008.
284. Lemaire SD. The glutaredoxin family in oxygenic photosynthetic organisms. *Photosynth Res* 79: 305-18, 2004.
285. Lemaire SD, Guillon B, Le Maréchal P, Keryer E, Miginiac-Maslow M, Decottignies P. New thioredoxin targets in the unicellular photosynthetic eukaryote *Chlamydomonas reinhardtii*. *Proc Natl Acad Sci U S A* 101: 7475-80, 2004.
286. Lemaire SD, Michelet L, Zaffagnini M, Massot V, Issakidis-Bourguet E. Thioredoxins in chloroplasts. *Curr Genet* 51: 343-65, 2007.
287. Lemaire SD, Miginiac-Maslow M. The thioredoxin superfamily in *Chlamydomonas reinhardtii*. *Photosynth Res* 82: 203-20, 2004.
288. Lennartz K, Plucken H, Seidler A, Westhoff P, Bechtold N, Meierhoff K. HCF164 encodes a thioredoxin-like protein involved in the biogenesis of the cytochrome b(6)f complex in Arabidopsis. *Plant Cell* 13: 2539-51, 2001.
289. Leonard SE, Reddie KG, Carroll KS. Mining the thiol proteome for sulfenic acid modifications reveals new targets for oxidation in cells. *ACS Chem Biol* 4: 783-99, 2009.
290. Lepisto A, Pakula E, Toivola J, Krieger-Liszkay A, Vignols F, Rintamaki E. Deletion of chloroplast NADPH-dependent thioredoxin reductase results in inability to regulate starch synthesis and causes stunted growth under short-day photoperiods. *J Exp Bot* 64: 3843-54, 2013.

291. Li L, Cheng N, Hirschi KD, Wang X. Structure of Arabidopsis chloroplastic monothiol glutaredoxin AtGRXcp. *Acta Crystallogr D Biol Crystallogr* 66: 725-32, 2010.
292. Li S, Zhu H, Wang J, Wang X, Li X, Ma C, Wen L, Yu B, Wang Y, Li J, Wang PG. Comparative analysis of Cu (I)-catalyzed alkyne-azide cycloaddition (CuAAC) and strain-promoted alkyne-azide cycloaddition (SPAAC) in O-GlcNAc proteomics. *Electrophoresis* 37: 1431-6, 2016.
293. Licausi F, Giorgi FM, Schmalzlin E, Usadel B, Perata P, van Dongen JT, Geigenberger P. HRE-type genes are regulated by growth-related changes in internal oxygen concentrations during the normal development of potato (*Solanum tuberosum*) tubers. *Plant Cell Physiol* 52: 1957-72, 2011.
294. Licausi F, Kosmacz M, Weits DA, Giuntoli B, Giorgi FM, Voesenek LA, Perata P, van Dongen JT. Oxygen sensing in plants is mediated by an N-end rule pathway for protein destabilization. *Nature* 479: 419-22, 2011.
295. Lim CJ, Kim WB, Lee BS, Lee HY, Kwon TH, Park JM, Kwon SY. Silencing of SIFTR-c, the catalytic subunit of ferredoxin:thioredoxin reductase, induces pathogenesis-related genes and pathogen resistance in tomato plants. *Biochem Biophys Res Commun* 399: 750-4, 2010.
296. Lin A, Wang Y, Tang J, Xue P, Li C, Liu L, Hu B, Yang F, Loake GJ, Chu C. Nitric oxide and protein S-nitrosylation are integral to hydrogen peroxide-induced leaf cell death in rice. *Plant Physiol* 158: 451-64, 2012.
297. Lind C, Gerdes R, Hamnell Y, Schuppe-Koistinen I, von Lowenhielm HB, Holmgren A, Cotgreave IA. Identification of S-glutathionylated cellular proteins during oxidative stress and constitutive metabolism by affinity purification and proteomic analysis. *Arch Biochem Biophys* 406: 229-40, 2002.
298. Lindahl M, Florencio FJ. Thioredoxin-linked processes in cyanobacteria are as numerous as in chloroplasts, but targets are different. *Proc Natl Acad Sci U S A* 100: 16107-12, 2003.
299. Lindahl M, Mata-Cabana A, Kieselbach T. The Disulfide Proteome and Other Reactive Cysteine Proteomes: Analysis and Functional Significance. *Antioxid Redox Signal* 14: 2581-642, 2011.

300. Lindermayr C. Crosstalk between reactive oxygen species and nitric oxide in plants: Key role of S-nitrosogluthione reductase. *Free Radic Biol Med*, 2017.
301. Lindermayr C, Saalbach G, Durner J. Proteomic identification of S-nitrosylated proteins in Arabidopsis. *Plant Physiol* 137: 921-30, 2005.
302. Liu CT, Benkovic SJ. Capturing a sulfenic acid with arylboronic acids and benzoxaborole. *J Am Chem Soc* 135: 14544-7, 2013.
303. Liu L, Hausladen A, Zeng M, Que L, Heitman J, Stamler JS. A metabolic enzyme for S-nitrosothiol conserved from bacteria to humans. *Nature* 410: 490-4, 2001.
304. Liu M, Hou J, Huang L, Huang X, Heibeck TH, Zhao R, Pasa-Tolic L, Smith RD, Li Y, Fu K, Zhang Z, Hinrichs SH, Ding SJ. Site-specific proteomics approach for study protein S-nitrosylation. *Anal Chem* 82: 7160-8, 2010.
305. Liu X, Liu S, Feng Y, Liu JZ, Chen Y, Pham K, Deng H, Hirschi KD, Wang X, Cheng N. Structural insights into the N-terminal GIY-YIG endonuclease activity of Arabidopsis glutaredoxin AtGRXS16 in chloroplasts. *Proc Natl Acad Sci U S A* 110: 9565-70, 2013.
306. Lo Conte M, Lin J, Wilson MA, Carroll KS. A Chemical Approach for the Detection of Protein Sulfinylation. *ACS Chem Biol* 10: 1825-30, 2015.
307. Longen S, Richter F, Kohler Y, Wittig I, Beck KF, Pfeilschifter J. Quantitative Persulfide Site Identification (qPerS-SID) Reveals Protein Targets of H₂S Releasing Donors in Mammalian Cells. *Sci Rep* 6: 29808, 2016.
308. Lu D, Wang T, Persson S, Mueller-Roeber B, Schippers JH. Transcriptional control of ROS homeostasis by KUODA1 regulates cell expansion during leaf development. *Nat Commun* 5: 3767, 2014.
309. Luo T, Fan T, Liu Y, Rothbart M, Yu J, Zhou S, Grimm B, Luo M. Thioredoxin Redox Regulates ATPase Activity of Magnesium Chelatase CHL1 Subunit and Modulates Redox-Mediated Signaling in Tetrapyrrole Biosynthesis and Homeostasis of Reactive Oxygen Species in Pea Plants. *Plant Physiol* 159: 118-30, 2012.
310. Luthje S, Moller B, Perrineau FC, Woltje K. Plasma membrane electron pathways and oxidative stress. *Antioxid Redox Signal* 18: 2163-83, 2013.

311. Maeda K, Finnie C, Svensson B. Cy5 maleimide labelling for sensitive detection of free thiols in native protein extracts: identification of seed proteins targeted by barley thioredoxin h isoforms. *Biochem J* 378: 497-507, 2004.
312. Maeda K, Finnie C, Svensson B. Identification of thioredoxin h-reducible disulphides in proteomes by differential labelling of cysteines: insight into recognition and regulation of proteins in barley seeds by thioredoxin h. *Proteomics* 5: 1634-44, 2005.
313. Maeda K, Hägglund P, Finnie C, Svensson B, Henriksen A. Structural basis for target protein recognition by the protein disulfide reductase thioredoxin. *Structure* 14: 1701-1710, 2006.
314. Maeda K, Hägglund P, Finnie C, Svensson B, Henriksen A. Crystal structures of barley thioredoxin h isoforms HvTrxh1 and HvTrxh2 reveal features involved in protein recognition and possibly in discriminating the isoform specificity. *Protein Sci* 17: 1015-24, 2008.
315. Mammarella ND, Cheng Z, Fu ZQ, Daudi A, Bolwell GP, Dong X, Ausubel FM. Apoplastic peroxidases are required for salicylic acid-mediated defense against *Pseudomonas syringae*. *Phytochemistry* 112: 110-21, 2015.
316. Marchal C, Delorme-Hinoux V, Bariat L, Siala W, Belin C, Saez-Vasquez J, Riondet C, Reichheld J-P. NTR/NRX define a new thioredoxin system in the nucleus of *Arabidopsis thaliana* cells. *Molecular Plant* 7: 30-44, 2014.
317. Marchand C, Le Marechal P, Meyer Y, Decottignies P. Comparative proteomic approaches for the isolation of proteins interacting with thioredoxin. *Proteomics* 6: 6528-37, 2006.
318. Marchand C, Le Maréchal P, Meyer Y, Miginiac-Maslow M, Issakidis-Bourguet E, Decottignies P. New targets of *Arabidopsis* thioredoxins revealed by proteomic analysis. *Proteomics* 4: 2696-706, 2004.
319. Marchand CH, Vanacker H, Collin V, Issakidis-Bourguet E, Marechal PL, Decottignies P. Thioredoxin targets in *Arabidopsis* roots. *Proteomics* 10: 2418-28, 2010.
320. Marino SM, Gladyshev VN. Structural analysis of cysteine S-nitrosylation: a modified acid-based motif and the emerging role of trans-nitrosylation. *J Mol Biol* 395: 844-59, 2010.

321. Marino SM, Gladyshev VN. Proteomics: mapping reactive cysteines. *Nat Chem Biol* 7: 72-3, 2011.
322. Marri L, Zaffagnini M, Collin V, Issakidis-Bourguet E, Lemaire SD, Pupillo P, Sparla F, Miginiac-Maslow M, Trost P. Prompt and easy activation by specific thioredoxins of Calvin cycle enzymes of *Arabidopsis thaliana* associated in the GAPDH/CP12/PRK supramolecular complex. *Mol Plant* 2: 259-69, 2009.
323. Martin BR, Cravatt BF. Large-scale profiling of protein palmitoylation in mammalian cells. *Nat Methods* 6: 135-8, 2009.
324. Marty L, Siala W, Schwarzlander M, Fricker MD, Wirtz M, Sweetlove LJ, Meyer Y, Meyer AJ, Reichheld JP, Hell R. The NADPH-dependent thioredoxin system constitutes a functional backup for cytosolic glutathione reductase in *Arabidopsis*. *Proc Natl Acad Sci U S A* 106: 9109-14, 2009.
325. Marx C, Wong JH, Buchanan BB. Thioredoxin and germinating barley: targets and protein redox changes. *Planta* 216: 454-60, 2003.
326. Mastrobuoni G, Irgang S, Pietzke M, Assmus HE, Wenzel M, Schulze WX, Kempa S. Proteome dynamics and early salt stress response of the photosynthetic organism *Chlamydomonas reinhardtii*. *BMC Genomics* 13: 215, 2012.
327. Mata-Perez C, Begara-Morales JC, Chaki M, Sanchez-Calvo B, Valderrama R, Padilla MN, Corpas FJ, Barroso JB. Protein Tyrosine Nitration during Development and Abiotic Stress Response in Plants. *Front Plant Sci* 7: 1699, 2016.
328. Matern S, Peskan-Berghoefer T, Gromes R, Kiesel RV, Rausch T. Imposed glutathione-mediated redox switch modulates the tobacco wound-induced protein kinase and salicylic acid-induced protein kinase activation state and impacts on defence against *Pseudomonas syringae*. *J Exp Bot* 66: 1935-50, 2015.
329. Menchise V, Corbier C, Didierjean C, Saviano M, Benedetti E, Jacquot JP, Aubry A. Crystal structure of the wild-type and D30A mutant thioredoxin h of *Chlamydomonas reinhardtii* and implications for the catalytic mechanism. *Biochem J* 359: 65-75, 2001.
330. Meng L, Wong JH, Feldman LJ, Lemaux PG, Buchanan BB. A membrane-associated thioredoxin required for plant growth moves from cell to cell, suggestive of a role in intercellular communication. *Proc Natl Acad Sci U S A* 107: 3900-5, 2010.

331. Merksamer PI, Trusina A, Papa FR. Real-time redox measurements during endoplasmic reticulum stress reveal interlinked protein folding functions. *Cell* 135: 933-47, 2008.
332. Meyer AJ, Brach T, Marty L, Kreye S, Rouhier N, Jacquot JP, Hell R. Redox-sensitive GFP in *Arabidopsis thaliana* is a quantitative biosensor for the redox potential of the cellular glutathione redox buffer. *Plant J* 52: 973-86, 2007.
333. Meyer AJ, Dick TP. Fluorescent protein-based redox probes. *Antioxid Redox Signal* 13: 621-50, 2010.
334. Meyer AJ, Riemer J, Rouhier N. Oxidative protein folding: state-of-the-art and current avenues of research in plants. *New Phytol*, 2018.
335. Meyer Y, Belin C, Delorme-Hinoux V, Reichheld JP, Riondet C. Thioredoxin and Glutaredoxin Systems in Plants: Molecular Mechanisms, Crosstalks, and Functional Significance. *Antioxid Redox Signal*, 2012.
336. Meyer Y, Siala W, Bashandy T, Riondet C, Vignols F, Reichheld JP. Glutaredoxins and thioredoxins in plants. *Biochim Biophys Acta* 1783: 589-600, 2008.
337. Mhamdi A, Noctor G, Baker A. Plant catalases: peroxisomal redox guardians. *Arch Biochem Biophys* 525: 181-94, 2012.
338. Michelet L, Zaffagnini M, Marchand C, Collin V, Decottignies P, Tsan P, Lancelin JM, Trost P, Miginiac-Maslow M, Noctor G, Lemaire SD. Glutathionylation of chloroplast thioredoxin f is a redox signaling mechanism in plants. *Proc Natl Acad Sci U S A* 102: 16478-83, 2005.
339. Michelet L, Zaffagnini M, Morisse S, Sparla F, Pérez-Pérez ME, Francia F, Danon A, Marchand CH, Fermani S, Trost P, Lemaire SD. Redox regulation of the Calvin-Benson cycle: something old, something new. *Front Plant Sci* 4: 470, 2013.
340. Michelet L, Zaffagnini M, Vanacker H, Le Marechal P, Marchand C, Schroda M, Lemaire SD, Decottignies P. In vivo targets of S-thiolation in *Chlamydomonas reinhardtii*. *J Biol Chem* 283: 21571-8, 2008.
341. Mignolet-Spruyt L, Xu E, Idänheimo N, Hoerberichts FA, Mühlenbock P, Brosché M, Van Breusegem F, Kangasjärvi J. Spreading the news: subcellular and organellar reactive oxygen species production and signalling. *J Exp Bot* 67: 3831-44, 2016.

342. Mikkelsen R, Mutenda KE, Mant A, Schürmann P, Blennow A. Alpha-glucan, water dikinase (GWD): a plastidic enzyme with redox-regulated and coordinated catalytic activity and binding affinity. *Proc Natl Acad Sci U S A* 102: 1785-90, 2005.
343. Mishanina TV, Libiad M, Banerjee R. Biogenesis of reactive sulfur species for signaling by hydrogen sulfide oxidation pathways. *Nat Chem Biol* 11: 457-64, 2015.
344. Mittard V, Blackledge MJ, Stein M, Jacquot JP, Marion D, Lancelin JM. NMR solution structure of an oxidised thioredoxin h from the eukaryotic green alga *Chlamydomonas reinhardtii*. *Eur J Biochem* 243: 374-83, 1997.
345. Mittler R. ROS Are Good. *Trends in Plant Science* 22: 11-19, 2017.
346. Mittler R, Vanderauwera S, Suzuki N, Miller G, Tognetti VB, Vandepoele K, Gollery M, Shulaev V, Van Breusegem F. ROS signaling: the new wave? *Trends Plant Sci* 16: 300-9, 2011.
347. Mock HP, Dietz KJ. Redox proteomics for the assessment of redox-related posttranslational regulation in plants. *Biochim Biophys Acta* 1864: 967-73, 2016.
348. Morgan B, Schwarzländer M. Fluoreszierende Proteinsensoren für die Redoxregulation in lebenden Zellen. *BIOspektrum* 22: 260-263, 2016.
349. Morisse S, Michelet L, Bedhomme M, Marchand CH, Calvaresi M, Trost P, Fermani S, Zaffagnini M, Lemaire SD. Thioredoxin-dependent redox regulation of chloroplastic phosphoglycerate kinase from *Chlamydomonas reinhardtii*. *Journal of Biological Chemistry* 289: 30012-30024, 2014.
350. Morisse S, Zaffagnini M, Gao XH, Lemaire SD, Marchand CH. Insight into protein S-nitrosylation in *Chlamydomonas reinhardtii*. *Antioxid Redox Signal* 21: 1271-84, 2014.
351. Moseler A, Aller I, Wagner S, Nietzel T, Przybyla-Toscano J, Mühlhoff U, Lill R, Berndt C, Rouhier N, Schwarzländer M. The mitochondrial monothiol glutaredoxin S15 is essential for iron-sulfur protein maturation in *Arabidopsis thaliana*. *Proc Natl Acad Sci U S A* 112: 13735-40, 2015.
352. Motohashi K, Hisabori T. HCF164 receives the reducing equivalents from stroma thioredoxin across thylakoid membrane and mediates reduction of target proteins in thylakoid lumen. *J Biol Chem*, 2006.

353. Motohashi K, Kondoh A, Stumpp MT, Hisabori T. Comprehensive survey of proteins targeted by chloroplast thioredoxin. *Proc Natl Acad Sci U S A* 98: 11224-9, 2001.
354. Mou Z, Fan W, Dong X. Inducers of plant systemic acquired resistance regulate NPR1 function through redox changes. *Cell* 113: 935-44, 2003.
355. Mubarakshina MM, Ivanov BN, Naydov IA, Hillier W, Badger MR, Krieger-Liszky A. Production and diffusion of chloroplastic H₂O₂ and its implication to signalling. *J Exp Bot* 61: 3577-87, 2010.
356. Mur LA, Mandon J, Persijn S, Cristescu SM, Moshkov IE, Novikova GV, Hall MA, Harren FJ, Hebelstrup KH, Gupta KJ. Nitric oxide in plants: an assessment of the current state of knowledge. *AoB Plants* 5: pls052, 2013.
357. Murmu J, Bush MJ, DeLong C, Li S, Xu M, Khan M, Malcolmson C, Fobert PR, Zachgo S, Hepworth SR. Arabidopsis basic leucine-zipper transcription factors TGA9 and TGA10 interact with floral glutaredoxins ROXY1 and ROXY2 and are redundantly required for anther development. *Plant Physiol* 154: 1492-504, 2010.
358. Murphy MP. How mitochondria produce reactive oxygen species. *Biochem J* 417: 1-13, 2009.
359. Murray CI, Uhrigshardt H, O'Meally RN, Cole RN, Van Eyk JE. Identification and quantification of S-nitrosylation by cysteine reactive tandem mass tag switch assay. *Mol Cell Proteomics* 11: M111 013441, 2012.
360. Murray R, Jindal S. The photosensitized oxidation of disulfides related to cystine. *Photochemistry and Photobiology* 16: 147-51, 1972.
361. Mustafa AK, Gadalla MM, Sen N, Kim S, Mu W, Gazi SK, Barrow RK, Yang G, Wang R, Snyder SH. H₂S signals through protein S-sulfhydration. *Sci Signal* 2: ra72, 2009.
362. Nagy P, Karton A, Betz A, Peskin AV, Pace P, O'Reilly RJ, Hampton MB, Radom L, Winterbourn CC. Model for the exceptional reactivity of peroxiredoxins 2 and 3 with hydrogen peroxide: a kinetic and computational study. *J Biol Chem* 286: 18048-55, 2011.
363. Naranjo B, Diaz-Espejo A, Lindahl M, Cejudo FJ. Type-f thioredoxins have a role in the short-term activation of carbon metabolism and their loss affects growth under short-day conditions in Arabidopsis thaliana. *J Exp Bot* 67: 1951-64, 2016.

364. Naranjo B, Mignee C, Krieger-Liszkay A, Hornero-Mendez D, Gallardo-Guerrero L, Javier Cejudo F, Lindahl M. The chloroplast NADPH thioredoxin reductase C, NTRC, controls non-photochemical quenching of light energy and photosynthetic electron transport in Arabidopsis. *Plant Cell Environ* 39: 804-22, 2016.
365. Nawrocki WJ, Tourasse NJ, Taly A, Rappaport F, Wollman FA. The plastid terminal oxidase: its elusive function points to multiple contributions to plastid physiology. *Annu Rev Plant Biol* 66: 49-74, 2015.
366. Ndamukong I, Abdallat AA, Thurow C, Fode B, Zander M, Weigel R, Gatz C. SA-inducible Arabidopsis glutaredoxin interacts with TGA factors and suppresses JA-responsive PDF1.2 transcription. *Plant J* 50: 128-39, 2007.
367. Nee G, Zaffagnini M, Trost P, Issakidis-Bourguet E. Redox regulation of chloroplastic glucose-6-phosphate dehydrogenase: a new role for f-type thioredoxin. *FEBS Lett* 583: 2827-32, 2009.
368. Nelson KJ, Parsonage D, Hall A, Karplus PA, Poole LB. Cysteine pK(a) values for the bacterial peroxiredoxin AhpC. *Biochemistry* 47: 12860-8, 2008.
369. Nikitovic D, Holmgren A. S-nitrosoglutathione is cleaved by the thioredoxin system with liberation of glutathione and redox regulating nitric oxide. *J Biol Chem* 271: 19180-5, 1996.
370. Nikkanen L, Toivola J, Diaz MG, Rintamäki E. Chloroplast thioredoxin systems: prospects for improving photosynthesis. *Phil. Trans. R. Soc. B* 372: 20160474, 2017.
371. Nikkanen L, Toivola J, Rintamaki E. Crosstalk between chloroplast thioredoxin systems in regulation of photosynthesis. *Plant Cell Environ*, 2016.
372. Nilsson T, Mann M, Aebersold R, Yates JR, 3rd, Bairoch A, Bergeron JJ. Mass spectrometry in high-throughput proteomics: ready for the big time. *Nat Methods* 7: 681-5, 2010.
373. Noctor G. Metabolic signalling in defence and stress: the central roles of soluble redox couples. *Plant Cell Environ* 29: 409-25, 2006.
374. Noctor G, Foyer CH. Intracellular Redox Compartmentation and ROS-Related Communication in Regulation and Signaling. *Plant Physiology* 171: 1581-1592, 2016.

375. Noctor G, Lelarge-Trouverie C, Mhamdi A. The metabolomics of oxidative stress. *Phytochemistry* 112: 33-53, 2015.
376. Noctor G, Mhamdi A, Foyer CH. Oxidative stress and antioxidative systems: recipes for successful data collection and interpretation. *Plant Cell Environ* 39: 1140-60, 2016.
377. Noctor G, Reichheld JP, Foyer CH. ROS-related redox regulation and signaling in plants. *Semin Cell Dev Biol*, 2017.
378. Noctor G, Veljovic-Jovanovic S, Driscoll S, Novitskaya L, Foyer CH. Drought and oxidative load in the leaves of C3 plants: a predominant role for photorespiration? *Ann Bot* 89 Spec No: 841-50, 2002.
379. Nordstrand K, slund F, Holmgren A, Otting G, Berndt KD. NMR structure of Escherichia coli glutaredoxin 3-glutathione mixed disulfide complex: implications for the enzymatic mechanism. *J Mol Biol* 286: 541-52, 1999.
380. Oelze M-L, Kandlbinder A, Dietz K-J. Redox regulation and overreduction control in the photosynthesizing cell: Complexity in redox regulatory networks. *Biochim Biophys Acta* 1780: 1261-72, 2008.
381. Oger E, Marino D, Guignon JM, Pauly N, Puppo A. Sulfenylated proteins in the Medicago truncatula-Sinorhizobium meliloti symbiosis. *J Proteomics* 75: 4102-13, 2012.
382. Ojeda V, Perez-Ruiz JM, Gonzalez M, Najera VA, Sahrawy M, Serrato AJ, Geigenberger P, Cejudo FJ. NADPH Thioredoxin Reductase C and Thioredoxins Act Concertedly in Seedling Development. *Plant Physiol* 174: 1436-48, 2017.
383. Okegawa Y, Motohashi K. Chloroplastic thioredoxin m functions as a major regulator of Calvin cycle enzymes during photosynthesis in vivo. *Plant J* 84: 900-13, 2015.
384. Onda Y. Oxidative protein-folding systems in plant cells. *Int J Cell Biol* 2013: 585431, 2013.
385. Ortega-Galisteo AP, Rodriguez-Serrano M, Pazmino DM, Gupta DK, Sandalio LM, Romero-Puertas MC. S-Nitrosylated proteins in pea (*Pisum sativum* L.) leaf peroxisomes: changes under abiotic stress. *J Exp Bot* 63: 2089-103, 2012.

386. Ostergaard H, Henriksen A, Hansen FG, Winther JR. Shedding light on disulfide bond formation: engineering a redox switch in green fluorescent protein. *Embo J* 20: 5853-62, 2001.
387. Ostergaard H, Tachibana C, Winther JR. Monitoring disulfide bond formation in the eukaryotic cytosol. *J Cell Biol* 166: 337-45, 2004.
388. Paige JS, Xu G, Stancevic B, Jaffrey SR. Nitrosothiol reactivity profiling identifies S-nitrosylated proteins with unexpected stability. *Chem Biol* 15: 1307-16, 2008.
389. Palmieri MC, Lindermayr C, Bauwe H, Steinhauser C, Durner J. Regulation of plant glycine decarboxylase by s-nitrosylation and glutathionylation. *Plant Physiol* 152: 1514-28, 2010.
390. Pan J, Carroll KS. Persulfide reactivity in the detection of protein s-sulfhydration. *ACS Chem Biol* 8: 1110-6, 2013.
391. Pattison DJ, Rahmanto AS, Davies MJ. Photo-oxidation of proteins. *Photochem Photobiol Sci* 11: 38-53, 2012.
392. Paul BD, Snyder SH. H₂S signalling through protein sulfhydration and beyond. *Nat Rev Mol Cell Biol* 13: 499-507, 2012.
393. Paul BD, Snyder SH. H₂S: A Novel Gasotransmitter that Signals by Sulfhydration. *Trends Biochem Sci* 40: 687-700, 2015.
394. Paul MV, Iyer S, Amerhauser C, Lehmann M, van Dongen JT, Geigenberger P. Oxygen Sensing via the Ethylene Response Transcription Factor RAP2.12 Affects Plant Metabolism and Performance under Both Normoxia and Hypoxia. *Plant Physiol* 172: 141-53, 2016.
395. Paulsen CE, Carroll KS. Cysteine-mediated redox signaling: chemistry, biology, and tools for discovery. *Chem Rev* 113: 4633-79, 2013.
396. Paulsen CE, Truong TH, Garcia FJ, Homann A, Gupta V, Leonard SE, Carroll KS. Peroxide-dependent sulfenylation of the EGFR catalytic site enhances kinase activity. *Nat Chem Biol* 8: 57-64, 2011.
397. Pedersen TA, Kirk M, Bassham JA. Light-dark transients in levels of intermediate compounds during photosynthesis in air-adapted *Chlorella*. *Physiol Plant* 19: 219-231, 1966.

398. Perez-Martin M, Blaby-Haas CE, Perez-Perez ME, Andres-Garrido A, Blaby IK, Merchant SS, Crespo JL. Activation of Autophagy by Metals in *Chlamydomonas reinhardtii*. *Eukaryot Cell* 14: 964-73, 2015.
399. Perez-Martin M, Perez-Perez ME, Lemaire SD, Crespo JL. Oxidative stress contributes to autophagy induction in response to endoplasmic reticulum stress in *Chlamydomonas reinhardtii*. *Plant Physiol* 166: 997-1008, 2014.
400. Pérez-Pérez ME, Couso I, Crespo JL. Carotenoid deficiency triggers autophagy in the model green alga *Chlamydomonas reinhardtii*. *Autophagy* 8: 376-88, 2012.
401. Pérez-Pérez ME, Florencio FJ, Crespo JL. Inhibition of target of rapamycin signaling and stress activate autophagy in *Chlamydomonas reinhardtii*. *Plant Physiol* 152: 1874-88, 2010.
402. Pérez-Pérez ME, Florencio FJ, Lindahl M. Selecting thioredoxins for disulphide proteomics: Target proteomes of three thioredoxins from the cyanobacterium *Synechocystis* sp. PCC 6803. *Proteomics* 6: S186-95, 2006.
403. Pérez-Pérez ME, Lemaire SD, Crespo JL. Reactive oxygen species and autophagy in plants and algae. *Plant Physiol* 160: 156-64, 2012.
404. Pérez-Pérez ME, Martin-Figueroa E, Florencio FJ. Photosynthetic regulation of the cyanobacterium *Synechocystis* sp. PCC 6803 thioredoxin system and functional analysis of TrxB (Trx x) and TrxQ (Trx y) thioredoxins. *Mol Plant* 2: 270-83, 2009.
405. Pérez-Pérez ME, Mauriès A, Maes A, Tourasse NJ, Hamon M, Lemaire SD, Marchand CH. The Deep Thioredoxome in *Chlamydomonas reinhardtii*: New Insights into Redox Regulation. *Mol Plant* 10: 1107-1125, 2017.
406. Pérez-Pérez ME, Zaffagnini M, Marchand CH, Crespo JL, Lemaire SD. The yeast autophagy protease Atg4 is regulated by thioredoxin. *Autophagy* 10: 1953-64, 2014.
407. Perez-Ruiz JM, Guinea M, Puerto-Galan L, Cejudo FJ. NADPH thioredoxin reductase C is involved in redox regulation of the Mg-chelatase I subunit in *Arabidopsis thaliana* chloroplasts. *Mol Plant* 7: 1252-5, 2014.
408. Pérez-Ruiz JM, Naranjo B, Ojeda V, Guinea M, Cejudo FJ. NTRC-dependent redox balance of 2-Cys peroxiredoxins is needed for optimal function of the photosynthetic apparatus. *Proc Natl Acad Sci U S A* 114: 12069-74, 2017.

409. Perez-Ruiz JM, Spinola MC, Kirchsteiger K, Moreno J, Sahrawy M, Cejudo FJ. Rice NTRC is a high-efficiency redox system for chloroplast protection against oxidative damage. *Plant Cell* 18: 2356-2368, 2006.
410. Peterson FC, Lytle BL, Sampath S, Vinarov D, Tyler E, Shahan M, Markley JL, Volkman BF. Solution structure of thioredoxin h1 from *Arabidopsis thaliana*. *Protein Sci* 14: 2195-200, 2005.
411. Pierella Karlusich JJ, Zurbriggen MD, Shahinnia F, Sonnewald S, Sonnewald U, Hosseini SA, Hajirezaei MR, Carrillo N. Chloroplast Redox Status Modulates Genome-Wide Plant Responses during the Non-host Interaction of Tobacco with the Hemibiotrophic Bacterium *Xanthomonas campestris* pv. *vesicatoria*. *Front Plant Sci* 8: 1158, 2017.
412. Plomion C, Aury JM, Amselem J, Leroy T, Murat F, Duplessis S, Faye S, Francillonne N, Labadie K, Le Provost G, Lesur I, Bartholomé J, Faivre-Rampant P, Kohler A, Leplé JC, Chantret N, Chen J, Diévarit A, Alaeitabar T, Barbe V, Belser C, Bergès H, Bodénès C, Bogeat-Triboulot MB, Bouffaud ML, Brachi B, Chancerel E, Cohen D, Couloux A, Da Silva C, Dossat C, Ehrenmann F, Gaspin C, Grima-Pettenati J, Guichoux E, Hecker A, Herrmann S, Hugueney P, Hummel I, Klopp C, Lalanne C, Lascoux M, Lasserre E, Lemainque A, Desprez-Loustau ML, Luyten I, Madoui MA, Mangenot S, Marchal C, Maumus F, Mercier J, Michotey C, Panaud O, Picault N, Rouhier N, Rué O, Rustenholz C, Salin F, Soler M, Tarkka M, Velt A, Zanne AE, Martin F, Wincker P, Quesneville H, Kremer A, Salse J. Oak genome reveals facets of long lifespan. *Nat Plants* 4: 440-52, 2018.
413. Poole LB, Klomsiri C, Knaggs SA, Furdui CM, Nelson KJ, Thomas MJ, Fetrow JS, Daniel LW, King SB. Fluorescent and affinity-based tools to detect cysteine sulfenic acid formation in proteins. *Bioconjug Chem* 18: 2004-17, 2007.
414. Poole LB, Schoneich C. Introduction: What we do and do not know regarding redox processes of thiols in signaling pathways. *Free Radic Biol Med* 80: 145-7, 2015.
415. Poole LB, Zeng BB, Knaggs SA, Yakubu M, King SB. Synthesis of chemical probes to map sulfenic acid modifications on proteins. *Bioconjug Chem* 16: 1624-8, 2005.
416. Poole TH, Reisz JA, Zhao W, Poole LB, Furdui CM, King SB. Strained cycloalkynes as new protein sulfenic acid traps. *J Am Chem Soc* 136: 6167-70, 2014.

417. Prescher JA, Bertozzi CR. Chemistry in living systems. *Nat Chem Biol* 1: 13-21, 2005.
418. Pucciariello C, Perata P. New insights into reactive oxygen species and nitric oxide signalling under low oxygen in plants. *Plant Cell Environ* 40: 473-482, 2017.
419. Pulido P, Spinola MC, Kirchsteiger K, Guinea M, Pascual MB, Sahrawy M, Sandalio LM, Dietz KJ, Gonzalez M, Cejudo FJ. Functional analysis of the pathways for 2-Cys peroxiredoxin reduction in *Arabidopsis thaliana* chloroplasts. *J Exp Bot* 61: 4043-54, 2010.
420. Puyaubert J, Baudouin E. New clues for a cold case: nitric oxide response to low temperature. *Plant Cell Environ* 37: 2623-30, 2014.
421. Puyaubert J, Fares A, Reze N, Peltier JB, Baudouin E. Identification of endogenously S-nitrosylated proteins in *Arabidopsis* plantlets: effect of cold stress on cysteine nitrosylation level. *Plant Sci* 215-216: 150-6, 2014.
422. Qu Z, Meng F, Bomgardner RD, Viner RI, Li J, Rogers JC, Cheng J, Greenlief CM, Cui J, Lubahn DB, Sun GY, Gu Z. Proteomic quantification and site-mapping of S-nitrosylated proteins using isobaric iodoTMT reagents. *J Proteome Res* 13: 3200-11, 2014.
423. Raja V, Majeed U, Kang H, Andrabi KI, John R. Abiotic stress: Interplay between ROS, hormones and MAPKs. *Environmental and Experimental Botany* 137: 142-57, 2017.
424. Reddie KG, Carroll KS. Expanding the functional diversity of proteins through cysteine oxidation. *Curr Opin Chem Biol* 12: 746-54, 2008.
425. Reichheld JP, Meyer E, Khafif M, Bonnard G, Meyer Y. AtNTRB is the major mitochondrial thioredoxin reductase in *Arabidopsis thaliana*. *FEBS Lett* 579: 337-42, 2005.
426. Reisz JA, Bechtold E, King SB, Poole LB, Furdui CM. Thiol-blocking electrophiles interfere with labeling and detection of protein sulfenic acids. *Febs J* 280: 6150-61, 2013.
427. Rey P, Becuwe N, Tourrette S, Rouhier N. Involvement of *Arabidopsis* glutaredoxin S14 in the maintenance of chlorophyll content. *Plant Cell Environ* 40: 2319-2332, 2017.

428. Ribeiro CW, Baldacci-Cresp F, Pierre O, Larousse M, Benyamina S, Lambert A, Hopkins J, Castella C, Cazareth J, Alloing G. Regulation of differentiation of nitrogen-fixing bacteria by microsymbiont targeting of plant thioredoxin s1. *Curr Biol* 27: 250-6, 2017.
429. Richter AS, Peter E, Rothbart M, Schlicke H, Toivola J, Rintamaki E, Grimm B. Posttranslational Influence of NADPH-Dependent Thioredoxin Reductase C on Enzymes in Tetrapyrrole Synthesis. *Plant Physiol* 162: 63-73, 2013.
430. Riemer J, Bulleid N, Herrmann JM. Disulfide formation in the ER and mitochondria: two solutions to a common process. *Science* 324: 1284-7, 2009.
431. Riondet C, Desouris JP, Montoya JG, Chartier Y, Meyer Y, Reichheld J-P. A dicotyledon-specific glutaredoxin GRXC1 family with dimer-dependent redox regulation is functionally redundant with GRXC2. *Plant Cell Environ* 35: 360-73, 2012.
432. Romero-Puertas MC, Campostrini N, Matte A, Righetti PG, Perazzolli M, Zolla L, Roepstorff P, Delledonne M. Proteomic analysis of S-nitrosylated proteins in *Arabidopsis thaliana* undergoing hypersensitive response. *Proteomics* 8: 1459-69, 2008.
433. Romero JM, Bizzozero OA. Intracellular glutathione mediates the denitrosylation of protein nitrosothiols in the rat spinal cord. *J Neurosci Res* 87: 701-9, 2009.
434. Roos G, Foloppe N, Messens J. Understanding the pKa of redox cysteines: the key role of hydrogen bonding. *Antioxid Redox Signal* 18: 94-127, 2013.
435. Roos G, Loverix S, Geerlings P. Origin of the pKa Perturbation of N-Terminal Cysteine in α - and 310-Helices: A Computational DFT Study. *J Phys Chem B* 110: 557-62, 2006.
436. Rosenwasser S, Graff van Creveld S, Schatz D, Malitsky S, Tzfadia O, Aharoni A, Levin Y, Gabashvili A, Feldmesser E, Vardi A. Mapping the diatom redox-sensitive proteome provides insight into response to nitrogen stress in the marine environment. *Proc Natl Acad Sci U S A* 111: 2740-5, 2014.
437. Rosenwasser S, Rot I, Sollner E, Meyer AJ, Smith Y, Leviatan N, Fluhr R, Friedman H. Organelles contribute differentially to reactive oxygen species-related events during extended darkness. *Plant Physiol* 156: 185-201, 2011.

438. Rouhier N, Cerveau D, Couturier J, Reichheld JP, Rey P. Involvement of thiol-based mechanisms in plant development. *Biochim Biophys Acta* 1850: 1479-96, 2015.
439. Rouhier N, Gelhaye E, Jacquot JP. Plant glutaredoxins: still mysterious reducing systems. *Cell Mol Life Sci* 61: 1266-77, 2004.
440. Rouhier N, Lemaire SD, Jacquot JP. The role of glutathione in photosynthetic organisms: emerging functions for glutaredoxins and glutathionylation. *Annu Rev Plant Biol* 59: 143-66, 2008.
441. Rouhier N, Unno H, Bandyopadhyay S, Masip L, Kim SK, Hirasawa M, Gualberto JM, Lattard V, Kusunoki M, Knaff DB, Georgiou G, Hase T, Johnson MK, Jacquot JP. Functional, structural, and spectroscopic characterization of a glutathione-ligated [2Fe-2S] cluster in poplar glutaredoxin C1. *Proc Natl Acad Sci U S A* 104: 7379-84, 2007.
442. Ruban AV. Nonphotochemical Chlorophyll Fluorescence Quenching: Mechanism and Effectiveness in Protecting Plants from Photodamage. *Plant Physiol* 170: 1903-16, 2016.
443. Rusterucci C, Espunya MC, Diaz M, Chabannes M, Martinez MC. S-nitrosoglutathione reductase affords protection against pathogens in Arabidopsis, both locally and systemically. *Plant Physiol* 143: 1282-92, 2007.
444. Saarinen M, Gleason FK, Eklund H. Crystal structure of thioredoxin-2 from *Anabaena*. *Structure* 3: 1097-108, 1995.
445. Samarasinghe KT, Munkanatta Godage DN, VanHecke GC, Ahn YH. Metabolic synthesis of clickable glutathione for chemoselective detection of glutathionylation. *J Am Chem Soc* 136: 11566-9, 2014.
446. Samarasinghe KT, Munkanatta Godage DN, Zhou Y, Ndombera FT, Weerapana E, Ahn YH. A clickable glutathione approach for identification of protein glutathionylation in response to glucose metabolism. *Mol Biosyst* 12: 2471-80, 2016.
447. Scheibe R. Malate valves to balance cellular energy supply. *Physiol Plant* 120: 21-26, 2004.

448. Scheibe R, Anderson LE. Dark modulation of NADP-dependent malate dehydrogenase and glucose-6-phosphate dehydrogenase in the chloroplast. *Biochim Biophys Acta* 636: 58-64, 1981.
449. Scheibe R, Dietz KJ. Reduction-oxidation network for flexible adjustment of cellular metabolism in photoautotrophic cells. *Plant Cell Environ* 35: 202-16, 2012.
450. Scheler C, Durner J, Astier J. Nitric oxide and reactive oxygen species in plant biotic interactions. *Curr Opin Plant Biol* 16: 534-9, 2013.
451. Schippers JHM, Foyer CH, van Dongen JT. Redox regulation in shoot growth, SAM maintenance and flowering. *Curr Opin Plant Biol* 29: 121-28, 2016.
452. Schmidt R, Schippers JH. ROS-mediated redox signaling during cell differentiation in plants. *Biochim Biophys Acta* 1850: 1497-508, 2015.
453. Schoneich C. Methionine oxidation by reactive oxygen species: reaction mechanisms and relevance to Alzheimer's disease. *Biochim Biophys Acta* 1703: 111-9, 2005.
454. Schoneich C. Mechanisms of protein damage induced by cysteine thiol radical formation. *Chem Res Toxicol* 21: 1175-9, 2008.
455. Schürmann P, Buchanan BB. Role of ferredoxin in the activation of sedoheptulose diphosphatase in isolated chloroplasts. *Biochim Biophys Acta* 376: 189-92, 1975.
456. Schürmann P, Buchanan BB. The ferredoxin/thioredoxin system of oxygenic photosynthesis. *Antioxid Redox Signal* 10: 1235-74, 2008.
457. Schürmann P, Wolosiuk RA, Breazeale VD, Buchanan BB. Two proteins function in the regulation of photosynthetic CO₂ assimilation in chloroplasts. *Nature* 263: 257-258, 1976.
458. Schwarzlander M, Dick TP, Meyer AJ, Morgan B. Dissecting Redox Biology Using Fluorescent Protein Sensors. *Antioxid Redox Signal* 24: 680-712, 2016.
459. Schwarzlander M, Fricker MD, Muller C, Marty L, Brach T, Novak J, Sweetlove LJ, Hell R, Meyer AJ. Confocal imaging of glutathione redox potential in living plant cells. *J Microsc* 231: 299-316, 2008.
460. Schwarzlander M, Fricker MD, Sweetlove LJ. Monitoring the in vivo redox state of plant mitochondria: effect of respiratory inhibitors, abiotic stress and assessment of recovery from oxidative challenge. *Biochim Biophys Acta* 1787: 468-75, 2009.

461. Scuffi D, Nietzel T, Di Fino LM, Meyer AJ, Lamattina L, Schwarzlander M, Laxalt AM, Garcia-Mata C. Hydrogen Sulfide Increases Production of NADPH Oxidase-Dependent Hydrogen Peroxide and Phospholipase D-Derived Phosphatidic Acid in Guard Cell Signaling. *Plant Physiol* 176: 2532-2542, 2018.
462. Sehrawat A, Abat JK, Deswal R. RuBisCO depletion improved proteome coverage of cold responsive S-nitrosylated targets in Brassica juncea. *Front Plant Sci* 4: 342, 2013.
463. Sehrawat A, Deswal R. S-nitrosylation analysis in Brassica juncea apoplast highlights the importance of nitric oxide in cold-stress signaling. *J Proteome Res* 13: 2599-619, 2014.
464. Selga T, Selga M, Ozoliņa A. Plastid-nuclear complexes in the photosynthesizing cells from their mitosis up to programmed death. *Photosynthetica* 51: 474-6, 2013.
465. Selles B, Jacquot JP, Rouhier N. Comparative genomic study of protein disulfide isomerases from photosynthetic organisms. *Genomics* 97: 37-50, 2011.
466. Seo YH, Carroll KS. Profiling protein thiol oxidation in tumor cells using sulfenic acid-specific antibodies. *Proc Natl Acad Sci U S A* 106: 16163-8, 2009.
467. Serrano I, Audran C, Rivas S. Chloroplasts at work during plant innate immunity. *J Exp Bot* 67: 3845-54, 2016.
468. Serrato AJ, Perez-Ruiz JM, Spinola MC, Cejudo FJ. A novel NADPH thioredoxin reductase, localized in the chloroplast, which deficiency causes hypersensitivity to abiotic stress in *Arabidopsis thaliana*. *J Biol Chem* 279: 43821-7, 2004.
469. Seth D, Stamler JS. The SNO-proteome: causation and classifications. *Curr Opin Chem Biol* 15: 129-36, 2011.
470. Sethuraman M, McComb ME, Heibeck T, Costello CE, Cohen RA. Isotope-coded affinity tag approach to identify and quantify oxidant-sensitive protein thiols. *Mol Cell Proteomics* 3: 273-8, 2004.
471. Sevilla F, Camejo D, Ortiz-Espin A, Calderon A, Lazaro JJ, Jimenez A. The thioredoxin/peroxiredoxin/sulfiredoxin system: current overview on its redox function in plants and regulation by reactive oxygen and nitrogen species. *J Exp Bot* 66: 2945-55, 2015.

472. Sewelam N, Kazan K, Schenk PM. Global Plant Stress Signaling: Reactive Oxygen Species at the Cross-Road. *Front Plant Sci* 7: 187, 2016.
473. Shaikhali J, Heiber I, Seidel T, Stroher E, Hiltcher H, Birkmann S, Dietz KJ, Baier M. The redox-sensitive transcription factor Rap2.4a controls nuclear expression of 2-Cys peroxiredoxin A and other chloroplast antioxidant enzymes. *BMC Plant Biol* 8: 48, 2008.
474. Shakir S, Vinh J, Chiappetta G. Quantitative analysis of the cysteine redoxome by iodoacetyl tandem mass tags. *Anal Bioanal Chem* 409: 3821-3830, 2017.
475. Simionato D, Basso S, Zaffagnini M, Lana T, Marzotto F, Trost P, Morosinotto T. Protein redox regulation in the thylakoid lumen: The importance of disulfide bonds for violaxanthin de-epoxidase. *FEBS Letters* 589: 919-923, 2015.
476. Skryhan K, Gurrieri L, Sparla F, Trost P, Blennow A. Redox Regulation of Starch Metabolism. *Frontiers in Plant Science* 9: 1344, 2018.
477. Sonntag C. *The chemical basis of radiation biology*: Taylor & Francis London; 1987.
478. Sparla F, Costa A, Lo Schiavo F, Pupillo P, Trost P. Redox regulation of a novel plastid-targeted beta-amylase of Arabidopsis. *Plant Physiol* 141: 840-50, 2006.
479. Sparla F, Pupillo P, Trost P. The C-terminal extension of glyceraldehyde-3-phosphate dehydrogenase subunit B acts as an autoinhibitory domain regulated by thioredoxins and nicotinamide adenine dinucleotide. *J Biol Chem* 277: 44946-52, 2002.
480. Sparla F, Zaffagnini M, Wedel N, Scheibe R, Pupillo P, Trost P. Regulation of photosynthetic GAPDH dissected by mutants. *Plant Physiology* 138: 2210-9, 2005.
481. Ströher E, Grassl J, Carrie C, Fenske R, Whelan J, Millar AH. Glutaredoxin S15 is involved in Fe-S cluster transfer in mitochondria influencing lipoic acid-dependent enzymes, plant growth and arsenic tolerance in Arabidopsis. *Plant Physiol* 170: 1284-99, 2015.
482. Subramani J, Kundumani-Sridharan V, Hilgers RH, Owens C, Das KC. Thioredoxin Uses a GSH-independent Route to Deglutathionylate Endothelial Nitric-oxide Synthase and Protect against Myocardial Infarction. *J Biol Chem* 291: 23374-89, 2016.

483. Sullivan DM, Wehr NB, Fergusson MM, Levine RL, Finkel T. Identification of oxidant-sensitive proteins: TNF-alpha induces protein glutathiolation. *Biochemistry* 39: 11121-8, 2000.
484. Suzuki N, Miller G, Morales J, Shulaev V, Torres MA, Mittler R. Respiratory burst oxidases: the engines of ROS signaling. *Curr Opin Plant Biol* 14: 691-9, 2011.
485. Szabo C. Hydrogen sulphide and its therapeutic potential. *Nat Rev Drug Discov* 6: 917-35, 2007.
486. Szabo C, Ischiropoulos H, Radi R. Peroxynitrite: biochemistry, pathophysiology and development of therapeutics. *Nat Rev Drug Discov* 6: 662-80, 2007.
487. Tada Y, Spoel SH, Pajerowska-Mukhtar K, Mou Z, Song J, Wang C, Zuo J, Dong X. Plant immunity requires conformational changes [corrected] of NPR1 via S-nitrosylation and thioredoxins. *Science* 321: 952-6, 2008.
488. Takahashi H, Kopriva S, Giordano M, Saito K, Hell R. Sulfur assimilation in photosynthetic organisms: molecular functions and regulations of transporters and assimilatory enzymes. *Annu Rev Plant Biol* 62: 157-84, 2011.
489. Takanishi CL, Ma LH, Wood MJ. A genetically encoded probe for cysteine sulfenic acid protein modification in vivo. *Biochemistry* 46: 14725-32, 2007.
490. Takanishi CL, Wood MJ. A genetically encoded probe for the identification of proteins that form sulfenic acid in response to H₂O₂ in *Saccharomyces cerevisiae*. *J Proteome Res* 10: 2715-24, 2011.
491. Tanou G, Filippou P, Belghazi M, Job D, Diamantidis G, Fotopoulos V, Molassiotis A. Oxidative and nitrosative-based signaling and associated post-translational modifications orchestrate the acclimation of citrus plants to salinity stress. *Plant J* 72: 585-99, 2012.
492. Tanou G, Ziogas V, Belghazi M, Christou A, Filippou P, Job D, Fotopoulos V, Molassiotis A. Polyamines reprogram oxidative and nitrosative status and the proteome of citrus plants exposed to salinity stress. *Plant Cell Environ* 37: 864-85, 2014.

493. Tao R, Zhao Y, Chu H, Wang A, Zhu J, Chen X, Zou Y, Shi M, Liu R, Su N, Du J, Zhou HM, Zhu L, Qian X, Liu H, Loscalzo J, Yang Y. Genetically encoded fluorescent sensors reveal dynamic regulation of NADPH metabolism. *Nat Methods* 14: 720-8, 2017.
494. Tarrago L, Laugier E, Zaffagnini M, Marchand C, Le Marechal P, Rouhier N, Lemaire SD, Rey P. Regeneration mechanisms of *Arabidopsis thaliana* methionine sulfoxide reductases B by glutaredoxins and thioredoxins. *J Biol Chem* 284: 18963-71, 2009.
495. Tarrago L, Laugier E, Zaffagnini M, Marchand CH, Le Marechal P, Lemaire SD, Rey P. Plant thioredoxin CDSP32 regenerates 1-cys methionine sulfoxide reductase B activity through the direct reduction of sulfenic acid. *J Biol Chem* 285: 14964-72, 2010.
496. Teo CF, Wells L. Monitoring protein O-linked beta-N-acetylglucosamine status via metabolic labeling and copper-free click chemistry. *Anal Biochem* 464: 70-2, 2014.
497. Terrile MC, Paris R, Calderon-Villalobos LI, Iglesias MJ, Lamattina L, Estelle M, Casalongue CA. Nitric oxide influences auxin signaling through S-nitrosylation of the Arabidopsis TRANSPORT INHIBITOR RESPONSE 1 auxin receptor. *Plant J* 70: 492-500, 2012.
498. Thormählen I, Meitzel T, Groysman J, Oechsner AB, von Roepenack-Lahaye E, Naranjo B, Cejudo FJ, Geigenberger P. Thioredoxin f1 and NADPH-Dependent Thioredoxin Reductase C Have Overlapping Functions in Regulating Photosynthetic Metabolism and Plant Growth in Response to Varying Light Conditions. *Plant Physiol* 169: 1766-86, 2015.
499. Thormählen I, Naranjo B, Trujillo-Hernandez JA, Reichheld J-P, Cejudo FJ, Geigenberger P. On the Elaborate Network of Thioredoxins in Higher Plants. *In: Progress in Botany. Springer, Berlin, Heidelberg, 2018.*
500. Thormählen I, Ruber J, Von Roepenack-Lahaye E, Ehrlich S-M, Massot V, Huemmer C, Tezycka J, Issakidis-Bourguet E, Geigenberger P. Inactivation of thioredoxin f1 leads to decreased light activation of ADP-glucose pyrophosphorylase and altered diurnal starch turnover in leaves of Arabidopsis plants. *Plant Cell Environ* 36: 16-29, 2013.

501. Thormählen I, Zupok A, Rescher J, Leger J, Weissenberger S, Groysman J, Orwat A, Chatel-Innocenti G, Issakidis-Bourguet E, Armbruster U. Thioredoxins play a crucial role in dynamic acclimation of photosynthesis in fluctuating light. *Mol Plant* 10: 168-82, 2017.
502. Thurlkill RL, Grimsley GR, Scholtz JM, Pace CN. pK values of the ionizable groups of proteins. *Protein Sci* 15: 1214-8, 2006.
503. Tikhonov AN. pH-dependent regulation of electron transport and ATP synthesis in chloroplasts. *Photosynth Res* 116: 511-34, 2013.
504. Tognetti VB, Bielach A, Hrtyan M. Redox regulation at the site of primary growth: auxin, cytokinin and ROS crosstalk. *Plant Cell Environ* 40: 2586-2605, 2017.
505. Toohey JI. Sulfur signaling: is the agent sulfide or sulfane? *Anal Biochem* 413: 1-7, 2011.
506. Trapet P, Kulik A, Lamotte O, Jeandroz S, Bourque S, Nicolas-Frances V, Rosnoblet C, Besson-Bard A, Wendehenne D. NO signaling in plant immunity: a tale of messengers. *Phytochemistry* 112: 72-9, 2015.
507. Traverso JA, Micallella C, Martinez A, Brown SC, Satiat-Jeunemaître B, Meinel T, Giglione C. Roles of N-terminal fatty acid acylations in membrane compartment partitioning: Arabidopsis h-type thioredoxins as a case study. *Plant Cell* 25: 1056-77, 2013.
508. Trost P, Fermani S, Calvaresi M, Zaffagnini M. Biochemical basis of sulphenomics: how protein sulphenic acids may be stabilized by the protein microenvironment. *Plant Cell Environ* 40: 483-90, 2017.
509. van Dongen JT, Licausi F. Oxygen sensing and signaling. *Annu Rev Plant Biol* 66: 345-67, 2015.
510. Vandenameele S, Vanderauwera S, Vuylsteke M, Rombauts S, Langebartels C, Seidlitz HK, Zabeau M, Van Montagu M, Inze D, Van Breusegem F. Catalase deficiency drastically affects gene expression induced by high light in Arabidopsis thaliana. *Plant J* 39: 45-58, 2004.
511. Vandiver MS, Paul BD, Xu R, Karuppagounder S, Rao F, Snowman AM, Ko HS, Lee YI, Dawson VL, Dawson TM, Sen N, Snyder SH. Sulfhydration mediates neuroprotective actions of parkin. *Nat Commun* 4: 1626, 2013.

512. Vanzo E, Ghirardo A, Merl-Pham J, Lindermayr C, Heller W, Hauck SM, Durner J, Schnitzler JP. S-nitroso-proteome in poplar leaves in response to acute ozone stress. *PLoS ONE* 9: e106886, 2014.
513. Verma PK, Verma S, Pande V, Mallick S, Deo Tripathi R, Dhankher OP, Chakrabarty D. Overexpression of rice glutaredoxin OsGrx_C7 and OsGrx_C2. 1 reduces intracellular arsenic accumulation and increases tolerance in *Arabidopsis thaliana*. *Front Plant Sci* 7: 740, 2016.
514. Vernoux T, Wilson RC, Seeley KA, Reichheld JP, Muroy S, Brown S, Maughan SC, Cobbett CS, Van Montagu M, Inze D, May MJ, Sung ZR. The ROOT MERISTEMLESS1/CADMIUM SENSITIVE2 gene defines a glutathione-dependent pathway involved in initiation and maintenance of cell division during postembryonic root development. *Plant Cell* 12: 97-110, 2000.
515. Vescovi M, Zaffagnini M, Festa M, Trost P, Lo Schiavo F, Costa A. Nuclear accumulation of cytosolic glyceraldehyde-3-phosphate dehydrogenase in cadmium-stressed *Arabidopsis* roots. *Plant Physiol* 162: 333-46, 2013.
516. Vetoshkina DV, Ivanov BN, Khorobrykh SA, Proskuryakov, II, Borisova-Mubarakshina MM. Involvement of the chloroplast plastoquinone pool in the Mehler reaction. *Physiol Plant* 161: 45-55, 2017.
517. Vieira Dos Santos C, Cuine S, Rouhier N, Rey P. The *Arabidopsis* plastidic methionine sulfoxide reductase B proteins. Sequence and activity characteristics, comparison of the expression with plastidic methionine sulfoxide reductase A, and induction by photooxidative stress. *Plant Physiol* 138: 909-22, 2005.
518. Vogel MO, Moore M, König K, Pecher P, Alsharafa K, Lee J, Dietz K-J. Fast Retrograde Signaling in Response to High Light Involves Metabolite Export, Mitogen-Activated Protein Kinase 6, and AP2/ERF Transcription Factors in *Arabidopsis*. *Plant Cell* 26: 1151-65, 2014.
519. von Sonntag C. Free-radical reactions involving thiols and disulphides. In: *Sulfur-centered reactive intermediates in chemistry and biology*. Springer; 1990. pp. 359-366.
520. Wang H, Xian M. Chemical methods to detect S-nitrosation. *Curr Opin Chem Biol* 15: 32-7, 2011.

521. Wang L, Li Y, Jacquot JP, Rouhier N, Xia B. Characterization of poplar GrxS14 in different structural forms. *Protein Cell* 5: 329-33, 2014.
522. Wang P, Du Y, Hou YJ, Zhao Y, Hsu CC, Yuan F, Zhu X, Tao WA, Song CP, Zhu JK. Nitric oxide negatively regulates abscisic acid signaling in guard cells by S-nitrosylation of OST1. *Proc Natl Acad Sci U S A* 112: 613-8, 2015.
523. Wang P, Liu J, Liu B, Feng D, Da Q, Wang P, Shu S, Su J, Zhang Y, Wang J, Wang H-B. Evidence for a Role of Chloroplastic m-Type Thioredoxins in the Biogenesis of Photosystem II in Arabidopsis. *Plant Physiol* 163: 1710-28, 2013.
524. Wang WH, He EM, Chen J, Guo Y, Liu X, Zheng HL. The reduced state of the plastoquinone pool is required for chloroplast-mediated stomatal closure in response to calcium stimulation. *Plant J* 86: 132-44, 2016.
525. Wang Y, Liu T, Wu C, Li H. A strategy for direct identification of protein S-nitrosylation sites by quadrupole time-of-flight mass spectrometry. *J Am Soc Mass Spectrom* 19: 1353-60, 2008.
526. Wang Z, Xing S, Birkenbihl RP, Zachgo S. Conserved Functions of Arabidopsis and Rice CC-Type Glutaredoxins in Flower Development and Pathogen Response. *Mol Plant* 2: 323-35, 2009.
527. Waszczak C, Akter S, Eeckhout D, Persiau G, Wahni K, Bodra N, Van Molle I, De Smet B, Vertommen D, Gevaert K, De Jaeger G, Van Montagu M, Messens J, Van Breusegem F. Sulfenome mining in Arabidopsis thaliana. *Proc Natl Acad Sci U S A* 111: 11545-50, 2014.
528. Waszczak C, Akter S, Jacques S, Huang J, Messens J, Van Breusegem F. Oxidative post-translational modifications of cysteine residues in plant signal transduction. *J Exp Bot* 66: 2923-34, 2015.
529. Wedel N, Soll J. Evolutionary conserved light regulation of Calvin cycle activity by NADPH-mediated reversible phosphoribulokinase/CP12/ glyceraldehyde-3-phosphate dehydrogenase complex dissociation. *Proc Natl Acad Sci U S A* 95: 9699-704, 1998.
530. Weerapana E, Wang C, Simon GM, Richter F, Khare S, Dillon MB, Bachovchin DA, Mowen K, Baker D, Cravatt BF. Quantitative reactivity profiling predicts functional cysteines in proteomes. *Nature* 468: 790-5, 2010.

531. Weits DA, Giuntoli B, Kosmacz M, Parlanti S, Hubberten H-M, Riegler H, Hoefgen R, Perata P, Van Dongen JT, Licausi F. Plant cysteine oxidases control the oxygen-dependent branch of the N-end-rule pathway. *Nat Commun* 5: 3425, 2014.
532. White MD, Kamps J, East S, Taylor Kearney LJ, Flashman E. The plant cysteine oxidases from *Arabidopsis thaliana* are kinetically tailored to act as oxygen sensors. *J Biol Chem* 293: 11786-11795, 2018.
533. White MD, Klecker M, Hopkinson RJ, Weits DA, Mueller C, Naumann C, O'Neill R, Wickens J, Yang J, Brooks-Bartlett JC, Garman EF, Grossmann TN, Dissmeyer N, Flashman E. Plant cysteine oxidases are dioxygenases that directly enable arginyl transferase-catalysed arginylation of N-end rule targets. *Nat Commun* 8: 14690, 2017.
534. Whiteman M, Moore PK. Hydrogen sulfide and the vasculature: a novel vasculoprotective entity and regulator of nitric oxide bioavailability? *J Cell Mol Med* 13: 488-507, 2009.
535. Wimmelbacher M, Bornke F. Redox activity of thioredoxin z and fructokinase-like protein 1 is dispensable for autotrophic growth of *Arabidopsis thaliana*. *J Exp Bot* 65: 2405-13, 2014.
536. Winterbourn CC, Hampton MB. Thiol chemistry and specificity in redox signaling. *Free Radic Biol Med* 45: 549-61, 2008.
537. Winterbourn CC, Metodiewa D. Reactivity of biologically important thiol compounds with superoxide and hydrogen peroxide. *Free Radic Biol Med* 27: 322-8, 1999.
538. Wolosiuk RA, Buchanan BB. Thioredoxin and glutathione regulate photosynthesis in chloroplasts. *Nature* 266: 565-7, 1977.
539. Wolosiuk RA, Buchanan BB. Activation of Chloroplast NADP-linked Glyceraldehyde-3-Phosphate Dehydrogenase by the Ferredoxin/Thioredoxin System. *Plant Physiol* 61: 669-71, 1978.
540. Wolosiuk RA, Buchanan BB. Regulation of chloroplast phosphoribulokinase by the ferredoxin/thioredoxin system. *Arch Biochem Biophys* 189: 97-101, 1978.

541. Wolosiuk RA, Buchanan BB, Crawford NA. Regulation of NADP-malate dehydrogenase by the light-actuated ferredoxin/thioredoxin system of chloroplasts. *FEBS Letters* 81: 253-258, 1977.
542. Wong JH, Balmer Y, Cai N, Tanaka CK, Vensel WH, Hurkman WJ, Buchanan BB. Unraveling thioredoxin-linked metabolic processes of cereal starchy endosperm using proteomics. *FEBS Lett* 547: 151-6, 2003.
543. Wong JH, Cai N, Balmer Y, Tanaka CK, Vensel WH, Hurkman WJ, Buchanan BB. Thioredoxin targets of developing wheat seeds identified by complementary proteomic approaches. *Phytochemistry* 65: 1629-40, 2004.
544. Wood MJ, Storz G, Tjandra N. Structural basis for redox regulation of Yap1 transcription factor localization. *Nature* 430: 917-21, 2004.
545. Wright MH, Paape D, Price HP, Smith DF, Tate EW. Global Profiling and Inhibition of Protein Lipidation in Vector and Host Stages of the Sleeping Sickness Parasite *Trypanosoma brucei*. *ACS Infect Dis* 2: 427-441, 2016.
546. Wu Q, Hu Y, Sprague SA, Kakeshpour T, Park J, Nakata PA, Cheng N, Hirschi KD, White FF, Park S. Expression of a monothiol glutaredoxin, AtGRXS17, in tomato (*Solanum lycopersicum*) enhances drought tolerance. *Biochem Biophys Res Commun* 491: 1034-9, 2017.
547. Wu Q, Lin J, Liu JZ, Wang X, Lim W, Oh M, Park J, Rajashekar C, Whitham SA, Cheng NH. Ectopic expression of Arabidopsis glutaredoxin AtGRXS17 enhances thermotolerance in tomato. *Plant Biotechnol J* 10: 945-55, 2012.
548. Xia XJ, Fang PP, Guo X, Qian XJ, Zhou J, Shi K, Zhou YH, Yu JQ. Brassinosteroid-mediated apoplastic H₂O₂-glutaredoxin 12/14 cascade regulates antioxidant capacity in response to chilling in tomato. *Plant Cell Environ* 41: 1052-64, 2017.
549. Xing S, Rosso MG, Zachgo S. ROXY1, a member of the plant glutaredoxin family, is required for petal development in *Arabidopsis thaliana*. *Development* 132: 1555-65, 2005.
550. Xing S, Zachgo S. ROXY1 and ROXY2, two Arabidopsis glutaredoxin genes, are required for anther development. *Plant J* 53: 790-801, 2008.

551. Xu S, Guerra D, Lee U, Vierling E. S-nitrosoglutathione reductases are low-copy number, cysteine-rich proteins in plants that control multiple developmental and defense responses in *Arabidopsis*. *Front Plant Sci* 4: 430, 2013.
552. Yamazaki D, Motohashi K, Kasama T, Hara Y, Hisabori T. Target proteins of the cytosolic thioredoxins in *Arabidopsis thaliana*. *Plant Cell Physiol* 45: 18-27, 2004.
553. Yang F, Bui HT, Pautler M, Llaca V, Johnston R, Lee B-h, Kolbe A, Sakai H, Jackson D. A Maize Glutaredoxin Gene, *Abphyl2*, Regulates Shoot Meristem Size and Phyllotaxy. *Plant Cell* 27: 121-31, 2015.
554. Yang J, Carroll KS, Liebler DC. The Expanding Landscape of the Thiol Redox Proteome. *Mol Cell Proteomics* 15: 1-11, 2016.
555. Yang J, Gupta V, Carroll KS, Liebler DC. Site-specific mapping and quantification of protein S-sulphenylation in cells. *Nat Commun* 5: 4776, 2014.
556. Yang J, Gupta V, Tallman KA, Porter NA, Carroll KS, Liebler DC. Global, in situ, site-specific analysis of protein S-sulfenylation. *Nat Protoc* 10: 1022-37, 2015.
557. Yang SS, Zhai QH. Cytosolic GAPDH: a key mediator in redox signal transduction in plants. *Biologia Plantarum* 61: 417-26, 2017.
558. Yano H, Kuroda M. Disulfide proteome yields a detailed understanding of redox regulations: a model study of thioredoxin-linked reactions in seed germination. *Proteomics* 6: 294-300, 2006.
559. Yano H, Wong JH, Lee YM, Cho MJ, Buchanan BB. A strategy for the identification of proteins targeted by thioredoxin. *Proc Natl Acad Sci U S A* 98: 4794-9, 2001.
560. Yao Y, He RJ, Xie QL, Zhao Xh, Deng Xm, He Jb, Song L, He J, Marchant A, Chen X-Y, Wu A-M. Ethylene response factor 74 (ERF74) plays an essential role in controlling a respiratory burst oxidase homolog D (RbohD)-dependent mechanism in response to different stresses in *Arabidopsis*. *New Phytol* 213: 1667-81, 2017.
561. Yoshida K, Hara A, Sugiura K, Fukaya Y, Hisabori T. Thioredoxin-like2/2-Cys peroxiredoxin redox cascade supports oxidative thiol modulation in chloroplasts. *Proc Natl Acad Sci U S A* 115: E8296-E8304, 2018.
562. Yoshida K, Hara S, Hisabori T. Thioredoxin Selectivity for Thiol-based Redox Regulation of Target Proteins in Chloroplasts. *J Biol Chem* 290: 14278-88, 2015.

563. Yoshida K, Hisabori T. Two distinct redox cascades cooperatively regulate chloroplast functions and sustain plant viability. *Proc Natl Acad Sci U S A* 113: E3967-76, 2016.
564. Yoshida K, Hisabori T. Distinct electron transfer from ferredoxin-thioredoxin reductase to multiple thioredoxin isoforms in chloroplasts. *Biochem J* 474: 1347-1360, 2017.
565. Yoshida K, Noguchi K, Motohashi K, Hisabori T. Systematic exploration of thioredoxin target proteins in plant mitochondria. *Plant Cell Physiol* 54: 875-92, 2013.
566. Yoshida K, Terashima I, Noguchi K. Up-Regulation of Mitochondrial Alternative Oxidase Concomitant with Chloroplast Over-Reduction by Excess Light. *Plant Cell Physiol* 48: 606-14, 2007.
567. Yu M, Yun BW, Spoel SH, Loake GJ. A sleigh ride through the SNO: regulation of plant immune function by protein S-nitrosylation. *Curr Opin Plant Biol* 15: 424-30, 2012.
568. Yu Q, Tian H, Yue K, Liu J, Zhang B, Li X, Ding Z. A P-Loop NTPase Regulates Quiescent Center Cell Division and Distal Stem Cell Identity through the Regulation of ROS Homeostasis in Arabidopsis Root. *PLOS Genetics* 12: e1006175, 2016.
569. Yu X, Pasternak T, Eiblmeier M, Ditengou F, Kochersperger P, Sun J, Wang H, Rennenberg H, Teale W, Paponov I, Zhou W, Li C, Li X, Palme K. Plastid-localized glutathione reductase2-regulated glutathione redox status is essential for Arabidopsis root apical meristem maintenance. *Plant Cell* 25: 4451-68, 2013.
570. Yun BW, Feechan A, Yin M, Saidi NB, Le Bihan T, Yu M, Moore JW, Kang JG, Kwon E, Spoel SH, Pallas JA, Loake GJ. S-nitrosylation of NADPH oxidase regulates cell death in plant immunity. *Nature* 478: 264-8, 2011.
571. Zaffagnini M, Bedhomme M, Groni H, Marchand CH, Puppo C, Gontero B, Cassier-Chauvat C, Decottignies P, Lemaire SD. Glutathionylation in the photosynthetic model organism *Chlamydomonas reinhardtii*: a proteomic survey. *Mol Cell Proteomics* 11: M111 014142, 2012.
572. Zaffagnini M, Bedhomme M, Lemaire SD, Trost P. The emerging roles of protein glutathionylation in chloroplasts. *Plant Sci* 185-186: 86-96, 2012.

573. Zaffagnini M, Bedhomme M, Marchand CH, Couturier JR, Gao XH, Rouhier N, Trost P, Lemaire SD. Glutaredoxin S12: unique properties for redox signaling. *Antioxid Redox Signal* 16: 17-32, 2012.
574. Zaffagnini M, Bedhomme M, Marchand CH, Morisse S, Trost P, Lemaire SD. Redox regulation in photosynthetic organisms: focus on glutathionylation. *Antioxid Redox Signal* 16: 567-86, 2012.
575. Zaffagnini M, De Mia M, Morisse S, Di Giacinto N, Marchand CH, Maes A, Lemaire SD, Trost P. Protein S-nitrosylation in photosynthetic organisms: A comprehensive overview with future perspectives. *Biochim Biophys Acta* 1864: 952-66, 2016.
576. Zaffagnini M, Fermani S, Calvaresi M, Orru R, Iommarini L, Sparla F, Falini G, Bottoni A, Trost P. Tuning Cysteine Reactivity and Sulfenic Acid Stability by Protein Microenvironment in Glyceraldehyde-3-Phosphate Dehydrogenases of *Arabidopsis thaliana*. *Antioxid Redox Signal* 24: 502-17, 2016.
577. Zaffagnini M, Fermani S, Costa A, Lemaire SD, Trost P. Plant cytoplasmic GAPDH: redox post-translational modifications and moonlighting properties. *Front Plant Sci* 4: 450, 2013.
578. Zaffagnini M, Michelet L, Massot V, Trost P, Lemaire SD. Biochemical characterization of glutaredoxins from *Chlamydomonas reinhardtii* reveals the unique properties of a chloroplastic CGFS-type glutaredoxin. *J Biol Chem* 283: 8868-76, 2008.
579. Zaffagnini M, Michelet L, Sciabolini C, Di Giacinto N, Morisse S, Marchand CH, Trost P, Fermani S, Lemaire SD. High-resolution crystal structure and redox properties of chloroplastic triosephosphate isomerase from *Chlamydomonas reinhardtii*. *Mol Plant* 7: 101-20, 2014.
580. Zaffagnini M, Morisse S, Bedhomme M, Marchand CH, Festa M, Rouhier N, Lemaire SD, Trost P. Mechanisms of nitrosylation and denitrosylation of cytoplasmic glyceraldehyde-3-phosphate dehydrogenase from *Arabidopsis thaliana*. *J Biol Chem* 288: 22777-89, 2013.
581. Zannini F, Roret T, Przybyla-Toscano J, Dhalleine T, Rouhier N, Couturier J. Mitochondrial *Arabidopsis thaliana* TRXo Isoforms Bind an Iron(-)Sulfur Cluster and Reduce NFU Proteins In Vitro. *Antioxidants (Basel)* 7, 2018.

582. Zechmann B. Compartment-specific importance of glutathione during abiotic and biotic stress. *Front Plant Sci* 5: 566, 2014.
583. Zechmann B. Compartment-Specific Importance of Ascorbate During Environmental Stress in Plants. *Antioxid Redox Signal*, 2017.
584. Zeida A, Gonzalez Lebrero MC, Radi R, Trujillo M, Estrin DA. Mechanism of cysteine oxidation by peroxynitrite: An integrated experimental and theoretical study. *Arch Biochem Biophys* 539: 81-6, 2013.
585. Zhang D, Macinkovic I, Devarie-Baez NO, Pan J, Park CM, Carroll KS, Filipovic MR, Xian M. Detection of protein S-sulfhydration by a tag-switch technique. *Angew Chem Int Ed Engl* 53: 575-81, 2014.
586. Zhang DW, Yuan S, Xu F, Zhu F, Yuan M, Ye HX, Guo HQ, Lv X, Yin Y, Lin HH. Light intensity affects chlorophyll synthesis during greening process by metabolite signal from mitochondrial alternative oxidase in Arabidopsis. *Plant Cell Environ* 39: 12-25, 2016.
587. Zhang N, Portis AR, Jr. Mechanism of light regulation of Rubisco: a specific role for the larger Rubisco activase isoform involving reductive activation by thioredoxin-f. *Proc Natl Acad Sci U S A* 96: 9438-43, 1999.
588. Zhang T, Zhu M, Zhu N, Strul JM, Dufresne CP, Schneider JD, Harmon AC, Chen S. Identification of thioredoxin targets in guard cell enriched epidermal peels using cystTMT proteomics. *J Proteomics* 133: 48-53, 2016.
589. Zhang X, Huang B, Chen C. SNO spectral counting (SNOSC), a label-free proteomic method for quantification of changes in levels of protein S-nitrosation. *Free Radic Res* 46: 1044-50, 2012.
590. Zhang X, Wang W, Li C, Zhao Y, Yuan H, Tan X, Wu L, Wang Z, Wang H. Structural insights into the binding of buckwheat glutaredoxin with GSH and regulation of its catalytic activity. *J Inorg Biochem* 173: 21-27, 2017.
591. Zhao Y, Wei T, Yin KQ, Chen Z, Gu H, Qu LJ, Qin G. Arabidopsis RAP2.2 plays an important role in plant resistance to *Botrytis cinerea* and ethylene responses. *New Phytol* 195: 450-60, 2012.
592. Zheng B, Zhu S, Wu X. Clickable analogue of cerulenin as chemical probe to explore protein palmitoylation. *ACS Chem Biol* 10: 115-21, 2015.

593. Zhou X, Han P, Li J, Zhang X, Huang B, Ruan HQ, Chen C. ESNOQ, proteomic quantification of endogenous S-nitrosation. *PLoS ONE* 5: e10015, 2010.
594. Zhu XG, Long SP, Ort DR. What is the maximum efficiency with which photosynthesis can convert solar energy into biomass? *Curr Opin Biotechnol* 19: 153-9, 2008.
595. Ziegler H, Ziegler I. Der Einfluss der Belichtung auf Die NADP+-Abhängige Glycerinaldehyd-3-Phosphat-Dehydrogenase. *Planta* 65: 369-380, 1965.

ABBREVIATIONS USED:

ACHT, atypical Cys histidine-rich thioredoxin;
APX, ascorbate peroxidase;
BASI, barley alpha-amylase/subtilisin inhibitor;
BiFC, bimolecular fluorescence complementation;
BST, Biotin Switch Technique;
CAT, catalase;
CB, Calvin-Benson;
CDSP32, chloroplastic drought-induced stress protein;
DTT, dithiothreitol;
FBPase, fructose-1,6-bisphosphate phosphatase;
FDX, ferredoxin;
Fe-S, iron-sulfur;
FNR, ferredoxin:NADPH reductase;
FTR, ferredoxin:thioredoxin reductase;
G6PDH, glucose-6-phosphate dehydrogenase;
GAPC, glyceraldehyde-3-phosphate dehydrogenase C (cytoplasmic isoform);
GAPDH, glyceraldehyde-3-phosphate dehydrogenase;
GFP, green fluorescent probe;
GOX, glycolate oxidase;
GPLX, glutathione peroxidases-like;
GR, glutathione reductase;
GRX, glutaredoxin;
GSH, reduced glutathione;
GSNO, nitrosoglutathione;
GSNOR, nitrosoglutathione reductase;
GSSG, oxidized glutathione;
GST, glutathione-S-transferase;
ICL, isocitrate lyase;
MMTS, methyl methanethiosulfonate;
MS, mass spectrometry;

NADP-MDH, NADP-malate dehydrogenase;
NEM, N-ethyl maleimide;
NOFNiR, NO-forming nitrate reductase;
NPQ, non-photochemical quenching;
NR, nitrate reductase;
NRX, nucleoredoxins;
NTR, NADPH:thioredoxin reductase;
NTRC, NADPH:thioredoxin reductase C;
OPPP, oxidative pentose phosphate pathway;
PCO, plant cysteine oxidase;
PDI, protein disulfide isomerase;
PET, photosynthetic electron transport;
PRK, phosphoribulokinase;
PRX, peroxiredoxin;
PS, photosystem;
PTM, post-translational modification;
QY, quantum yield;
RBOH, respiratory burst oxidase homolog;
RMS, reactive molecular species;
RNS, reactive nitrogen species;
ROS, reactive oxygen species;
RSS, reactive sulfur species;
RubisCO, ribulose-1,5-bisphosphate carboxylase/oxygenase;
SiR, sulfite reductase;
SOD, superoxide dismutase;
TDX, tetratricopeptide domain-containing thioredoxin;
TR, thioredoxin reductase;
TRX, thioredoxin;
TRXL, thioredoxin-like;
YFP, yellow fluorescent probe

Table 1. Gene content in the GRX and TRX families in representative organisms of the green lineage*

	<i>At</i>	<i>Os</i>	<i>Sm</i>	<i>Pp</i>	<i>Cr</i>	<i>Syn</i>
GRXs	33	29	17	15	7	3
Class I	6	5	4	5	2	2
C1	1	0	0	0	-	-
C2	1	2	2	3	-	-
C3	1	1	0	1	-	-
C4	1	1	1	0	-	-
C5	1	0	0	0	-	-
S12	1	1	1	1	-	-
Class II	4	5	9	8	4	1
S14	1	1	3	2	1	-
S15	1	2	3	2	1	-
S16	1	1	1	1	1	-
S17	1	1	2	3	1	-
Class III	21	17	3	2	0	0
Class IV	2	2	1	0	1	0
TRXs	37	30	22	28	20	4
TRX f	2	1	2	3	2	0
TRX h	11	7	5	5	2	0
TRX m	4	4	2	6	1	1
TRX o	2	1	0	1	1	0
TRX x	1	1	1	2	1	1
TRX y	2	1	1	1	1	1
TRX z	1	1	1	2	1	0
TRX-like 1	1	1	2	1	1	0
TRX-like 2	2	1	2	2	0	0
TRX-lilium 1	3	2	0	0	0	0
TRX-lilium 2	1	1	2	1	1	0
TRX-lilium 3	1	1	0	1	1	0
TDX	1	1	0	0	0	0
CDSP32	1	1	1	1	1	0
CLOT	1	1	1	1	1	0
HCF164	1	1	1	1	1	1
NRX1	1	2	0	0	5 [†]	0
NRX2	0	1	1	0	0	0
NRX3	1	1	0	0	0	0
TR	4	4	3	6	4	2
NTRA/B	2	2	1	2	3 [†]	0 [§]
NTRC	1	1	1	2	1	0
FTR-b	1	1	1	2	1	1

* Sequences from *O. sativa* (*Os*), *S. moellendorffii* (*Sm*), *P. patens* (*Pp*), *C. reinhardtii* (*Cr*) and *Synechocystis* sp. PCC 6803 (*Syn*) have been retrieved from genomic data available through Phytozome V12 portal or cyanobase by BLAST-p analysis using *A. thaliana* (*At*) sequences as references. The classes in the GRX and TRX families have been previously defined (87,100).

[†] The five NRXs found in *C. reinhardtii* have been arbitrarily classified as NRX1 but they group independently from land plant NRXs.

[‡] This indicates the existence among NTRA/B from *C. reinhardtii* of a mammalian-type selenocysteine-containing NTR.

[§] *Synechocystis* sp. PCC 6803 does not possess an authentic NTR, but another type of diflavin protein of unknown function (59).

Table 2. 3D-structures of TRXs and GRXs from photosynthetic organisms

PROTEIN (redox state)	ORGANISM	PDB ID (reference)	METHOD
TRX <i>h</i> (ox)	<i>C. reinhardtii</i>	1TOF (344)	NMR
TRX <i>h</i> (ox)	<i>C. reinhardtii</i>	1EP7 (329)	X-ray
TRX <i>h</i> D30A (ox)	<i>C. reinhardtii</i>	1EP8 (329)	X-ray
TRX <i>h</i> 1 (red)	<i>H. vulgare</i>	2VM1, 2VM2 (314)	X-ray
TRX <i>h</i> 2 (ox)	<i>H. vulgare</i>	2VLT (314)	X-ray
TRX <i>h</i> 2 (partially red)	<i>H. vulgare</i>	2VLU, 2VLV (314)	X-ray
TRX <i>h</i> 1 (ox)	<i>A. thaliana</i>	1XFL (410)	NMR
TRX <i>h</i> 1 (red)	<i>P. trichocarpa</i> x <i>P. deltoides</i>	1TI3 (98)	NMR
TRX <i>h</i> 4 (ox)	<i>P. trichocarpa</i> x <i>P. deltoides</i>	3D21 (264)	X-ray
TRX <i>h</i> 4 C61S (red)	<i>P. trichocarpa</i> x <i>P. deltoides</i>	3D22 (264)	X-ray
TRX <i>h</i> (red)	<i>O. sativa</i>	1WMJ (/)	NMR
TRX <i>f</i> (short form; ox)	<i>S. oleracea</i>	1F9M (65)	X-ray
TRX <i>f</i> (long form; ox)	<i>S. oleracea</i>	1FAA (65)	X-ray
TRX <i>m</i> (red)	<i>S. oleracea</i>	1FB0 (65)	X-ray
TRX <i>m</i> (ox)	<i>S. oleracea</i>	1FB6 (65)	X-ray
TRX <i>m</i> CH2 (ox)	<i>C. reinhardtii</i>	1DBY (277)	NMR
TRX 2 (ox)	<i>Anabaena</i> sp. PCC 7120	1THX (444)	X-ray
TRX <i>o</i> 1 (ox)	<i>A. thaliana</i>	6G61 (581)	X-ray
TRX <i>o</i> 2 (ox)	<i>A. thaliana</i>	6G62 (581)	X-ray
TRX-like2.1 (ox/red)	<i>P. tremula</i> x <i>P. tremuloides</i>	5NYK, 5NYM (84)	X-ray

GRXC1-Fe ₂ S ₂ -GSH (red)	<i>P. trichocarpa</i> x <i>P. deltooides</i>	2E7P (441)	X-ray
GRXC1 (red)	<i>P. trichocarpa</i> x <i>P. deltooides</i>	1Z7P (142)	NMR
GRXC1 (red)	<i>P. trichocarpa</i> x <i>P. deltooides</i>	1Z7R (142)	NMR
GRXC5-GSH (red)	<i>A. thaliana</i>	3RHB (104)	X-ray
GRXC5-Fe ₂ S ₂ -GSH (red)	<i>A. thaliana</i>	3RHC (104)	X-ray
GRXS12-GSH	<i>P. trichocarpa</i> x <i>P. deltooides</i>	3FZ9 (102)	X-ray
GRXS12-GSH-BME*	<i>P. trichocarpa</i> x <i>P. deltooides</i>	3FZA (102)	X-ray
GRXS14 (GRXcp, red)	<i>A. thaliana</i>	3IPZ (291)	X-ray
GRXS14 (red)	<i>P. tremula</i> x <i>P. tremuloides</i>	2LKU (521)	NMR
GRXS16 (N-terminal endonuclease domain, red)	<i>A. thaliana</i>	2LWF (305)	NMR
GRX-GSH	<i>Fagopyrum tataricum</i>	5KQA (590)	X-ray
GRX A (red)	<i>Synechocystis</i> sp. PCC 6803	3QMX (258)	X-ray

*BME: Beta-mercaptoethanol

FIGURE LEGENDS

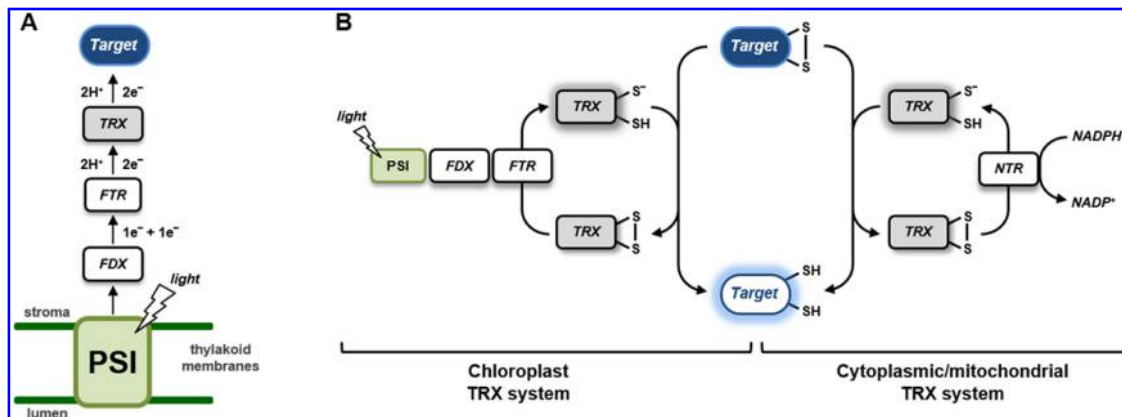


Figure 1. TRX-dependent redox systems

(A) Schematic representation of the FDX-TRX system of oxygenic photosynthetic organisms. In illuminated chloroplasts, FDX distributes PSI-driven electrons ($1e^-$ plus $1e^-$) to oxidized TRX in a reaction catalyzed by FTR ($2e^-$ plus $2H^+$). In turn, TRX reduces target proteins via a dithiol/disulfide exchange reaction ($2e^-$ plus $2H^+$). (B) Dithiol/disulfide interchanges of chloroplastic and cytoplasmic/mitochondrial TRX systems. Chloroplastic TRXs are reduced as described above whereas cytoplasmic/mitochondrial TRXs are reduced by NADPH:TRX reductase that uses NADPH as electron donor. Once reduced, TRX catalyzes the reduction of regulatory disulfides on target proteins. Abbreviations: FDX, ferredoxin; FTR, ferredoxin:thioredoxin reductase; NTR, NADPH:TRX reductase; PSI, photosystem I; TRX, thioredoxin. To see this illustration in color, the reader is referred to the online version of this article at www.liebertpub.com/ars.

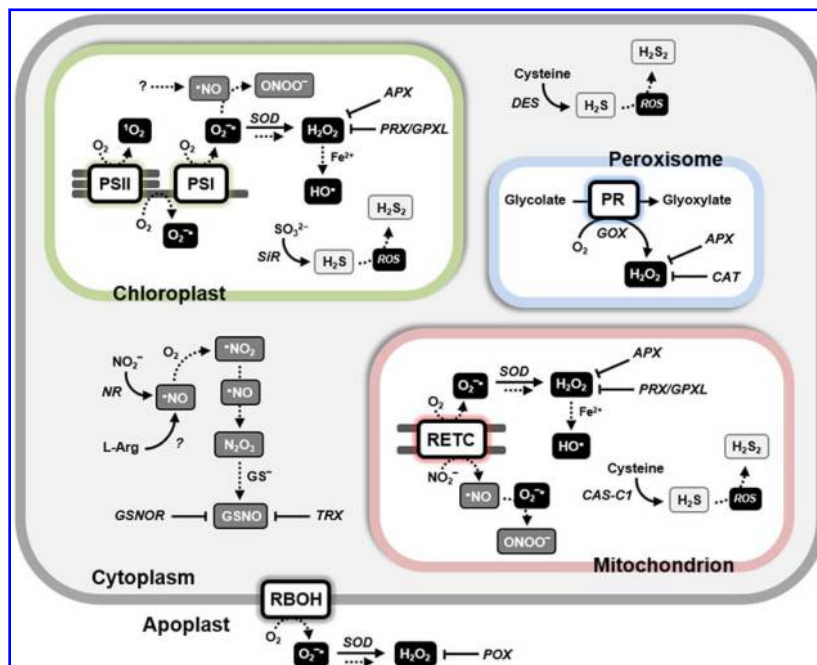


Figure 2. Reactive molecular species (RMS): production and scavenging systems

Biologically relevant RMS are based on oxygen (ROS, indicated in white on black rectangles), nitrogen (RNS, indicated in white on dark grey rectangles) or sulfur (RSS, indicated in black on light grey rectangles). The generation of RMS occurs through diverse enzymatic and non-enzymatic pathways and involves all subcellular compartments as depicted in the figure (for further details please refer to the text). The scavenging system mainly relies on antioxidant enzymes that are localized in all subcellular compartments including apoplast. Abbreviations: APX, ascorbate peroxidase; CAS-C1, β -cyanoalanine synthase; CAT, catalase; DES, cysteine desulfhydrase; GPXL, glutathione peroxidase-like; GOX, glyoxylate oxidase; GSNOR, nitrosogluthathione reductase; NR, nitrite reductase; POX, peroxidase; PR, photorespiration; PRX, peroxiredoxin; RBOH, respiratory burst oxidase homolog; RETC, respiratory electron transport chain; SiR, sulfite reductase, SOD, superoxide dismutase; TRX, thioredoxin. To see this illustration in color, the reader is referred to the online version of this article at www.liebertpub.com/ars.

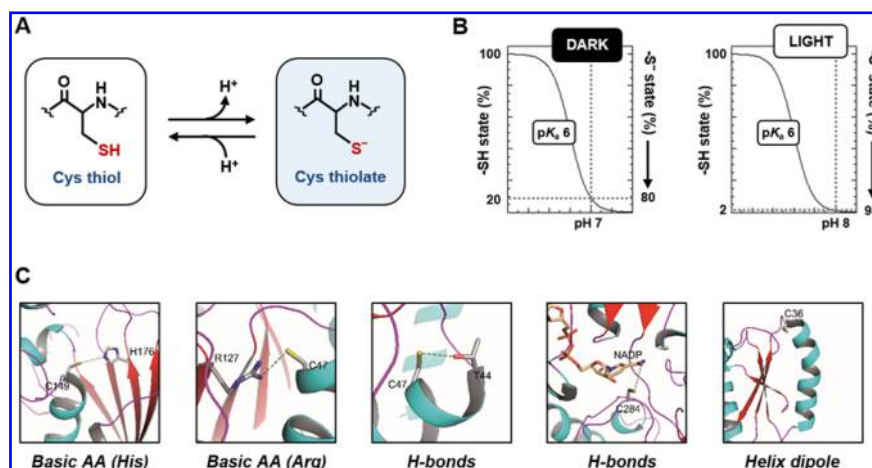


Figure 3. Biochemical and structural features of protein Cys

(A) Representation of a protein Cys in equilibrium between its thiol form ($-SH$, left side) and thiolate form ($-S^-$, right side). (B) Estimation of thiol/thiolate percentage of the catalytic Cys of photosynthetic GAPDH ($pK_a = 6$) at the indicated pH values (7.0 and 8.0 for stromal pH under dark and light conditions, respectively). (C) Examples of the main structural determinants of the Cys thiol reactivity by known protein crystal structures. From left to right: interactions with basic amino acids (His and Arg; PDB IDs: 4Z0H (576) and 1HD2 (114)), H-bond networks (PDB IDs: 1HD2 (114) and 2EUH (91)), and positioning of reactive Cys at the N-terminus of an α -helix (helix dipole; PDB ID: 1EP7 (329)). To see this illustration in color, the reader is referred to the online version of this article at www.liebertpub.com/ars.

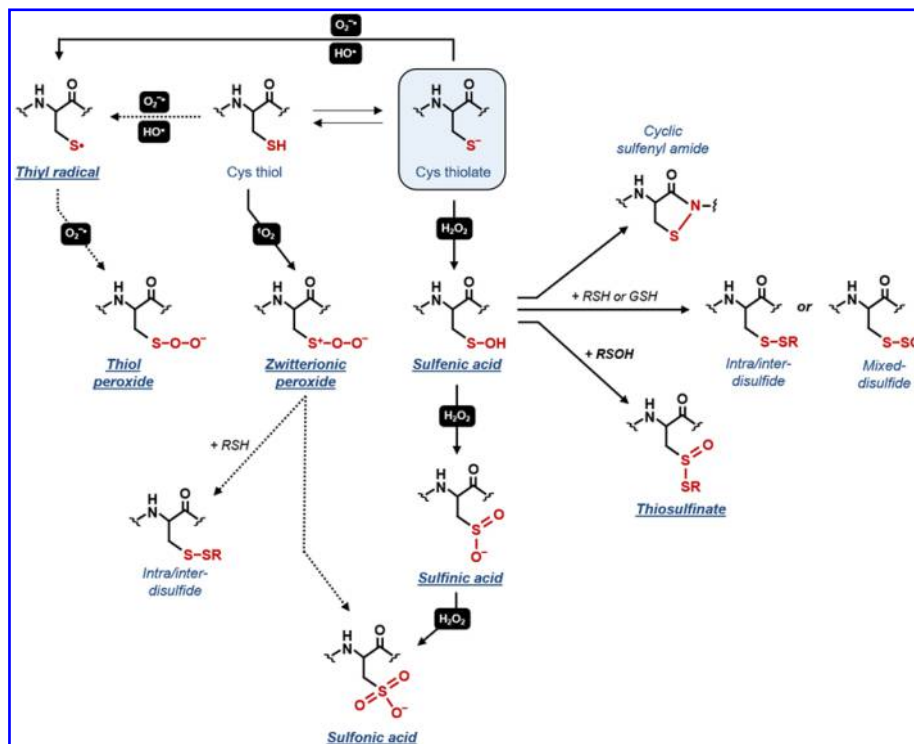


Figure 4. ROS-dependent thiol-based redox modifications

Biologically relevant ROS-dependent Cys modifications are depicted (underlined) together with secondary redox modifications. For further details, please refer to the text. ROS are indicated in white on black rectangles. Continuous and dotted lines indicate recognized and possible reactions, respectively. To see this illustration in color, the reader is referred to the online version of this article at www.liebertpub.com/ars.

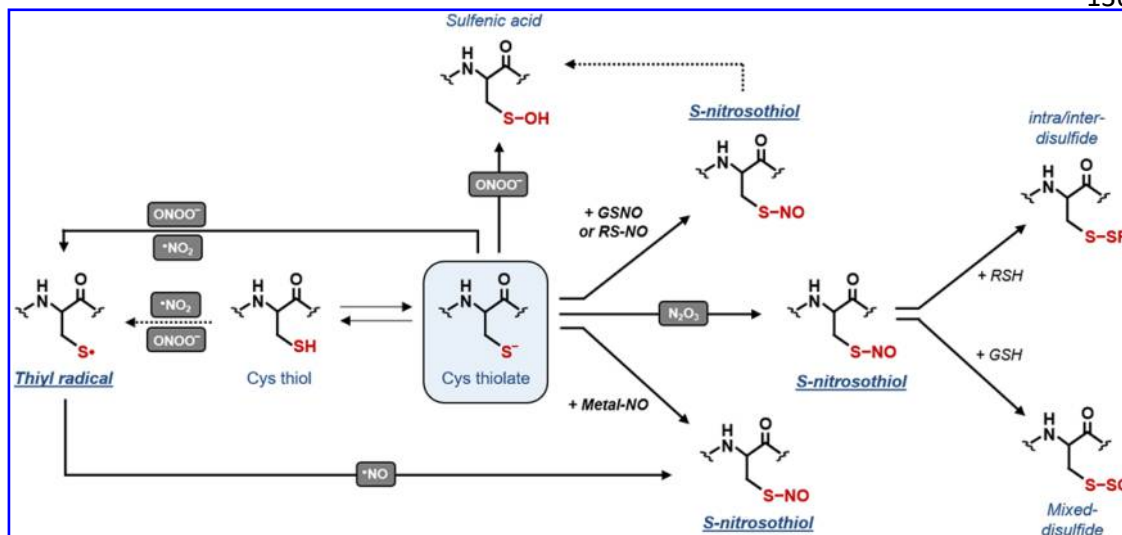


Figure 5. RNS-dependent thiol-based redox modifications

Biologically relevant RNS-dependent Cys modifications are depicted (underlined) together with secondary redox modifications. For further details, please refer to the text. RNS are indicated in white on dark grey rectangles. Continuous and dotted lines indicate recognized and possible reactions, respectively. To see this illustration in color, the reader is referred to the online version of this article at www.liebertpub.com/ars.

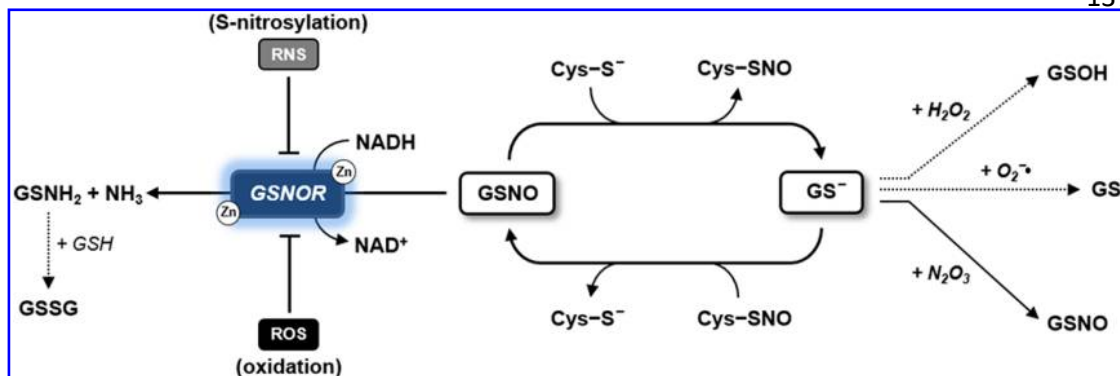


Figure 6. Redox homeostasis of protein and low-molecular S-nitrosothiols

Protein S-nitrosylation is generally induced by GSNO-dependent trans-nitrosylation with concomitant release of GSH. The reduction of protein S-nitrosylation is mainly controlled by GSH leading to the formation of GSNO. Once formed, GSNO is reduced to NH₃ and GSSG (if GSH is present) by the Zn-containing GSNOR using NADH as electron donor. The reactivity of GSH thiolate (GS⁻) with H₂O₂, O₂^{•-}, and N₂O₃ is also represented and indicated by continuous and dotted lines for established and hypothetical reactions, respectively. To see this illustration in color, the reader is referred to the online version of this article at www.liebertpub.com/ars.

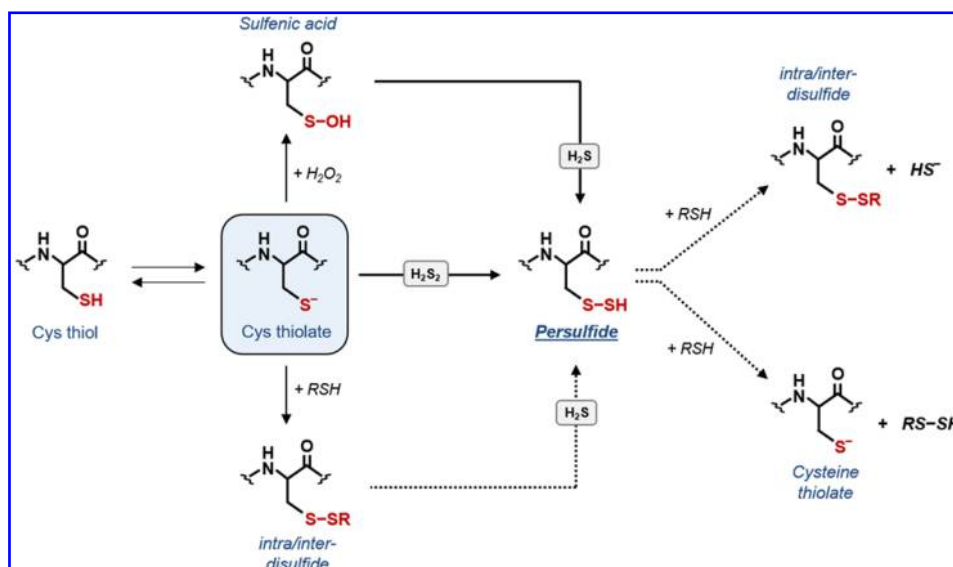


Figure 7. RSS-dependent thiol-based redox modifications

Biologically relevant RSS-dependent Cys modifications are depicted (underlined) together with secondary redox modifications. For further details, please refer to the text. RSS are indicated in black on light grey rectangles. Continuous and dotted lines indicate recognized and possible reactions, respectively. To see this illustration in color, the reader is referred to the online version of this article at www.liebertpub.com/ars.

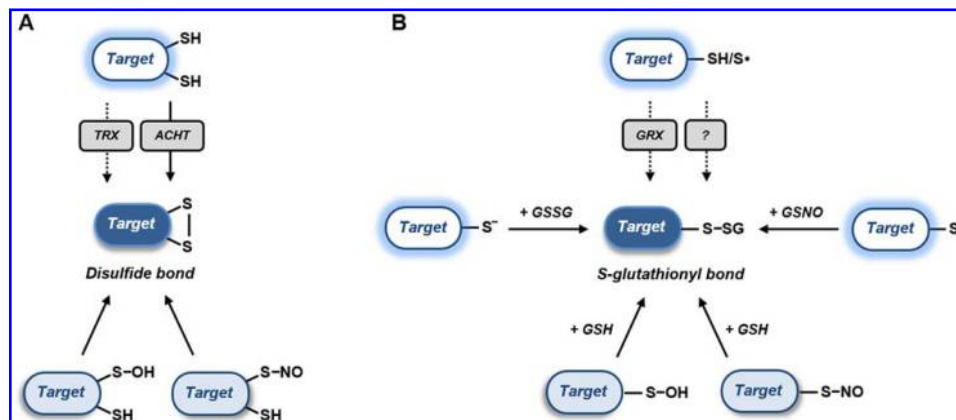


Figure 8. Major mechanisms of protein disulfide formation

(A) Enzymatic (upper panel) and non-enzymatic (lower panel) mechanisms of disulfide formation involving diverse enzymes (TRX or ACHT) or Cys oxoforms (sulfenic acid or S-nitrosothiol). Continuous and dotted lines indicate recognized and possible reactions, respectively. (B) Enzyme-catalyzed protein S-glutathionylation (–SSG, mixed disulfide formation) involving GRX or other not identified enzymes (upper panel). Non-enzymatic mechanisms (side and lower panels) of protein S-glutathionylation involving diverse oxidizing molecules (GSNO, GSSG) or Cys oxoforms (sulfenic acid or S-nitrosothiol). Continuous and dotted lines indicate recognized and possible reactions, respectively. To see this illustration in color, the reader is referred to the online version of this article at www.liebertpub.com/ars.

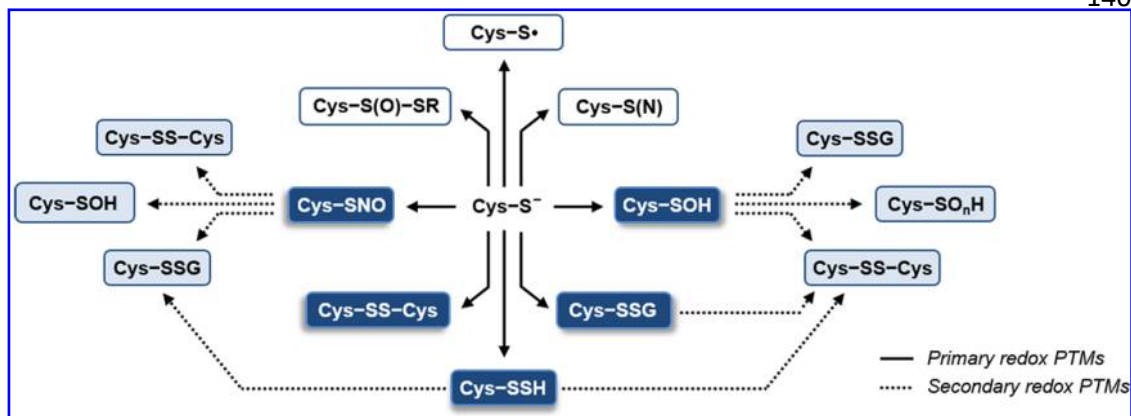


Figure 9. Primary and secondary thiol-based redox modifications

Biologically relevant RMS-dependent Cys PTMs (*i.e.* redox PTMs) are represented as follow: proteomic-suited primary redox modifications (white on dark blue rectangles), non-proteomic-suited primary redox modifications (black on white rectangles), and secondary redox modifications (black on light blue rectangles) occurring through further oxidative reactions of primary Cys oxoforms (S-nitrosothiols, sulfenic acid, S-glutathionyl and persulfide). Continuous and dotted lines indicate primary and secondary redox reactions, respectively. To see this illustration in color, the reader is referred to the online version of this article at www.liebertpub.com/ars.

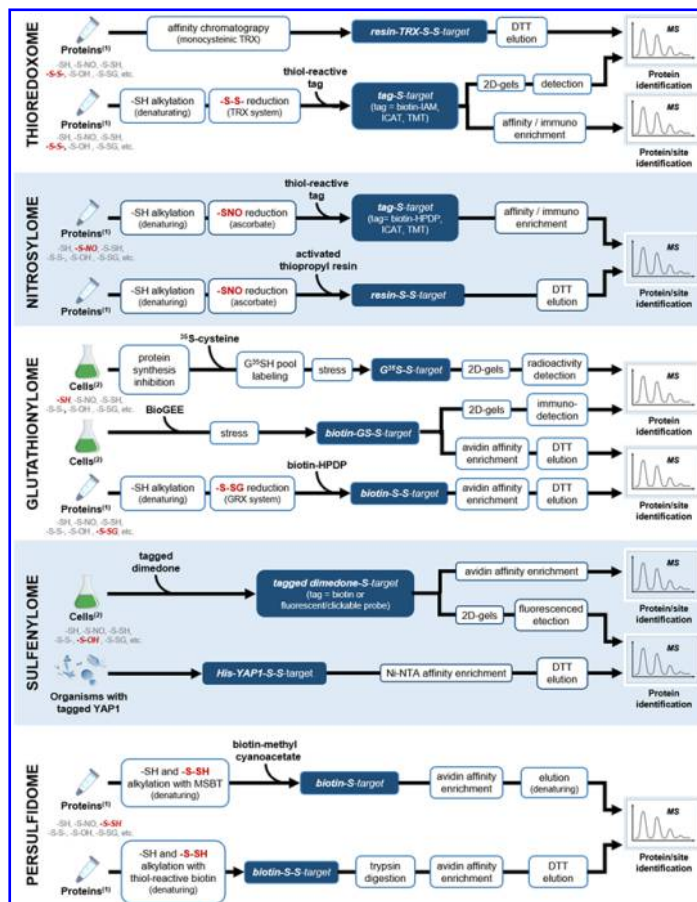


Figure 10. Methodological principles of redox proteomic-based approaches

Workflows of current redox proteomic strategies are depicted according to the targeted redox PTM. The starting material (proteins, cells or organisms) is indicated at the beginning of each workflow. The main steps are indicated in black/white on white/blue boxes, and the information level obtained by MS (identification of the modified protein and/or the modified Cys) is indicated at the end of each workflow. The initial modification state of Cys (-SH: reduced Cys; -S-S-: disulfide bond; -S-NO: nitrosylated Cys; -S-SG: glutathionylated Cys; -S-OH: sulfenylated Cys; -S-SH: persulfidated Cys) subjected to the redox proteomic strategy is indicated in bold. (1), proteins: cell-free protein extracts; (2), cells: intact cells. To see this illustration in color, the reader is referred to the online version of this article at www.liebertpub.com/ars.

Antioxidants and Redox Signaling
 REDOX HOMEOSTASIS IN PHOTOSYNTHETIC ORGANISMS: NOVEL AND ESTABLISHED THIOL-BASED MOLECULAR MECHANISMS (DOI: 10.1089/ars.2018.7617)
 This paper has been peer-reviewed and accepted for publication, but has yet to undergo copyediting and proof correction. The final published version may differ from this proof.

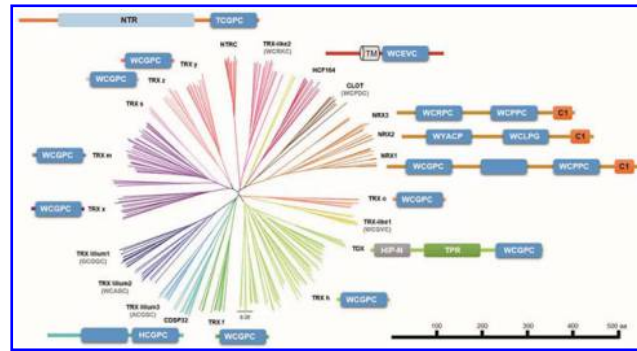


FIGURE 11. Phylogenetic analysis of plant TRXs and schematic representation of the architecture of TRX members

A total of 267 sequences have been retrieved by blastp analyses from 10 genomes found in the cyanobase (<http://genome.microbedb.jp/cyanobase/>) for cyanobacterial genomes and from the version 12 of the Phytozome portal (<http://phytozome.jgi.doe.gov/pz/portal.html>) for algal and terrestrial plant genomes. Sequences were aligned using ClustalOmega and the phylogenetic tree was constructed with BioNJ (168) in Seaview using the observed distance methods and ignoring all sequence gaps. The robustness of the branches was assessed by the bootstrap method with 1000 replications. The scale marker represents 0.1 substitutions per residue. The tree was then edited with Figtree software (<http://tree.bio.ed.ac.uk/software/figtree/>). The names of individual sequences have been indicated and proteins possessing classical or additional domains as predicted by the pfam or NCBI conserved domain tools have been represented with the exception of TRX lilium1-3, CLOT, TRX-like1-2, and TRX s. The TRX domain of a chosen *A. thaliana* representative is colored in light blue with the active site signature in white. The TRX domains without active site signatures have lost both catalytic cysteines. Among additional domains, NTR stands for NADPH thioredoxin reductase, HIP-N for N-terminal domain of HSP70-interacting proteins, C1 for C1 domain (short domain rich in cysteines and histidines) and TPR for tetratricopeptide repeat. The only protein with a membrane-anchoring domain, represented as a cylinder, is HFC164. The size of the boxes and strings is proportional to the length in amino acids. Note that TRX s and NRX2 are absent in *A. thaliana* and that poplar NRX2 was used as the plant representative. To see this illustration in color, the reader is referred to the online version of this article at www.liebertpub.com/ars.

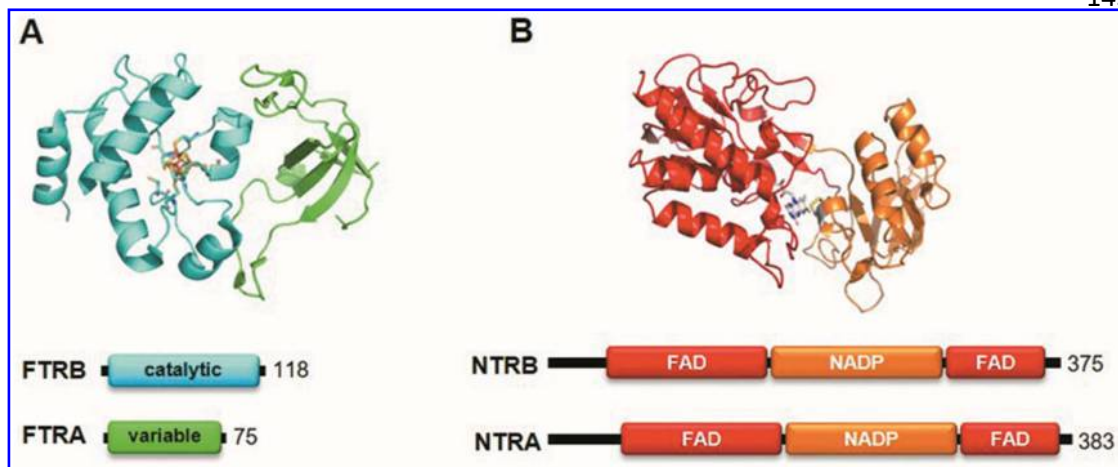


FIGURE 12. Structural and schematic representation of the architecture of plant TRX reductases (TRs)

(A) The catalytic (FTRB) and variable (FTRA) subunits of FTR from *Synechocystis* sp. PCC 6803 are represented (upper panel: ribbon, PDB ID: 2PVD; lower panel: schematic subunits), and colored in cyan and light green, respectively. Accession numbers: catalytic FTR subunit, Q55389; variable FTR subunit, Q55781. (B) The FAD- and NADP(H)- binding domains of NTRB/A from *Arabidopsis thaliana* are represented as ribbon (upper panel, PDB ID for *Arabidopsis* NTRB: 1VDC) and schematic domains (lower panel), and colored in red and orange, respectively. Accession numbers: NTRB, Q39243; NTRA, Q39242. For both panels, the size of the boxes is proportional to the length in amino acids. To see this illustration in color, the reader is referred to the online version of this article at www.liebertpub.com/ars.

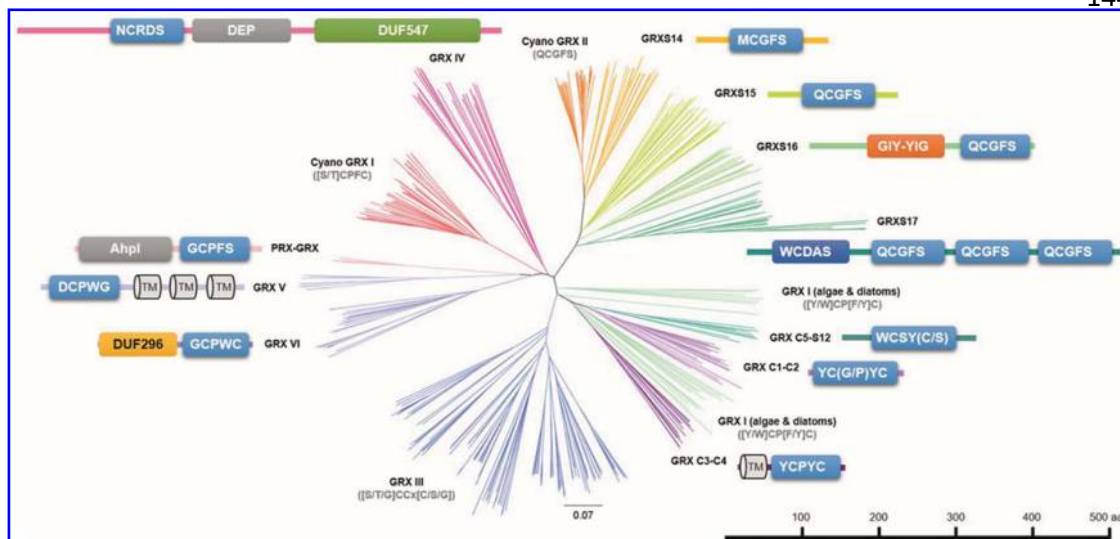


FIGURE 13. Phylogenetic analysis of plant GRXs and schematic representation of the architecture of GRX members

The retrieval and alignment of amino acid sequences (415 from 58 organisms) and the building of the phylogenetic tree were achieved exactly as described in the legend of Figure 11. The names of individual sequences have been indicated and proteins possessing classical or additional domains as predicted by the pfam or NCBI conserved domain tools have been represented. The GRX domain is colored in light blue with the active site signature of a chosen *A. thaliana* representative shown in white, except when there was no Arabidopsis representative, which is the case for the PRX-GRX, GRX V and GRX VI clades specifically found in cyanobacteria. Among additional domains, DEP stands for domain found in Dishweller, Egl10 and Pleckstrin, DUF547 for domain of unknown function 547, GIY-YIG for domain similar to the catalytic domain of I-Tev and UvrC endonucleases, DUF296 for domain of unknown function 296 and Ahpl for an alkyl hydroperoxide/PRX domain. Membrane-anchoring domains have been represented as cylinders, when the predicted score using the Tmpred server was above 1000. The size of the boxes and strings is proportional to the length in amino acids. To see this illustration in color, the reader is referred to the online version of this article at www.liebertpub.com/ars.

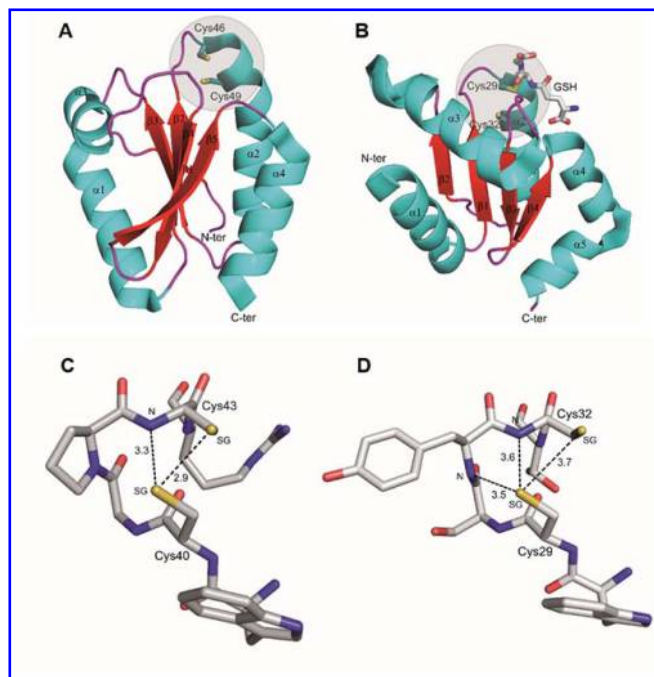


FIGURE 14. Structural features of typical TRX (TRX *h1*) and class I GRX (GRXC5)

Ribbon representation of the crystal structure of (A) reduced TRX *h1* from *Hordeum vulgare* (PDB ID 2VM1; (314)) and (B) GRXC5 from *Arabidopsis thaliana* (PDB ID 3RHB; (104)). The secondary structure elements are differently colored. The two protein present a very similar fold and the active sites formed by two close cysteine residues, are located at the N-terminus of helix $\alpha 2$ and quite solvent exposed. Representation of the hydrogen bonds formed by the N-terminal catalytic cysteine in (C) reduced TRX *h1* from *Hordeum vulgare* (PDB ID 2VM1; (314)) and (D) GRXC5 from *Arabidopsis thaliana* (PDB ID 3RHB; (104)). To see this illustration in color, the reader is referred to the online version of this article at www.liebertpub.com/ars.

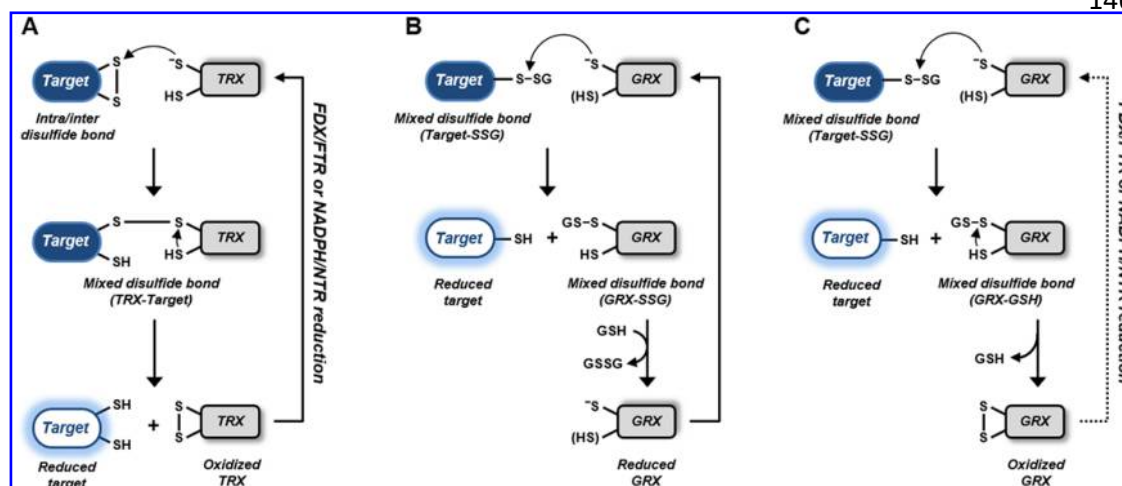


FIGURE 15. Schematic representation of TRX and GRX reduction mechanisms.

(A) TRX-dependent molecular mechanism of protein disulfide reduction. Under physiological conditions, the thiolate form of the N-terminal Cys of the CXXC active site initiates a nucleophilic attack on the disulfide bond in a protein target. Due to local conformational perturbations, the transient intermolecular disulfide formed is resolved by the C-terminal Cys in TRX, resulting in the formation of an intramolecular disulfide in TRX and the release of reduced target. The reduction of oxidized TRX is then catalyzed by the FDX-FTR or NADPH-NTR systems. (B) GRX-dependent monothiol de-glutathionylation mechanism. In GRX, the nucleophilic active site Cys forms a mixed-disulfide with GSH upon reaction with an S-glutathionylated target. Typically, a second GSH resolves the enzyme-glutathione mixed disulfide bond to generate the reduced GRX. (C) GRX-dependent dithiol de-glutathionylation mechanism. Some GRXs, such as *Chlamydomonas* GRX3, can also follow a mechanism in which the mixed-disulfide in GRX is resolved by a second non active site Cys resulting yielding an oxidized GRX. In chloroplasts, GRX3 is believed to be reduced via the FDX-FTR system. To see this illustration in color, the reader is referred to the online version of this article at www.liebertpub.com/ars.

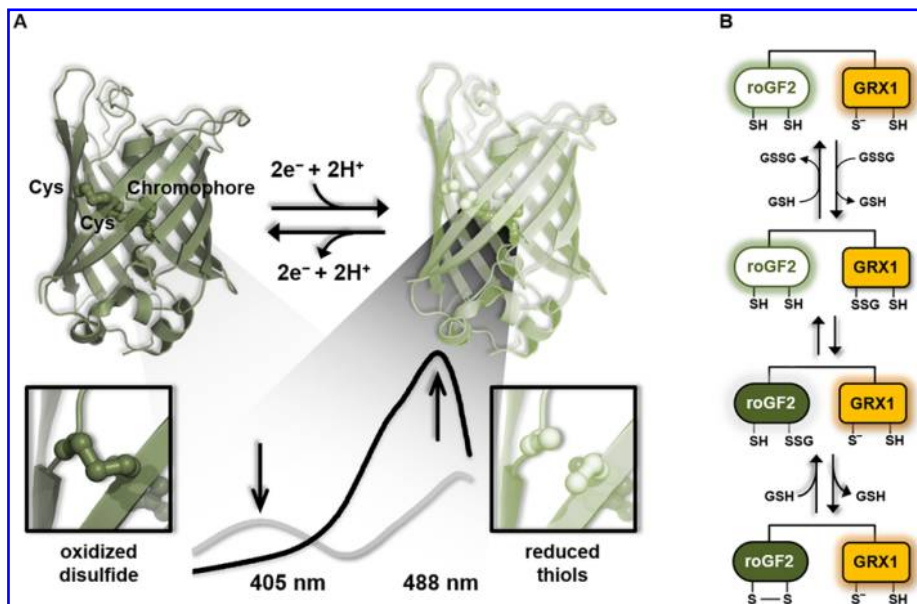


FIGURE 16. Spectroscopic and biochemical features of roGFP-based redox sensors

(A) Ribbon representation of roGFP with chromophore and Cys residues involved in the disulfide bond formation represented as ball-and-sticks. The change in the oxidation state of the Cys residues affects the spectral properties of the fluorescent protein by inducing a change in its absorption profile. The gray and black lines correspond to the absorption spectrum of the roGFP2 in the oxidized and reduced form, respectively. Adapted from (348) (B) Redox equilibration mechanism of GRX1-roGFP2 sensor. As depicted, each individual reaction step of dithiol-disulfide exchange cascade is fully reversible. To see this illustration in color, the reader is referred to the online version of this article at www.liebertpub.com/ars.

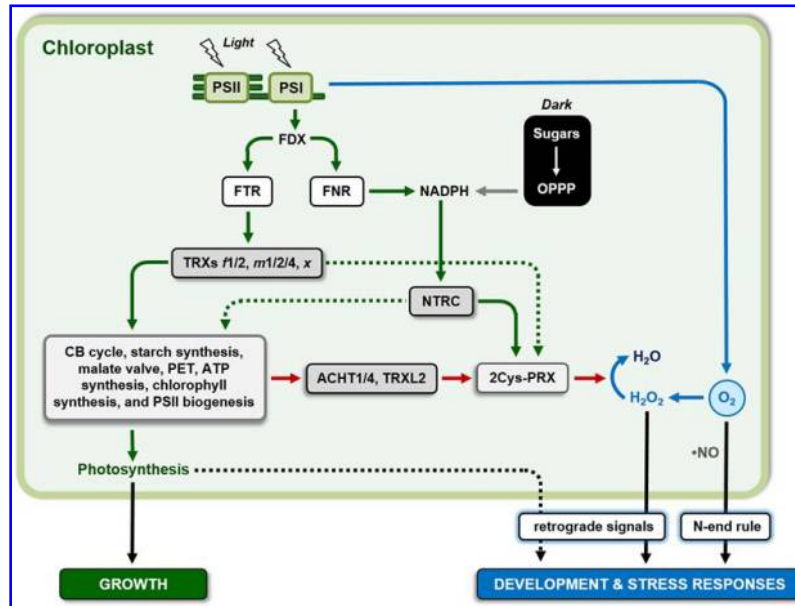


FIGURE 17. Proposed model for the *in vivo* role of the chloroplast redox network in light-dependent regulation of photosynthesis, growth, vegetative development and stress responses

Two different TRX systems coordinately participate to ensure light-responsive control of chloroplast functions CB by reducing regulatory dithiols in various target enzymes (171). The FDX-TRX system is reduced by electrons provided by PSI in the light, whereas NTRC consists of an NTR and TRX domain providing a separate reduction system that depends on NADPH. Joint operation of these two different reduction systems has been found to be crucial for the regulation of photosynthetic performance, biosynthetic activities and growth in acclimation to varying light conditions (69,108,371,382,383,498,501,563). The photosynthetic light reactions also produce O_2 and ROS/NO providing a feedback loop to oxidize the regulatory thiols of TRX target proteins via 2-Cys PRX and the atypical TRXs ACHT1/4 (111,133) and TRXL2 (561), while they also serve as retrograde signals to the nucleus regulating leaf development (14) and stress responses (119,123,134). NTRC is the major system to provide electrons for reduction of 2-Cys PRXs (419,563), thereby diminishing the oxidation loop (371,382) and maintaining the reducing capacity of the pool of FDX-TRXs (408) allowing increased reduction of targets of the FDX-TRX system to promote photosynthesis and growth (408), while it modulates ROS (H_2O_2) dependent retrograde signals to promote early plant development (382), abiotic stress (257) and immune responses (234). ROS levels and related immune and developmental responses

were also found to be affected by chloroplast GPX-like (75), however the TRXs involved in their reduction have not been identified yet. In addition to ROS there are also more direct O₂ and NO sensing and signaling pathways via cysteine oxidases that lead to proteasomal degradation of transcription factors via the N-end rule pathway affecting leaf development and stress responses at the transcriptional level (180,394,451). The individual specificities of TRXs *f1*, *f2*, *m1*, *m2*, *m4* and *x* for the different photosynthetic target processes, as well as the role of TRXs *m3*, *y1*, *y2* and *z* are not shown in this figure for clarity (see text for further information). Reduction signals are indicated with green lines whereas oxidation signals are indicated with red lines. Dotted lines indicate pathways of minor importance. Abbreviations: FDX, ferredoxin; FNR, FDX:NADPH reductase; FTR, ferredoxin:thioredoxin reductase; NO, nitric oxide; OPPP, oxidative pentose phosphate pathway; PET, photosynthetic electron transport chain; PRX, peroxiredoxin; PS, photosystem; ROS, reactive oxygen species; TRX, thioredoxin; TRXL2, TRX-like2. To see this illustration in color, the reader is referred to the online version of this article at www.liebertpub.com/ars.